THE JOURNAL OF CHEMICAL PHYSICS

VOLUME 14 NUMBER 10

OCTOBER, 1946

Published by the

AMERICAN INSTITUTE OF PHYSICS

Lancaster, Pa., and New York, N. Y.

EMICA

OTORS

Editor

Cross

Fuoss.

wood

Coryell.

Rice

Tuttle

W.

R. Bu[illegible], Jr.

...ponent. The solidus (/) should be used wherever possible for fractions.

All illustrations should accompany manuscript and should always be referred to in the text. Line drawings must be made with India ink on white paper or on tracing cloth. Coordinate paper is not desirable, but if used must be blue-lined with all coordinates to be reproduced drawn with India ink. Lettering should be of sufficient size to be legible after reduction.

Proof and all correspondence concerning papers in the process of publication should be addressed to the Publications Manager, American Institute of Physics, 57 East 55 Street, New York 22, New York.

Subscription Price

The United States and Possessions, Canada and Mexico, ... $10.00

Foreign..... 11.00

Back Numbers

Complete set: Vol. 1, 1933—Vol. 13, 1945..... $130.00

Library rate: $11.00.

Single copies: $3.00 each.

Subscriptions and orders for single copies should be addressed to Prince and Lemon Streets, Lancaster, Pennsylvania, or to the American Institute of Physics, 57 East 55 Street, New York 22, New York.

Changes of address should be sent to the Business Manager, American Institute of Physics.

Prince and Lemon Streets, Lancaster, Pennsylvania.

Entered as second class matter at the Post Office at Lancaster, Pa., under the Act of March 3, 1879. Acceptance for mailing at special rate of postage provided for in paragraph (d-2) Section 538, P. L. & R., authorized

THE JOURNAL
OF
CHEMICAL PHYSICS

VOLUME 14, NUMBER 10 OCTOBER, 1946

Intensities of Electronic Transitions in Ammonia

ROBERT J. THOMPSON* AND A. B. F. DUNCAN
Department of Chemistry, University of Rochester, Rochester, New York
(Received April 11, 1946)

Absolute intensity measurements of the transitions in ammonia vapor with maxima at 52,500, 66,000, and 77,000 cm^{-1} are reported. Calculations are made of the intensities of the first and third transitions, using non-bonding nitrogen orbitals, of the form suggested by Slater. The calculated values are considerably lower than the measured values, but may be improved by variation of the effective nuclear charge. Similar calculations for the second transition are less conclusive, but seem to indicate that it also may originate from a nearly non-bonding nitrogen orbital. Some other possible origins of this transition are considered and rejected on the basis of either their energy or their intensity.

INTRODUCTION

PREVIOUS investigation of the absorption spectrum of ammonia vapor[1,2] has revealed the presence of four electronic levels in the frequency range 45,000–120,000 cm^{-1}. We report here absolute intensity measurements of transitions from the normal level to the two lowest of these electronic levels, designated as transitions I and II, with intensity maxima at about 52,500 and 66,000 cm^{-1}. In addition, the intensity of the transition III with maximum at about 77,000 cm^{-1} may be estimated by comparison with I and II using previously obtained appearance-pressure data. There appears to be little hope of obtaining a direct measurement of the intensity of III or IV with present experimental techniques.

As is well known, an experimental value of the absolute intensity of absorption associated with an electronic transition in a pure vapor is found by evaluation of $\int \alpha_\nu d\nu$ over the entire absorption region. At a single frequency, $\alpha_\nu = (1/l_0) \log_e (I_0/I)$, where I_0 is the intensity of the incident light and I is the intensity after passage through a column of the absorbing gas of length l_0 measured at 0°C and 760-mm pressure. The light source used should emit sharp, well-resolved lines of known frequency, well distributed over the wave-length region in question.

Values of α_ν in cm^{-1} are plotted against wave number, and the value of $\int \alpha_\nu d\nu$ determined with a precision planimeter. The value of the integral multiplied by $mc^2/n\pi e^2 (=4.2\times10^{-8}\ cm^2)$ gives the f number or oscillator strength of the transition. In order to compare experimental intensities with calculated values, we may compute the square of the dipole moment integral (in square angstroms) from the approximate relation

$$Q^2(\text{exptl}) \cong (3hf/8\pi^2\nu mc)\times10^{16} (\cong 9.12\times10^4 f/\nu_m),$$

where ν_m is the wave number of the intensity maximum of the transition.

* Part of a dissertation presented to the Faculty of the Graduate School of the University of Rochester in partial fulfillment of the requirements for the degree of Doctor of Philosophy.

[1] A. B. F. Duncan, Phys. Rev. **47**, 822 (1935).

[2] A. B. F. Duncan, Phys. Rev. **50**, 700 (1936).

Two methods of photographic photometry may be used to evaluate I_0/I at a single known frequency from measurements of photographic density. In both methods the intensity of the source must be kept as constant as possible. In the first method (intensity scale method) the intensity through the absorption cell is varied by a system of calibrated diaphragms. On each plate a series of exposures for equal time intervals is made through each of the diaphragms with the cell evacuated, then one or more exposures are made through one of the diaphragms with the cell filled with vapor at a measured pressure.

For every line within the absorption band, a series of density values corresponding to the series of exposures is recorded with a Moll type microphotometer. From a plot of density against $\log_{10}(I_0/I)$ for each line, I_0/I for the exposure through the vapor, and hence α_ν, may be obtained directly.

In the second method (time scale method) the intensity through the evacuated cell is kept constant and a similar series of exposures is made for different time intervals. In this case, density $-\log$ time curves give $\log_{10}(t_0/t)$, which is equivalent to $\log_{10}(I_0/I)$ by the usual photographic reciprocity law. The exposure through the vapor is then made for time t_0. In this work we have used both methods.

The general method outlined in the preceding five paragraphs should give correct intensity values in the case of strictly continuous spectra. While the absorption spectrum of ammonia is not truly continuous, it approximates continuity sufficiently under the experimental conditions used here, since α_ν does not change anywhere very abruptly with frequency. At considerably lower pressures than were used in the present work and with slit widths 0.008–0.015 mm, vibrational structure is easily resolved, and in transition II, rotational structure is partly resolved.[1] In the present work, with slit 0.2 mm wide, and with pressures 5–10 times that used to resolve fine structure, vibrational structure can be recognized as broad low maxima in the absorption curves for transition II. The frequencies, at which α_ν were measured, are sufficiently close together to show the detailed shapes of these curves. Not even vibrational maxima are clearly recognized in the curves for transition I, and no rotational structure is apparent in any case.

The integrated absorption coefficients for transitions I and II are independent of the pressure in the range used, or rather, any pressure dependence is concealed and included in the total experimental error in the f numbers (5–10 percent).

EXPERIMENTAL

The ammonia gas used in this study was purified by a large number of distillations in vacuum through KOH pellets, and subsequent fractionation. It was dissolved in dried NH_4NO_3 and NH_4SCN in the molar proportions 1:3 for storage, the resulting solution giving a convenient NH_3 pressure of about 180 mm. The desired pressures were obtained by expansion through calibrated volumes, and the pressure in the cell was read with a McLeod gauge.

The apparatus used to study transitions I and II was in all essentials the same as that of Ladenburg and Van Voorhis[3] and need not be described in detail. The background for observation of absorption was a discharge in pure CO_2 for the region 45,000 to 61,000 cm^{-1} (transition I) and in pure H_2 for the region 60,000 to 71,000 (transition II). In the former case the well-known $A^1\Pi - X^1\Sigma$ bands of CO appeared with great intensity and the heads were sufficiently sharp to serve as lines for photometric measurement. The wave-lengths given by D. N. Read[4] were used. In the second case the rotational lines in the H_2 bands of the Lyman ($^1\Sigma_u^+ - {}^1\Sigma_g^+$) system[5] were used.

The discharge tube was operated at a constant direct current of 0.065 ampere through a voltage regulator and a transformer-rectifier unit. Less than 0.001-ampere variation in current was observed with the longest exposures. The light from this discharge was made parallel by a LiF lens, passed through an absorption cell 17.7 cm long, and was focused on the slit of the vacuum spectrograph by a second LiF lens. The spectra were photographed from a 2-meter radius,

[3] R. Ladenburg and C. C. Van Voorhis, Phys. Rev. **43**, 315 (1933).
[4] D. N. Read, Phys. Rev. **46**, 571 (1934).
[5] T. Lyman, Astrophys. J. **23**, 181 (1906).

TABLE I.

Transition	Frequency maximum (cm^{-1})	Assumed type	Q/a_0 obs.	Q/a_0 calc.	f obs.	f calc.
I	52500	$2p_z-3s$	0.90	0.29	0.13	0.0134
II	66000	$2p_z-3d_z$	0.22	0.092	0.0095	0.0017
III	77000	$2p_z-4s$	0.52	0.02	0.064	0.0001
IV	85000	$2p_z-5s$	—	0.01	—	0.00003

120,000-line grating, used in the first order.[6] The dispersion was about 4.15A per mm. The exposure times were 40 to 60 minutes. Eastman III-O and I-O ultraviolet sensitized plates were used, and were processed with the special precautions required in photographic photometry.

The decrease in effective transmission of the LiF lenses became quite appreciable below 1400A (70,000 cm^{-1}) when used in the optical system described. To observe transition III (and IV, with maximum at 85,000 cm^{-1}) would have required prohibitively long exposures. We considered the possibility of using the spectrograph as an absorbing column and moving the discharge close to the slit, with a very thin LiF plate separating the two. However, we did not believe that the pressure of ammonia could be maintained sufficiently constant in the spectrograph, especially at the low pressures required.

RESULTS

Seven plates, four on the intensity and three on the time scale, were used to obtain $\int \alpha_\nu d\nu$ for transition I. The pressure of ammonia ranged from 0.150 to 0.875 mm, the most useful range being 0.2 to 0.5 mm. For transition II eight plates on the intensity scale and one on the time scale were used. The pressure range was 0.3 to 3.0 mm, the most useful range being between 1.0 and 2.0 mm. The results from the intensity and time scales checked within the experimental accuracy. Reciprocity law failure was negligible in these experiments.

Average experimental values of the dipole strength Q and the f number of transitions I, II, and III are given in Table I, together with two sets of calculated values for transitions I, II, III, and IV. These calculations will be discussed in the next section. a_0 is 0.528A, the Bohr radius of the normal hydrogen atom.

[6] A. B. F. Duncan, J. Chem. Phys. **8**, 444 (1940).

The experimental results for transitions I and II are estimated to be accurate to within 5 to 10 percent. The indirect values for transition III are subject to somewhat larger error, although this is not necessarily much larger. The probable accuracy of these values is difficult to estimate.

DISCUSSION OF RESULTS

The electronic configuration of the ground state of ammonia, omitting the 1s electrons of N, is given by Mulliken[7,8] as $(sa_1)^2(\pi e)^4(za_1)^2$. The orbital sa_1 is primarily a N atom $2s$ orbital which, however, contributes a little to the three N−H bonds. The two πe orbitals are strongly bonding. The orbital za_1 is non-bonding and is approximately just a $2p_z$ orbital of the N atom. Mulliken suggests that the lower excited states correspond to the excitation of one za_1 electron from this configuration, and that the lowest electronic transition should be $2za_1-3sa_1$.

Dipole Moment Integrals for Transitions I, III, and IV[9]

We have assumed that the transitions $(za_1)-(nsa_1)$ in ammonia may be approximated, for the purpose of intensity calculations, by the transitions $2p_z-ns$ in the N atom. The dipole moment integrals will be of the form

$$Q=Q_z=(2)^{\frac{1}{2}}\int \psi_{2p_z} z \psi_{ns} d\tau$$

and may be evaluated in spherical polar coordinates, with $z=r\cos\theta$. The factor $(2)^{\frac{1}{2}}$ allows for the fact that there are two equivalent $2p_z$ electrons, either of which may make the transition. The functions ψ_{2p_z} and ψ_{ns} may be approximated

[7] R. S. Mulliken, J. Chem. Phys. **1**, 492 (1933).
[8] R. S. Mulliken, J. Chem. Phys. **3**, 506 (1935).
[9] The general method used here is discussed by R. S. Mulliken, J. Chem. Phys. **7**, 14 (1939); *Reports on Progress in Physics* (1941), Vol. VIII.

by the radial functions given by Slater,[10] multiplied by the appropriate angular factors. The normalized radial parts of the functions are:

$$R_{nl}(r)=\frac{(2Z^*/n^*)^{n^*+\frac{1}{2}}}{a_0^{\frac{1}{2}}(\Gamma(2n^*+1))^{\frac{1}{2}}}(r/a_0)^{n^*-1} \times\exp\left[-(z^*r/n^*a_0)\right].$$

The complete ψ_{2p_z} function is obtained by multiplying $R_{2p}(r)$ by $(6)^{\frac{1}{2}}\cos\theta/2(2\pi)^{\frac{1}{2}}$; the complete ψ_{ns} function is obtained by multiplying R_{ns} by $(2)^{\frac{1}{2}}/2(2\pi)^{\frac{1}{2}}$. a_0 is the radius of the Bohr orbit on normal hydrogen. Substitution of these functions and integration yields

$$\frac{Q}{a_0}=(2)^{\frac{1}{2}}(3^{\frac{1}{2}}/3)\left\{\frac{(2Z_1^*/n_1^*)^{n_1^*+\frac{1}{2}}(2Z_2^*/n_2^*)^{n_2^*+\frac{1}{2}}}{[\Gamma(2n_1^*+1)\Gamma(2n_2^*+2)]^{\frac{1}{2}}}\right\} \times\left\{\frac{\Gamma(n_1^*+n_2^*+2)}{[(Z_1^*/n_1^*)+(Z_2^*/n_2^*)]^{(n_1^*+n_2^*+2)}}\right\}. \quad (1)$$

The factor $(3)^{\frac{1}{2}}/3$ is the result of integration over the angles θ and φ. Subscripts 1 and 2 refer to the lower $(2p_z)$ and upper (ns) states.

The values of the parameters Z^* and n^* in the states considered are given by Slater as:

State	$2p$	$3s$	$4s$	$5s$
Z^*	3.9	1.6	1.0	1.0
n^*	2.0	3.0	3.7	4.0

The values of Q/a_0 calculated with these values of the parameters are listed in Table I. The values of f were calculated for the transitions $2p_z-ns$ on the assumption that these correspond to the observed transitions I, III, and IV, which were found earlier[2] to fit into a Rydberg series.

Table I shows that the experimental values of the dipole moment integrals associated with transitions I and III and the values calculated by means of Slater functions differ by factors of 3 and 26, respectively. The experimental value of the mean oscillator strength f (which is proportional to the intensity of the transition) is 10 times the calculated value for transition I and 550 times the calculated value for transition III.

This disagreement between theory and experiment may be considered from two viewpoints. First, the electron involved in the transitions I and III may not be completely non-bonding. Second, the functions used in the numerical evaluation of the dipole moment integrals are probably crude approximations to the true functions. Even if the form of the wave functions is approximately correct, the appropriate values of the parameters Z^* and n^* for our use may not be those given by Slater.

The first viewpoint suggests that improvement in the calculated values may result from admixture of the orbitals $2s(N)$, $2p_z(N)$, and $1s(H)$ for the normal state wave function (as suggested by Mulliken[7]). Perhaps the upper states in the transitions should not be regarded as pure N atom states and a linear combination of orbitals should be used there also. Calculations employing such mixed functions appear to offer considerable difficulty and may be inconclusive in view of the undetermined coefficients appearing in these linear combinations. We have not made such calculations.

The second viewpoint suggests that we might vary Z^* in the Slater function to obtain better agreement between calculation and experiment. The variation of Slater's Z^* has been discussed by Mulliken.[11] We have varied the Z^* in Eq. (1) and find that if $Z_{2p}{}^*$ is to be near the Slater value 3.9, then $Z_{3s}{}^*$ must be increased to about 3.5 to get agreement with experiment in transition I. This is indeed a large increase, in comparison with the increases suggested by Mulliken in other cases.

This large increase in $Z_{3s}{}^*$ appears improbable on the basis of simple energy considerations, such as have been used by Slater. Using the method of reference 10, the lowest ionization potential of ammonia, taken as the energy difference of the configurations $1s^22s^22p^2-1s^22s^22p^3$ is close to the experimental value (11.56 ev obs., 12.88 calc.). Similarly, with $Z_{3s}{}^*=1.6$, the Slater value, the difference between $1s^22s^22p^2$ and $1s^22s^22p^23s$ is 3.85 ev (obs. in ammonia, 5.05). An increase of $Z_{3s}{}^*$ to 1.8 gives exact agreement with the observed term value, while an increase to 3.5 gives a term value greater than the normal state. It is uncertain how seriously these energy calculations should be considered.

It is well known that the upper level of

[10] J. C. Slater, Phys. Rev. **36**, 57 (1930).

[11] R. S. Mulliken, J. Chem. Phys. **8**, 234 (1940); *Reports on Progress in Physics* (1941), Vol. VIII, pages 244, 250, 269.

transitions I in ammonia is predissociated. The origin of this predissociation has not been examined theoretically in detail. If the perturbation causing the predissociation is merely of a vibrational nature, it should have no effect in a comparison of experimental and theoretical intensities. If the perturbation is caused by another electronic level, the experimental intensity may well be higher than the intensity calculated for a single, atom-like transition. It appears at least that no simple explanation can be offered at the present time for the intensity of transition I.

Discussion of Transition II

It was suggested previously[2] that this transition might be to a triplet level associated with the upper level of transition III. From the present quantitative measurements, the experimental ratio of intensities of III to II is about 7:1, which appears to be too low for a singlet-triplet ratio. In some previous unreported work, we looked for transitions at frequencies lower than transition I, in an absorption tube 10 meters long with ammonia at one atmosphere pressure. None was found, indicating a very low intensity for any possible triplet transition associated with I. We would expect the triplet associated with III to have an even lower intensity. Accordingly, we withdraw this previous suggestion.

We will discuss briefly other possible explanations for this transition. Discussion will be limited to parallel transitions, since analysis of the rotational structure of the bands of transition II showed it to be of this type.[12]

Of the other atom-like transitions of a za_1 electron we considered $2za_1-3da_1$, which we have assumed may be approximated by the N atom $2p_z-3d_z$ transition. The dipole moment integral was calculated in the same way as before. The value of the integral is given by Eq. (1), except that integration over the angles now gives $2(15)^{\frac{1}{2}}/15$. The calculation was made using Slater's value of $Z_{2p}^*=3.9$, $Z_{3d}^*=1.0$, $n_{2p}^*=2.0$, and $n_{3d}^*=3.0$. The experimental and calculated results are compared in Table I. If Z_{3d}^* is increased from 1.0 to 1.5, complete agreement with experiment is obtained, without adjustment of any other parameters. By analogy with the energy levels of the nitrogen atom, this transition should occur at a higher frequency (about 80,000 cm^{-1}) in ammonia. However, as Mulliken points out,[8] the lower members of the Rydberg series in a polyatomic molecule may show abnormalities because of their relationship to orbitals in the core. For example, the frequency of transition I in ammonia is about 13,000 cm^{-1} lower than would be expected by analogy with the corresponding transition in nitrogen. The transition $2p_z-3d_z$ should therefore be considered as a possible explanation for transition II.

Transition II may, however, be caused by excitation of another electron in ammonia. The estimated ionization potential of an sa_1 electron is given as 27 volts,[8] which indicates that even the first member of the (sa_1-nza_1) series should lie above the ionization potential of the za_1 electron, and should not appear in the spectral region investigated. The ionization potential of a πe bonding electron is estimated to be about 16 volts, so it is quite possible that the first transition due to this electron may be in the region of transition II. The possible transitions consistent with parallel rotational structure are the $N-V_\pi$ bonding to anti-bonding transition and the $(\pi e)-(\pi e)'$ bonding to bonding transitions in which the upper state orbitals may possess atom-like characteristics. It should be interesting to attempt calculations of the intensities of such transitions in ammonia.

[12] A. B. F. Duncan and G. R. Harrison, Phys. Rev. **49**, 211 (1936).

THE JOURNAL OF CHEMICAL PHYSICS VOLUME 14, NUMBER 10 OCTOBER, 1946

The Experimental Determination of the Intensities of Infra-Red Absorption Bands

I. Theory of the Method*

E. BRIGHT WILSON, JR. AND A. J. WELLS**
Mallinckrodt Chemical Laboratory, Harvard University, Cambridge, Massachusetts

(June 28, 1946)

With spectrographs of available resolving power, the apparent integrated absorption coefficients of infra-red bands usually differ greatly from the true coefficients because the spectrograph yields at each setting a weighted average of the fractional light transmitted in a band of frequencies, whereas what is desired is the unweighted average of the logarithm of the fractional light transmitted. It is shown that true absorption coefficients can be obtained by (a) eliminating the violent fluctuations in intensity with frequency by broadening the rotational lines with a non-absorbing foreign gas and (b) eliminating the error due to the intensity variation of the envelope by extrapolating the apparent integrated absorption coefficient divided by the partial pressure to zero partial pressure of the absorbing gas. These two steps permit vibrational intensities to be measured to a reasonable accuracy even with a spectrograph of low resolving power.

FEW accurate measurements on the intensities of infra-red absorption bands have been published in spite of the utility of such data. Many of the results which have been obtained have been in error by as much as several hundred percent. This error is mainly caused by the lack of adequate resolving power in the spectrographs used. In this paper a method will be described which permits fairly accurate results to be obtained on most substances, even with a spectrograph of low resolving power. This method is primarily useful in handling the vibration-rotation bands of gases whose rotational spacing is not too wide.

I. DEFINITIONS

It will be assumed that the absorption of strictly monochromatic light is governed by the familiar law

$$I = I_0 \exp(-\alpha p L), \tag{1}$$

where I is the light transmitted by a cell of length L containing a gas at pressure p, and I_0 is the incident intensity. α is the absorption coefficient divided by the pressure and is assumed to be independent of p and L but dependent on the frequency.[1] The quantity which is desired for comparison with theory is the integrated absorption coefficient for unit pressure

$$A = \int \alpha d\nu = (1/pL) \int \ln (I_0/I) d\nu, \tag{2}$$

where the integration is carried out over the frequency range covered by a given band. If a spectrograph of infinite resolving power were available, I_0/I could be measured directly and there would be no problem.

No actual spectrograph measures I or I_0 for a single frequency but instead measures the integral of the intensity in a range of frequencies. Let T be the apparent intensity registered by the instrument at a setting ν' (representing the central frequency admitted by the finite slit). Then

$$T = \int I(\nu) g(\nu, \nu') d\nu, \tag{3}$$

where $g(\nu, \nu')$ is the fraction of the light of actual frequency ν which is registered by the instrument when its setting is ν'. The integration is carried out over all values of ν for which $g(\nu, \nu') \neq 0$. Since g will diminish rapidly outside of a narrow band centered at ν', the limits of integration can be extended to $\pm\infty$ without harm. A similar expression holds for T_0 in which I_0 replaces I. It is convenient to define an apparent absorption coefficient $p\beta$ for frequency ν' by the equation

$$p\beta = (1/L) \ln (T_0/T), \tag{4}$$

* Much of the material in this paper is taken from a thesis by A. J. Wells, submitted to the Department of Chemistry, Harvard University, in May, 1941. A short note was published in J. Chem. Phys. 9, 659 (1941).

** Now at Experimental Station, E. I. du Pont de Nemours and Company, Wilmington, Delaware.

[1] Actually α is not strictly independent of p due to self-broadening, but this does not affect the later arguments, when the total pressure, including that of a foreign gas, is held constant.

and, for each band, an integrated apparent absorption coefficient B for unit pressure

$$B=\int \beta d\nu' = (1/pL)\int \ln (T_0/T)d\nu'. \quad (5)$$

T and B are measurable quantities from which A is to be obtained.

II. EXTRAPOLATION THEOREM

It is desired to prove that

$$\operatorname*{Lim}_{pL\to 0} B=A.$$

To do so examine the difference

$$A-B=(1/pL)\int \ln (TI_0/T_0I)d\nu'$$

$$=(1/pL)\int \ln \frac{\int f(\nu)g(\nu,\nu')d\nu}{f(\nu')\int g(\nu,\nu')d\nu}d\nu', \quad (6)$$

where

$$f(\nu)=\exp(-\alpha pL)=I/I_0, \quad (7)$$

and I_0 has been assumed to be constant over a slit width.[2]

If f were constant over a slit width, it could be removed from the inner integral and the expression would vanish, so that, for resolving power large compared with the variations of $\exp(-\alpha pL)$, A and B are equal. But in practice this exponential will go rapidly from nearly zero to nearly one through each rotation line, if there is enough gas to make the average absorption appreciable. Under these conditions A and B will diverge widely.

Now consider the limit as $pL\to 0$. Differentiate the integral and the quantity pL in (6). The result is, after a few steps,

$$\operatorname{Lim}(A-B)=\operatorname{Lim}\int\left\{\alpha-\frac{\int \alpha f g d\nu}{\int f g d\nu}\right\}d\nu' = \int\left\{\alpha-\frac{\int \alpha g d\nu}{\int g d\nu}\right\}d\nu', \quad (8)$$

since $f\to 1$ in the limit.

[2] This assumption may break down in regions of absorption by water vapor or carbon dioxide in the atmosphere unless these materials are excluded from the light path.

If this expression vanishes, the desired theorem is proved. But it will vanish if the absorption coefficient α is constant over a slit width, a much less stringent condition than that its exponential be considered constant. Moreover, under certain conditions this expression will vanish regardless of the variations of α. Thus if $g(\nu,\nu')=g(\nu-\nu')$ only, i.e., if the resolving power is constant over the width of the band, and if $g(\nu-\nu')=g(\nu'-\nu)$, then

$$\int g(\nu-\nu')d\nu=\int g(\nu-\nu')d(\nu-\nu')=G, \quad (9)$$

which is independent of ν'. Also

$$\int\int \alpha g d\nu d\nu' = \int \alpha \int g d\nu' d\nu = G\int \alpha d\nu, \quad (10)$$

so the expression in Eq. (8) will reduce to[3]

$$\int \alpha d\nu' - \int \alpha d\nu = 0. \quad (11)$$

Consequently, if the incident intensity I_0 does not vary rapidly over a slit width and if either the resolving power is high compared with the variations in α or the resolving power does not change much over the band,

$$\operatorname*{Lim}_{pL\to 0} B=A. \quad (12)$$

Therefore by measuring B at a series of values of pL (either by changing p or L) and extrapolating to zero pL, the true integrated absorption A can be found.

III. PRESSURE BROADENING

In practice the fluctuations of $f=\exp(-\alpha pL)$ will be very extreme on passing through each line of the rotational fine structure. Consequently, where such fine structure exists, it might be necessary to carry the measurements to impractically low values of pL before a good limit could be estimated. To remedy this, the rotational fine structure can be eliminated by pressure broadening with the use of a sufficiently high pressure of a non-absorbing foreign gas, as was done by Bartholomé[4] for HCl.

[3] A similar argument has been used by D. M. Dennison, Phys. Rev. **31**, 503 (1928), for a slightly different purpose.

[4] E. Bartholomé, Zeits. f. physik. Chemie **B23**, 131 (1933).

With spectrographs of high resolving power, the use of a foreign gas to eliminate the rotational fine structure may be sufficient to make B essentially equal to A without extrapolation but for poorer spectrographs the variation of $f=\exp(-\alpha pL)$ over the band envelope may still be sufficiently great to cause very large differences between A and B, as was pointed out by Kemble.[5] The extrapolation procedure then takes care of this.

IV. ABSORPTION AREAS

Bourgin,[6] in studying the intensity of individual HCl rotation-vibration lines, extrapolated the integral ("absorption area")

$$pLC=\int[(T_0-T)/T_0]d\nu', \tag{13}$$

instead of B. By expansion of the logarithm in B, one gets

$$B=(1/pL)\int(x+\tfrac{1}{2}x^2+\cdots)d\nu', \tag{14}$$

where

$$x=(T_0-T)/T_0, \tag{15}$$

so that in the limit B and C are also equal. However, B is always larger than C and various arguments indicate that B is normally less than A so that B extrapolates to A more conveniently and rapidly than C. As shown by Dennison,[3] C is independent of the resolving power whereas B is not (at finite values of pL). Therefore the use of a better spectrograph assists the extrapolation when B is used but does not with C.

V. EFFECT OF STRAY LIGHT

In most spectrographs light of a frequency quite foreign to that being studied enters the detecting instrument, which if not taken into consideration will falsify the results. If the amount of stray is known, it can be corrected for, either by subtracting the stray intensity S from each observation T' or by correcting B after integration. If the stray is greater than about 10 percent of the total intensity T_0, it is more accurate to correct each observation.

Let $T_0=T_0'-S$ and $T=T'-S$ so that the uncorrected integral B' is

$$B'=(1/pL)\int\ln[T_0'/T')d\nu'$$

$$=(1/pL)\int\ln[(T_0+S)/(T+S)]d\nu'.$$

If S is independent of pL, then by differentiation one gets

$$\text{Lim } B'=-\text{Lim}\int[1/(T+S)][dT/d(pL)]d\nu'$$

$$=-\text{Lim}\int\frac{dT/d(pL)}{[1+(S/T_0)]T_0}d\nu'$$

$$=(1/[1+(S/T_0)])\text{ Lim } B,$$

if $1+(S/T_0)$ is constant over the band. If the stray is not too large, it should therefore not interfere with the accuracy of the extrapolation method, since it can be corrected for. It should be noted, however, that the stray may also be absorbed by the material under study, thus introducing a further source of error.

VI. SUMMARY OF METHOD

The above considerations show that it should be possible under proper conditions to obtain values of the intensity of an infra-red vibrational absorption band (integrated over the various rotational lines) by measuring the integrated apparent absorption coefficient for unit pressure B (see Eq. (5)) at a series of partial pressures of the absorbing gas and extrapolating this quantity to zero partial pressure. The rotational fine structure should be eliminated by means of a sufficiently high pressure of some suitable non-absorbing gas. The extrapolated value of B should then equal the true integrated absorption coefficient at unit pressure, A.

Care needs to be taken that the presence of atmospheric absorption bands does not cause the intensity of the incident beam to vary rapidly in the frequency band admitted by the slit and also that the resolving power of the instrument does not vary excessively from one end of a band to the other. Correction needs also to be made for stray light.

[5] E. C. Kemble, J. Chem. Phys. **3**, 316 (1935).
[6] D. G. Bourgin, Phys. Rev. **29**, 794 (1927).

THE JOURNAL OF CHEMICAL PHYSICS VOLUME 14, NUMBER 10 OCTOBER, 1946

The Mercury Photosensitized Reactions of 1-Butene and 2-Butene*

H. E. GUNNING AND E. W. R. STEACIE
Division of Chemistry, National Research Laboratories, Ottawa, Canada

(Received July 25, 1946)

An investigation has been made of the reactions of 1-butene and 2-butene with mercury ($^3P_1$) atoms at 30°C in a static system. The main products of the 1-butene reaction are 2-butene and liquid polymer. A large number of other products are also formed especially at low pressures. The rate of isomerization increases rapidly with pressure in the region of complete quenching, while the rate of polymerization falls off rapidly. The over-all rate of consumption of 1-butene increases very slightly with increasing pressure. The over-all quantum yield of 1-butene consumption is 0.32 at 20-mm pressure. The principal steps in the mechanism proposed for the reaction are:

$$1-C_4H_8+Hg(^3P_1)\rightarrow 1-C_4H_8^*+Hg(^1S_0),$$
$$1-C_4H_8^*+1-C_4H_8\rightarrow 2-C_4H_8+1-C_4H_8,$$
$$1-C_4H_8^*\rightarrow C_4H_7+H,$$

followed by polymerization reactions of the type

$$1-C_4H_8+C_4H_7\rightarrow C_8H_{15}, \text{ etc.}$$

It is therefore possible for the first time, to obtain a direct measurement of the rate of collisional deactivation merely by determining the rate of formation of 2-butene. 2-butene is much less reactive than 1-butene. The over-all quantum yield of 2-butene consumption has a maximum value of 0.11 at an initial pressure of 1–2 mm. Above this pressure the rate of 2-butene consumption falls off rapidly. The main product of the reaction is a liquid polymer. Smaller amounts of hydrogen and methane are also formed. An activated molecule mechanism is proposed which accounts for the essential aspects of the reaction.

INTRODUCTION

IN earlier papers from this laboratory it has been shown that ethylene,[1] butadiene,[2] propylene,[3] and isoprene[3] all react with mercury ($^3P_1$) atoms, at room temperature, by an activated molecule mechanism. Isobutene,[4] on the other hand seems to decompose initially into C_4H_7 radicals and H atoms. In other words, with isobutene, the activated molecule formed by collision of the hydrocarbon molecule with the mercury ($^3P_1$) atom seems to have a shorter life than the interval between successive collisions.

The present investigation on 1-butene and 2-butene was undertaken in order to investigate further the relation between structure and mechanism of reaction in the unsaturated hydrocarbons.

EXPERIMENTAL

A general description of the apparatus employed, and the experimental technique has already been given in a previous paper.[2]

The cylindrical quartz cell had a volume of 240 cc, and was immersed in a water thermostat, maintained at 30.00±0.01°C. The total volume of the system was 1050 cc.

The analyses of the condensible products of the reaction reported in this paper were made on the mass spectrometer through arrangement with the National Bureau of Standards. The sampling technique employed, as well as the method of analysis of the products, non-condensible in liquid air, have been previously described.[4]

The 1-butene and 2-butene were the C.P. grade manufactured by the Matheson Company, East Rutherford, New Jersey. After several trap-to-trap distillations, the middle fractions were collected and stored in one-liter flasks provided with Warrick-Fugassi valves.[5]

TABLE I. Composition of original reactants.

Component	1-butene (mole percent)	2-butene (mole percent)
C_3H_4	—	0.3
Propylene	—	0.4
1-Butene	98.91	—
2-Butene	0.87	99.0
Butanes	0.13	0.2
2-methyl-2-butene	—	0.03
Methyl pentenes	—	0.02
Dimethyl pentanes	—	0.05
Carbon dioxide	0.09	—

* Contribution No. 1414 from the National Research Laboratories, Ottawa, Canada.

[1] D. J. LeRoy and E. W. R. Steacie, J. Chem. Phys. **9**, 829 (1941).

[2] H. E. Gunning and E. W. R. Steacie, J. Chem. Phys. **12**, 484 (1944).

[3] H. E. Gunning and E. W. R. Steacie, J. Chem. Phys. **14**, 57 (1946).

[4] H. E. Gunning and E. W. R. Steacie, J. Chem. Phys. **14**, 534 (1946).

[5] E. Warrick and P. Fugassi, Ind. Eng. Chem. Anal. Ed. **15**, 13 (1943).

TABLE II. 1-Butene.

Run No.	Po (mm)	$\frac{-\Delta P}{\Delta t}\times 10^2$ mm/min.	$\frac{A}{\frac{d(CH_4)}{dt}\times 10^6}$ moles/min.	$\frac{B}{\frac{d(H_2)}{dt}\times 10^6}$ moles/min.	A/B
80G	2.12	1.45	0.0280	0.0186	1.50
81G	4.92	1.82	0.0540	0.0290	1.86
76G	6.03	1.73	0.0719	0.0427	1.68
77G	7.91	1.88	0.0686	0.0504	1.36
83G	8.66	1.83	0.0762	0.0599	1.27
73G	9.90	2.02	0.0704	0.0585	1.26
84G	15.35	1.83	0.0712	0.0536	1.33
79G	16.36	1.86	0.0619	0.0422	1.47
75G	17.49	1.87	0.0550	0.0426	1.29
71G	20.92	1.73	0.0520	0.0375	1.39
85G	22.52	1.70	0.0579	0.0416	1.39
74G	23.67	1.71	0.0522	0.0377	1.39
78G	24.74	1.62	0.0542	0.0429	1.27
86G	44.81	1.28	0.0340	0.0273	1.25
82G	62.38	1.00	0.0286	0.0227	1.26
87G	67.23	0.92	0.0257	0.0208	1.24

The compositions of the gases used, as determined on the mass spectrometer, are given in Table I.

RESULTS

1-Butene

1-butene shows a similar behavior to propylene,[3] isoprene,[3] and isobutene[4] in that the pressure decreases linearly with time even in the initial stages of the reaction. The polymer forms in colorless droplets on the window of the cell through which the light enters. The gas, noncondensible in liquid air, present at the end of each run was shown to be a mixture of hydrogen and methane. These data are summarized in Table II.

From Table II we see that the rate of pressure decrease as well as the rates of formation of hydrogen and methane all reach a maximum at an initial pressure of 10 mm. Measurements of the actual amounts of methane and hydrogen formed, as functions of the time, were made at initial pressures of 15 mm and 30 mm. These quantity-time curves were all straight lines passing through the origin.

The last column of Table II shows that the ratio $[d(CH_4)]/dt/[d(H_2)]/dt$ is constant, within experimental error, at 1.39 ± 0.12.

THE PRODUCTS OF THE REACTION

A detailed analysis of the products of the reaction has been made on the mass spectrometer at the National Bureau of Standards by Dr. A. Keith Brewer[6] and these results are reported in Tables III, IV, V, VI, and VII. There are a large number of products at the lower pressures owing undoubtedly to radical recombination reactions. At the higher pressures, the main products are 2-butene and polymer. The polymer is a clear, viscous, colorless liquid, completely soluble in benzene.

TABLE III. 1-butene. Mass spectrometric analysis—run 80G. Po=2.12 mm.

Product	Moles products formed per mole 1-butene decomposed
Hydrogen	0.0166
Methane	0.0250
Ethane	0.1372
Propane	0.0230
2-Butene	0.00204
n-Butane	0.00353
Pentenes	0.00676
Pentanes	0.0366
Benzene	0.00101
Methyl cyclopentane	0.00605
Hexanes	0.00524
Methyl cyclohexanes	0.00232
Ethyl cyclohexenes	0.00030
Heptanes	0.00434
Octenes	0.00040

The data in Table VII on the composition of the polymer, and the rate of polymerization of 1-butene, were obtained by a carbon-balance calculation.

In Fig. 1 the over-all rate of consumption of 1-butene, the rate of formation of 2-butene, and the rate of polymerization are plotted as

TABLE IV. 1-butene. Mass spectrometric analysis—run 81G. Po=4.92 mm.

Product	Moles product formed per mole 1-butene decomposed
Hydrogen	0.0141
Methane	0.0263
Ethane	0.1126
Propane	0.0240
2-Butene	0.2124
n-Butane	0.0207
Pentadienes	0.00296
Pentenes	0.0416
Pentanes	0.0124
Benzene	0.00104
Hexenes	0.0108
Hexanes	0.0137
Methyl cyclohexenes	0.00226
Ethyl cyclohexenes	0.00191
Heptenes	0.00330
Heptanes	0.00834
Octanes	0.00070

[6] For a description of the method of analysis, see A. Keith Brewer and Vernon H. Dibeler, J. Research Nat. Bur. Stand. **35**, 125 (1945).

TABLE V. 1-butene. Mass spectrometric analysis—run 87G. Po=67.23.

Product	Moles product formed per mole of 1-butene decomposed
Hydrogen	0.0091
Methane	0.0113
2-Butene	0.742

functions of the initial pressure, using the data of Tables VI and VII.

QUANTUM YIELD

Four determinations were made of the quantum input to the cell from the mercury resonance lamp by filling the cell with ethylene at an initial pressure of 13 mm. LeRoy and Steacie[1] have shown that this reaction has a quantum yield of 0.37 at this pressure. The mean quantum input to the cell, on this basis, was $7.07\pm0.11\times10^{-6}$ einstein per minute. The values of the over-all quantum yield of 1-butene consumption are given for each pressure in the last column of Table VI.

RESULTS

2-Butene

The results for the runs on 2-butene are summarized in Table VIII.

It is apparent from Table VIII that 2-butene is considerably less reactive than 1-butene. The main product of the reaction is a liquid polymer. Smaller amounts of hydrogen and methane are also formed. The maximum rate of consumption of 2-butene seems to occur at an initial pressure of 1–2 mm corresponding to the maximum over-all quantum yield of approximately 0.11.

TABLE VI. 1-butene.

Run No.	Po mm.	$-d(1-C_4H_8)/dt$ moles/min. $\times10^6$	$d(2-C_4H_8)/dt$ moles/min. $\times10^6$	Quantum yield $\varphi(1-C_4H_8)$
80G	2.12	1.12	0.00229	0.159
81G	4.92	2.06	0.437	0.291
83G	8.66	1.71	0.526	0.242
84G	15.35	2.23	0.967	0.316
85G	22.52	2.25	1.115	0.318
86G	44.81	2.13	1.285	0.301
87G	67.23	2.28	1.693	0.323

TABLE VII. 1-Butene.

Run No.	Polymer composition	Rate of polymerization of 1-butene moles per min. $\times10^6$
80G	$n(C_4H_{7.4})$	0.92
81G	$n(C_4H_{7.2})$	1.10
83G	$n(C_4H_{7.8})$	1.16
84G	$n(C_4H_{7.8})$	1.24
85G	$n(C_4H_{7.8})$	1.12
86G	$n(C_4H_{7.9})$	0.83
87G	$n(C_4H_{7.8})$	0.58

DISCUSSION

1-Butene

Before attempting to devise a mechanism for this reaction, it might be well to summarize briefly the salient results of our investigation. These are:

(a) The pressure *vs.* time curve is linear even in the initial stages of the reaction.

(b) The rate of pressure decrease is maximum at 10 mm.

(c) The main products of the reaction are 2-butene and a liquid polymer. Smaller amounts of a large number of other substances are also formed, including methane and hydrogen.

(d) The rate of isomerization increases rapidly with pressure in the region of complete quenching, while the rate of polymerization falls off rapidly.

(e) The over-all rate of consumption of 1-butene increases only very slightly with increasing pressure in the complete quenching region. The quantum yield is approximately constant in this region at 0.32.

(f) The rates of formation of methane and hydrogen reach a maximum at 10-mm pressure. Furthermore the ratio

$$[d(CH_4)/dt]/[d(H_2)/dt]$$

is constant throughout the entire pressure range at 1.39 ± 0.12. These products are only of minor importance compared to isomerization and polymerization.

(g) The polymer is a clear, colorless liquid, completely soluble in benzene.

The fact that the rate of isomerization increases with pressure, in the complete quenching region, while the rate of polymerization decreases, suggests the sequence

$$1-C_4H_8+Hg(^3P_1)\rightarrow1-C_4H_8^*+Hg(^1So), \quad (1)$$

$$1-C_4H_8^*\rightarrow C_4H_7+H, \quad (2)$$

$$1-C_4H_8^*+1-C_4H_8\rightarrow2-C_4H_8+1-C_4H_8, \quad (3)$$

$$1-C_4H_8^*+1-C_4H_8\rightarrow2(1-C_4H_8). \quad (4)$$

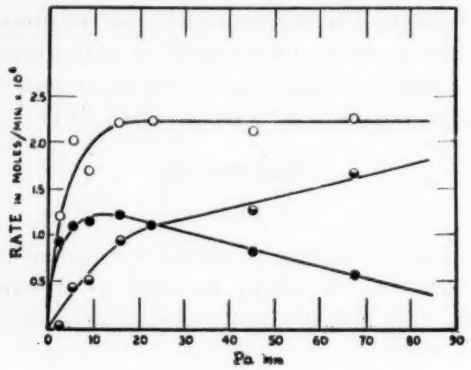

FIG. 1.

Polymerization will then be initiated by the radicals formed in (2)

$$C_4H_8+H\rightarrow C_4H_9, \tag{5}$$

$$C_4H_7+1-C_4H_8\rightarrow C_8H_{15}, \text{ etc.}, \tag{6}$$

$$C_4H_9+1-C_4H_8\rightarrow C_8H_{17}, \text{ etc.} \tag{7}$$

On this basis, isomerization would be virtually the only reaction occurring at high pressures. An examination of Table VI will show that this conclusion is consistent with our findings. At Po = 15.35 mm, 0.967/2.23 or 0.43 mole of 2-butene are formed per mole of 1-butene decomposed. While at Po = 67.23, 1.693/2.28 or 0.74 mole of 2-butene are formed per mole of 1-butene decomposed. Consequently one would expect that at pressures above, say, 150 mm, free radical formation, and hence polymerization would be of negligible importance, the only reaction occurring being the isomerization of 1-butene to 2-butene. It is interesting to note at this point that LeRoy and Steacie[7] found that 2-butene was a significant product in the cadmium ($^3P_1$) sensitized reaction of 1-butene.

With increasing pressure, then, reaction (2) will eventually become completely suppressed and under these conditions the rate equations assume the asymptotic form

$$\frac{d(2-C_4H_8)}{dt}\Big/Iab=\frac{-d(1-C_4H_8)}{dt}\Big/Iab$$

$$=k_1\left(\frac{k_4}{k_3+k_4}\right)=0.32$$

from Table VI or

$$\frac{k_4}{k_3}=\left(\frac{k_1-0.32}{0.32}\right).$$

Now if all collisions between activated 1-butene molecules and normal 1-butene molecules lead to isomerization $k_4=0$, and hence $k_1=0.32$. This is not an improbable assumption in view of the fact that it has been shown that the initial step in the mercury photo-sensitized reaction of isobutene[4] is only about 16 percent efficient. In other words, if we assume that reaction (1) is only 32 percent efficient, the rate of formation of 2-butene becomes a direct measure of the rate of deactivation of the excited molecules.

This conclusion is of considerable interest. Collisional deactivation has been postulated in a large number of reactions in order to explain, for example, a decrease in rate with increasing pressure. Now, for the first time, it becomes possible to follow deactivation directly simply by measuring the rate of formation of 2-butene.

The small amounts of methane and hydrogen formed probably arise from the unimolecular decomposition of the activated butyl radical formed in (5). This radical will contain excess energy of hydrogenation[4] and may decompose to some extent by the reactions

$$C_4H_9\rightarrow H_2+C_4H_7, \tag{8}$$

$$C_4H_9\rightarrow CH_4+C_3H_5. \tag{9}$$

These reactions would explain the fact that the ratio of the rates of formation to methane to hydrogen is constant, since under these conditions

$$\frac{d(CH_4)}{dt}\Big/\frac{d(H_2)}{dt}=\frac{k_8}{k_9}=1.39 \text{ from Table II.}$$

At low pressures atomic cracking reactions of the type

$$H+C_4H_9\rightarrow CH_3+C_3H_7, \tag{10}$$

$$H+C_4H_9\rightarrow 2C_2H_5, \tag{11}$$

would become significant. The important products listed in Tables III and IV could easily be accounted for by radical recombination reactions involving CH_3, C_2H_5, C_3H_7, C_4H_7, and C_4H_9 radicals.

[7] D. J. LeRoy and E. W. R. Steacie, J. Chem. Phys. **10**, 683 (1942).

2-Butene

The salient features of the 2-butene reaction are:

(a) The rate of pressure decrease, as well as the rate of consumption of 2-butene both fall off with increasing pressure above 2 mm.
(b) The maximum over-all quantum yield of 2-butene consumption is 0.11.
(c) The main product of the reaction is a liquid polymer. Smaller amounts of hydrogen and methane are also formed.

The falling off in the rate of consumption of 2-butene with increasing pressure again suggests an activated molecule mechanism.

$$2-C_4H_8+Hg(^3P_1)\rightarrow 2-C_4H_8^*+Hg(^1So), \quad (12)$$

$$2-C_4H_8^*+2-(C_4H_8)\rightarrow 2(2-C_4H_8), \quad (13)$$

$$2-C_4H_8^*\rightarrow C_4H_7+H, \quad (14)$$

$$2-C_4H_8+H\rightarrow C_4H_9, \quad (15)$$

$$C_4H_9+2-C_4H_8\rightarrow C_8H_{17}, \text{ etc.}, \quad (16)$$

$$C_4H_7+2-C_4H_8\rightarrow C_8H_{15}, \text{ etc.} \quad (17)$$

A comparison of Tables VII and VIII shows that the maximum in the polymerization rate curves occurs at an initial pressure of 1–2 mm for 2-butene, and at about 10 mm for 1-butene. Now since the quenching cross sections for the two molecules should not be significantly different, we are lead to conclude that the activated state has a longer life in the case of 2-butene than in 1-butene, i.e., $(1/k_{14})>(1/k_2)$. This assumption would also offer a plausible explanation for the fact that the rate of polymerization of 2-butene is only about one-half that of 1-butene.

The small amounts of hydrogen formed suggest the step

$$H+2-C_4H_8\rightarrow H_2+C_4H_7, \quad (18)$$

which would involve an activated C_4H_9 radical as an intermediate.

The methane is present in significant amounts only at low pressures. The reaction

$$C_4H_9\rightarrow CH_4+C_3H_5 \quad (19)$$

would require that the rate of methane formation fall off even more rapidly with pressure than the rate of hydrogen formation, in agreement with our results.

TABLE VIII. 2-butene.

Po mm	$\frac{-\Delta P}{\Delta t}\times 10^2$ mm/min.	$\frac{-d(2-C_4H_8)}{dt}$ moles/min. $\times 10^8$	$\frac{d(H_2)}{dt}$ moles/min. $\times 10^8$	$\frac{d(CH_4)}{dt}$ moles/min. $\times 10^8$	Quantum yield $\varphi(2-C_4H_8)$
2.02	0.93	0.77	0.041	0.047	0.11
4.63	0.82	0.74	0.047	0.024	0.10
8.32	0.65	0.49	0.038	0.009	0.07
21.52	0.52	0.36	0.027	0.003	0.05
32.36	0.57	0.35	0.025	0.001	0.05
42.14	0.37	0.30	0.022	0.001	0.04
49.02	0.33	0.21	0.022	0.0008	0.03
61.14	0.27	0.28	0.020	0.0007	0.04
70.64	0.37	0.28	0.020	0.0002	0.04

It is interesting to note that the reaction

$$2-C_4H_8^*+2-C_4H_8\rightarrow 1-C_4H_8+2-C_4H_8$$

does not seem to occur, since no 1-butene was found in the products. Thermodynamically, of course, 2-butene is more stable than 1-butene, although their heats of formation differ only by 1-2 kcal.[8]

CONCLUSIONS

It is apparent that, with the striking exception of isobutene, the activated molecule mechanism seems to be common to all the lower olefines and alkadienes.

The collisional isomerization reaction of 1-butene to 2-butene is of considerable interest since it gives us a direct means of determining the extent of collisional deactivation. Virtually every activated molecule formed seems to undergo a deactivating collision above an initial pressure of 150 mm. We are therefore lead to the important conclusion that, with the exception of isobutene, free radicals play an important part in the mercury photo-sensitized reactions of the lower olefines and alkadienes only at relatively low pressures.

ACKNOWLEDGMENT

It is a great pleasure to acknowledge our indebtedness to Dr. A. Keith Brewer and Dr. Fred L. Mohler of the Mass Spectrometry Section of the National Bureau of Standards for their kindness in performing the mass spectrometric analyses reported in this paper.

Our thanks are also due to Mr. Yves Lupien for assistance in making the measurements.

[8] F. D. Rossini, Chem. Rev. **27**, 1 (1940).

Bending Force Constants for Halogenated Ethylenes

KENNETH S. PITZER AND N. K. FREEMAN
Department of Chemistry, University of California, Berkeley

(Received August 8, 1946)

Force constants have been calculated for the out-of-plane bending motions of the vinyl halides and for *cis-* and *trans-* 1,2-dichloroethylene. Published vibrational assignments have been followed for the most part, but several changes were found necessary. A generally consistent set of force constants was obtained in which the values are also similar to those for the methyl halides.

WHILE bending force constants in general have received less attention than stretching force constants, they are important in establishing the assignments of the lower fundamental vibration frequencies. In thermodynamic calculations the lower frequencies take on primary significance. In this investigation, an attempt has been made to evaluate the force constants for the non-planar vibrations in certain halogenated ethylenes, and to find some correlation among them for this series of compounds.

Complete assignments of fundamental vibration frequencies for the vinyl halides have been made by Torkington and Thompson[1,2] on the basis of their own infra-red spectra. These assignments appear to be straightforward and unambiguous except in the case of vinyl fluoride. Here some anomalies occur that are not yet satisfactorily explained. The fluoride, furthermore, is the only one of these substances for which Raman data are lacking. Wu[3] and Herzberg[4] have summarized the data on the dichloroethylenes.

TABLE I. Non-planar frequencies and force constants of vinyl halides.

	C_2H_3F	C_2H_3Cl	C_2H_3Br	C_2H_3I
C−X distance, A	1.36	1.69	1.85	2.03
Frequencies (cm^{-1})				
ω_1	924 (860)	940	940	946
ω_2	860 (732)	895	902	909
ω_3	715 (715)	622	497	435
Assumed force constants				
F_{11} (from ethylene)	0.37	0.39	0.39	0.39
F_{12} ($=F_{21}$) (ethylene)	0.045	0.054	0.054	0.054
F_{13} ($=F_{31}$)	0.00	0.00	0.00	0.00
Calculated force constants				
F_{22}	0.48	0.43	0.36	0.32
F_{23} ($=F_{32}$)	−0.21	−0.10	0.03	0.09
F_{33}	0.90	0.82	0.64	0.60

The calculations were carried out by the method of Wilson[5] for which the following coordinates were chosen:

θ_1 = angle of wag of CH_2 group (angle between extension of C=C bond and HCH plane).
θ_2 = angle of wag of CHX group.
θ_3 = angle of twist of groups at opposite ends of C=C bond.

The elements of the reciprocal kinetic energy matrix then take the following form for the vinyl halides:

$$G_{11}=2\epsilon^2\mu_H+\mu_C(4\epsilon^2+4\epsilon\rho+2\rho^2);$$
$$G_{12}=G_{21}=-\mu_C\rho(3\epsilon+\eta+2\rho);$$
$$G_{13}=G_{31}=0;$$
$$G_{22}=\epsilon^2\mu_H+\eta^2\mu_X+\mu_C(\epsilon^2+\eta^2+2\rho^2+2\epsilon\eta+2\epsilon\rho+2\eta\rho);$$
$$G_{23}=G_{32}=(\epsilon^2\mu_H-\eta^2\mu_X)/\sqrt{3};$$
$$G_{33}=\epsilon^2\mu_H+\tfrac{1}{3}\eta^2\mu_X,$$

where the μ's refer to reciprocal masses, and ϵ, ρ, and η are the reciprocals of the C−H, C=C, and C−X bond distances, respectively. The C−C and C−H bond lengths (1.353 and 1.071A) are taken to be those in ethylene, as determined by Gallaway and Barker.[6] These authors report a bond angle of 119° 55′ for H−C−H in ethylene, whereas electron diffraction measurements on vinyl chloride by Brockway, Pauling, and Beach[7] indicate a C−C−Cl angle of 122±2°.

[1] P. Torkington and H. W. Thompson, J. Chem. Soc. 303 (1944).
[2] P. Torkington and H. W. Thompson, Trans. Faraday Soc. **41**, 236 (1945).
[3] T. Y. Wu, Phys. Rev. **46**, 465 (1934).
[4] G. Herzberg, *Infra-Red and Raman Spectra* (D. Van Nostrand Company, New York, 1945), p. 330.
[5] E. B. Wilson, Jr., J. Chem. Phys. **7**, 1047 (1939) and **9**, 76 (1941). See also A. G. Meister and F. F. Cleveland, Am. J. Phys. **14**, 13 (1946).
[6] W. S. Gallaway and E. F. Barker, J. Chem. Phys. **10**, 88 (1942).
[7] L. O. Brockway, L. Pauling, and J. Y. Beach, J. Am. Chem. Soc. **57**, 2693 (1935).

For simplicity, 120° has been used for all bond angles in these calculations. The experimental value of 1.69A given by Brockway, Pauling, and Beach,[7] for the C−Cl distance is accepted. This represents a shortening of the bond compared with 1.76A in CCl_4, and a corresponding relationship is assumed to exist in the other halides, i.e., the =C−X length is decreased with respect to that of −C−X. This is corroborated in the case of vinyl iodide, in which the C−I length is reported by Huggill, Coop, and Sutton[8] as 2.03A, while in CI_4 it is 2.12A (Finbak and Hassel[9]). The C−X distances are included in Table I.

In these calculations the force constant for CH_2 wagging, F_{11}, and the interaction constant, F_{12}, were assigned the values obtained from ethylene.[10] This proved satisfactory in all cases except vinyl fluoride, where the noticeably lower value of ω_1 (compared with ethylene and the other halides) made it necessary to lower these constants slightly. All constants are expressed in "atomic weight-angstrom" units, which for angle bending constants is (ergs/radian^2)$\times 1.698 \times 10^{+11}$. The frequencies and constants are listed in Table I. In parentheses are given Torkington and Thompson's[2] assignment for vinyl fluoride.

In an attempt to confirm the F_{22} value for C_2H_3Cl, some calculations were made of the out-of-plane force constants in the *cis-* and *trans-* forms of 1,2-dichloroethylene. The appropriate equations are readily derived by the same methods. In spite of some uncertainties in the assignments of these frequencies,[3,4] it is believed that the results obtained provide some measure of verification for the vinyl chloride wagging constant. The choice and classification of the frequencies is given by Table II, which also shows the force constants obtained from them.

These molecules have higher symmetry than the vinyl compounds, so that the non-planar motions may be further subdivided. The B_2 "unsymmetrical" wagging frequency in *cis*-1,2-dichloroethylene, and the B_g "symmetrical" wagging frequency in *trans*-1,2-dichloroethylene are both (by symmetry) free from interaction with the other non-planar vibrations. This leads to a rather simple and direct evaluation of these force constants, which in the case of the *trans-* molecule can also be checked with the deuterated compound. Then if the "symmetrical" wagging constant in *trans-* is accepted for the corresponding motion in *cis-*, and the "unsymmetrical" wagging constant in *cis-* is accepted similarly for *trans-*, the torsional and interaction constants for the A_2 and A_u vibrations may be calculated and a set of values consistent with the most probable frequencies obtained. The greatest uncertainties in the assigned frequencies are in the A_u vibrations of *trans*-1,2-dichloroethylene. While Wu[3] and Herzberg[4] both suggest 620 cm^{-1} for the "unsymmetrical" wagging vibration of this group, it gives too low a force constant. Wood and Stevenson[11] have used 820 cm^{-1} for this frequency in connection with studies of the *cis-trans* isomerization, and the present calculations seem to confirm the latter value. The A_u torsional frequency is too low to be observed. The 620 cm^{-1} band, left unassigned by the choice of 820 cm^{-1} for the A_u wagging fundamental, may now be assumed to be a combination of two low frequencies. One of these must be the 350 cm^{-1} C−Cl planar bending, leaving a difference of 270 cm^{-1}. This is taken as the twisting fundamental.

The symmetrical and unsymmetrical wagging constants for the dichloroethylenes should be approximately $F_{22}-F_{12}$ and $F_{22}+F_{12}$, respectively, from vinyl chloride. While the agreement with these combinations from vinyl chloride is

TABLE II. 1,2-dichloroethylenes.

Vibration	Frequency (cm^{-1})	Force constant
cis-		
B_2 (unsym. wagging)	694	0.45
A_2 (sym. wagging)	876	0.36*
A_2 (torsion)	406	0.78
(A_2 interaction constant)		−0.08
trans-		
B_g (sym. wagging)	765	0.36
A_u (unsym. wagging)	820	0.45†
A_u (torsion)	270	0.87
(A_u interaction constant)		−0.17
deutero-trans-		
B_g (sym. wagging)	657	0.36

* Assumed from B_g (sym.) in *trans-*.
† Assumed from B_2 (unsym.) in *cis-*.

[8] J. A. C. Huggill, I. E. Coop, and L. E. Sutton, Trans. Faraday Soc. **34**, 1518 (1938).
[9] C. Finbak and O. Hassel, Zeits. f. physik. Chemie **36B**, 301 (1937).
[10] J. E. Kilpatrick and K. S. Pitzer, to be published.
[11] R. E. Wood and D. P. Stevenson, J. Am. Chem. Soc. **63**, 1650 (1941).

not very close, it is about what one might expect. Likewise, the torsion constants of the *cis*- and *trans*-molecules differ somewhat. However, the pattern of constants shows such general consistency as to lend considerable support to their validity.

To examine the trend of the force constants in passing through the series of vinyl halides, it is informative to see whether or not a similar trend exists in some comparable series. The methyl halides afford such a comparison, and the force constants for bending of the H−C−X angles in these molecules are given by Crawford and Brinkley.[12] Their values, expressed in terms of our units are as follows:

	CH_3F	CH_3Cl	CH_7Br	CH_3I
k	0.41	0.31	0.28	0.24

The relative values of k may be properly compared with those of F_{22} in the vinyl compounds (see Table I). In both series, it is observed that progression from the fluoride to successively heavier halides leads to successively lower force constants.

We are aware that our assignment for vinyl fluoride will make it difficult to explain the published spectrum completely; however, any other assignment gives unreasonable force constants. Further investigation is needed here.

[12] B. L. Crawford, Jr. and S. R. Brinkley, Jr., J. Chem. Phys. 9, 69 (1941).

THE JOURNAL OF CHEMICAL PHYSICS VOLUME 14, NUMBER 10 OCTOBER, 1946

The Differential Entropy of Dilution in Aqueous Solutions of Amino Acids

A. L. ROBINSON
Department of Chemistry, University of Pittsburgh, Pittsburgh, Pennsylvania
(Received July 22, 1946)

The relative partial molal entropy of water, $\bar{S}_1-\bar{S}_1^0$, in aqueous solutions of seven amino acids is calculated from existing data. For all solutions, $\bar{S}_1-\bar{S}_1^0=km^2$ approximately; k is positive for glycine solutions and negative for solutions of the two alanines and four aminobutyric acids. The $\bar{S}_1-\bar{S}_1^0$ values are determined largely by the size and structure of the hydrocarbon part of the amino acid and only to a minor degree by its dipole moment. Positive $\bar{S}_1-\bar{S}_1^0$ values are interpreted as indicating a structure breaking effect of glycine on water; negative $\bar{S}_1-\bar{S}_1^0$ values indicate a structure strengthening effect which increases with size of the hydrocarbon residue. The data are consistent with the recent discussion of Frank. Heat capacity and viscosity values for some of these solutions qualitatively show expected behavior.

STUDIES of the heats of dilution of aqueous solutions of amino acids[1–3] have shown that the dipole moment is not the main factor determining the thermodynamic properties of these solutions. The quantity ΦL_2 (apparent relative molal heat content) is negative for glycine, has positive values for α-alanine and shows a further increment for α-amino-*n*-butyric acid, although the dielectric increments for these three substances are approximately equal;[4] in contrast, α-amino-*n*-butyric and γ-aminobutyric acids show nearly identical ΦL_2 values up to 1.2 *m* although the dielectric increment of the γ-acid is more than twice as large as that of the α-acid. The hydrocarbon residue is evidently an important factor. Its influence may be exerted through hydrocarbon-hydrocarbon, hydrocarbon-dipole, and hydrocarbon-solvent interactions.

An examination of the differential entropies of dilution $(\bar{S}_1-\bar{S}_1^0)$ of aqueous electrolyte solutions[5] permitted an attempt to correlate the sizes, shapes, and hydrogen bonding powers of ions with changes in the structure of water in

[1] W. E. Wallace, W. F. Offutt, and A. L. Robinson, J. Am. Chem. Soc. **65**, 347 (1943).
[2] Data for α- and β-alanine, L. S. Mason, H. Benesi, and A. L. Robinson, J. Am. Chem. Soc., to be published.
[3] Data for four aminobutyric acids, L. S. Mason and A. L. Robinson, J. Am. Chem. Soc., submitted for publication.
[4] E. J. Cohn and J. T. Edsall, *Proteins, Amino Acids, and Peptides* (Reinhold Publishing Corporation, New York, 1943), p. 146.
[5] H. S. Frank and A. L. Robinson, J. Chem. Phys. **8**, 933 (1940). A recent paper by G. W. Stewart, J. Chem. Phys. **11**, 72 (1943) is a particular interest in this connection.

TABLE I. Differential entropy of dilution ($\bar{S}_1-\bar{S}_1^0$), in calorie-degree^{-1}-mole^{-1}, in aqueous solutions at 25°.

amino acid \ m	0.2	0.4	0.6	0.8	1.0	1.2
glycine	0.0_312	0.0_338	0.0_382	0.0015	0.0023	
α-alanine	-0.0_488	-0.0_335	-0.0_379	−0.0014	−0.0022	−0.0032
β-alanine	-0.0_311	-0.0_336	-0.0_366	−0.0013	−0.0020	−0.0026
α-amino-*n*-butyric	-0.0_323	-0.0_391	−0.0021	−0.0037	−0.0058	−0.0084
α-amino-*i*-butyric	-0.0_330	−0.0012	−0.0027	−0.0048	−0.0076	−0.0107
β-amino-*n*-butyric	-0.0_325	-0.0_395	−0.0021	−0.0037	−0.0056	−0.0080
γ-aminobutyric	-0.0_335	−0.0013	−0.0029	−0.0050	−0.0076	−0.0107

the solutions. Recently Frank[6] has discussed entropies of vaporization of solutes from solutions and has interpreted the data to indicate that frozen patches or microscopic icebergs form around non-polar solutes and the non-polar parts of polar solute molecules in aqueous solutions. Data are now available for calculating $\bar{S}_1-\bar{S}_1^0$ values for aqueous solutions of seven amino acids. These values lead to some possible conclusions regarding the effect of the hydrocarbon residues on the structure of the solvent, which are consistent with the interpretations of Frank.

The $\bar{S}_1-\bar{S}_1^0$ values of Table I were calculated from

$$\bar{S}_1-\bar{S}_1^0=(\bar{L}_1-RT\ln(a_1/N_1))/T. \quad (1)$$

$\bar{L}_1$ is the relative partial molal heat content of the water ($\bar{H}_1-\bar{H}_1^0$) and a_1 is its activity, referred to pure water as the standard state. N_1, the mole fraction of water in the solution, takes account of the entropy of mixing; the values of Table I give the non-ideal part of the differential entropy of dilution. For consistent comparison all activity values were derived from the vapor pressure measurements of Smith and Smith.[7–9] For the same reason, all $\bar{L}_1$ values were derived from heat of dilution measurements made in this laboratory. Figure 1 shows the plots of the values of Table I against the molality.

There is no satisfactory theory to explain the thermodynamic behavior of these dipolar ions in aqueous solution.[10–13] Purely electrostatic interactions, calculated for various simplified models, do not suffice. From a consideration of activity data Cohn[4] has concluded that the nature and number of polar and non-polar groups, and their positions in the molecule, must be considered in order to obtain a better explanation of the facts.

$\bar{S}_1-\bar{S}_1^0$ is the entropy change for the transfer of a mole of water from an infinitely dilute solution to a solution of finite concentration. Since entropy is related to structural order, the $\bar{S}_1-\bar{S}_1^0$ values should reflect the effect of the dipolar ions on the quasi-solid structure of water, positive values indicating structure weakening and negative values pointing to structure strengthening effects. For the seven amino acids studied the relation $\bar{S}_1-\bar{S}_1^0=km^2$ holds fairly well, but only for glycine does the constant have a positive value.* The net effect of glycine is thus similar to that of sodium and potassium halides and nitrates at 1 m while the behavior of the other six amino acids parallels the effect of ions such as H_3O^+, OH^-, NH_4^+, Li^+, and F^-, whose structure strengthening effect has been attributed to their small size or their hydrogen bridging capacity.[5]

The structure strengthening effect of the amino acids obviously cannot be attributed to these same factors. The order shown by glycine, α-alanine, and α-amino-*n*-butyric acid, and also by β-alanine and β-amino-*n*-butyric acid, is the reverse of the order expected from constant dipole moment and increasing size. Another factor, the non-polar hydrocarbon groups, seems to play the dominant role, giving rise to a structure strengthening interaction with the water. The values of Table I are derived from accurate data and the differences shown by the

[6] H. S. Frank, J. Chem. Phys. **13**, 507 (1945).
[7] E. R. B. Smith and P. K. Smith, J. Biol. Chem. **117**, 209 (1937).
[8] E. R. B. Smith and P. K. Smith, J. Biol. Chem. **121**, 607 (1937).
[9] E. R. B. Smith and P. K. Smith, J. Biol. Chem. **132**, 47 (1940).
[10] G. Scatchard and J. G. Kirkwood, Physik. Zeits. **33**, 297 (1932).
[11] J. G. Kirkwood, Chem. Rev. **19**, 275 (1936).
[12] R. M. Fuoss, J. Am. Chem. Soc. **56**, 1027 (1934).
[13] R. M. Fuoss, J. Am. Chem. Soc. **58**, 982 (1936).

* The dependence on m^2 is a reflection of the relative importance of the term in $\bar{L}_1$ in Eq. (1). There is some uncertain evidence that $\bar{L}_1$ for glycine[1] may also become negative at very small concentrations.

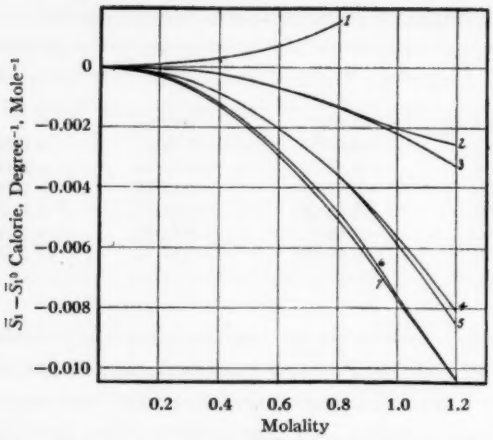

FIG. 1. Relative partial molal entropy of water, $\bar{S}_1-\bar{S}_1^0$, in aqueous amino acid solutions: 1, glycine; 2, β-alanine; 3, α-alanine; 4, β-*N*-butyric acid; 5, α-*N*-butyric acid; 6, α-iso-butyric acid; 7, γ-butyric acid.

members of an isomeric group are undoubtedly real, but it is interesting that $\Delta\bar{S}_1$ at 1 *m* is -0.0044 in going from glycine to the alanines (average) and almost the same, -0.0046, in passing from the alanines to the aminobutyric acids (average). Small differences are noted between α- and β-*n*-acids; hydrocarbon branching and the γ position for the NH_3^+ group give the most negative values of $\bar{S}_1-\bar{S}_1^0$, but further study will be required to clarify these effects.

The structure strengthening effect on water shown by the non-polar parts of these dipolar ions is consistent with the recent discussion by Frank[6] of the abnormally high entropies of vaporization of rare gases and hydrocarbon gases from water. Frank suggests that when a rare gas atom or a non-polar molecule or a polar molecule with non-polar parts dissolves in water at room temperature it modifies the water structure in the direction of greater "crystallinity." This effect increases with the size of the solute molecule. Our own study leads to similar conclusions and simply suggests that this "freezing" of the water (Frank's calculations are for infinite dilution) increases with concentration in the range of this study. For glycine the structure breaking interaction, always present, is not compensated by the "iceberg" effect because of the small non-polar part.

The high apparent heat capacities of amino acids and fatty acids and alcohols in aqueous solutions have attracted comment.[14] In a homologous series of liquids the increment in C_p per CH_2 group is only 6 to 8 cal./mole while in aqueous solution the increment in $\Phi(C_p)$ is 20 to 30 cal./mole. Similar behavior is shown by aqueous solutions of the rare gases, the effect also increasing with the size of the rare gas atom. The explanation for these large heat capacities given by Frank[6] should apply equally well to solutions of the amino acids. With increase of temperature the melting of the quasi-crystalline patches of water, which the entropy values indicate increase in size with increasing size of the hydrocarbon residue, will add an increasingly positive term to the heat capacities.

We may also call attention to the viscosities of aqueous solutions of glycine and α-alanine.[15] Previous discussions of the effect of solutes[16, 6] on the structure of water have pointed to the relation between the viscosities of solutions and the structure weakening or strengthening influence of the solute. At 18° the relative viscosities of 1 *m* solutions of glycine and α-alanine are 1.153 and 1.310, respectively. Qualitatively such a difference would be expected in terms of the present discussion. More extensive data, both for entropies of dilution and viscosities, would be of interest for a further discussion of the effects of amino acids on the structure of water.

[14] J. T. Edsall, J. Am. Chem. Soc. **57**, 1506 (1935). See also reference 4, p. 168.

[15] G. Hedestrand, Zeits. f. anorg. Chemie **124**, 153 (1922).

[16] J. D. Bernal and R. H. Fowler, J. Chem. Phys. **1**, 515 (1933).

THE JOURNAL OF CHEMICAL PHYSICS VOLUME 14, NUMBER 10 OCTOBER, 1946

Notes on the Rate Process Theory of Flow*

A. BONDI
International Lubricant Corporation, New Orleans, Louisiana

(Received March 11, 1946)

This paper deals with the separation of the contributing terms of the energy and entropy of activation for viscous flow and the identification of some of the molecular constants entering into these terms, as a step toward the prediction of the viscosity of liquids from first principles. The energy of activation for hole formation $\Delta H_{\ddagger}^{h}$ is found to be determined mainly by the magnitude of the dispersion energy and by the extent of displacement of the hole forming molecules from their equilibrium position. The latter, in the form of the viscosity-pressure coefficient $\Delta V_{\ddagger}$, is, at present, not predictable from any molecular constant. The energy of activation for motion into the hole $\Delta H_{\ddagger}^{j}$ was found for many substances to be numerically equal to the excess energy of vaporization $\Delta E_{\text{vap}}^{j}$ and is thus an additional measure of restricted external rotation. The cases in which $\Delta H_{\ddagger}^{j} > \Delta E_{\text{vap}}^{j}$ offer strong evidence for the requirement of deformation of the flowing molecule against internal potential energy barriers. The rotational, translational, and cooperative terms which contribute to the entropy of activation have been separated, but can so far be determined only from viscosity data. Numerical examples show that the stereometric arrangement of molecular structure determines the magnitude of $\Delta V_{\ddagger}$ and $\Delta H_{\ddagger}^{j}$ and thereby the viscosity of liquids to a far greater extent than chemical composition (except for OH groups). The existence of aliphatic fatty acids as double molecules in the liquid state over a wide range of temperatures is confirmed viscosimetrically, while the viscosity data of aliphatic alcohols suggest the presence of distinguishable multiple molecules only at very low temperatures but the existence of a continuous OH-bond network structure at ordinary temperatures. One of the important consequences of the rate process theory of flow is the recognition that the viscosity of a liquid is determined by the (very small) concentration of molecules in relatively shallow potential energy walls from which the activated molecules are preferentially recruited. Viscosity is therefore not a bulk property in the commonly accepted sense and depends only to a minor extent on the structure of a liquid, i.e., on its state of order.

THE object of this investigation was to separate the terms contributing to the energy and entropy of activation for viscous flow occurring in Eyring's[1] equation

$$\eta = \frac{\lambda_1 h}{\lambda_2 \lambda_3 \lambda^2} \exp(-\Delta S_{\ddagger}/R) \exp(\Delta H_{\ddagger}/RT) \sim \frac{Nh}{V} \exp(-\Delta S_{\ddagger}/R) \exp(\Delta H_{\ddagger}/RT)$$

(where $\lambda_{1,2,3}$ = intermolecular distances in the three space coordinates, λ = length of path over potential energy barrier, h = Planck constant, V = molar volume (used where $\lambda = \lambda_1$), $\Delta S_{\ddagger}$ = entropy of activation, and $\Delta H_{\ddagger}$ = heat of activation), in order to facilitate the prediction of the absolute value of the viscosity of liquids from first principles.

1. THE HEAT OF ACTIVATION $\Delta H_{\ddagger}$

$\Delta H_{\ddagger}$ is also defined by

$$\Delta H_{\ddagger} = R\left(\frac{\partial \ln (V\eta)}{\partial 1/T}\right)_P. \quad (1)$$

It has been suggested by Eyring[1] and his co-workers that $\Delta H_{\ddagger}$ consists of two elements: the energy required to form a hole in the liquid structure and the energy required to move into this hole. The latter is

$$\Delta H_{\ddagger}^{j} = R\left(\frac{\partial \ln \eta}{\partial 1/T}\right)_V, \quad (2)$$

so that the energy of hole formation is

$$\Delta H_{\ddagger}^{h} = \Delta H_{\ddagger} - \Delta H_{\ddagger}^{j} \equiv R\left\{\left(\frac{\partial \ln (V\eta)}{\partial 1/T}\right)_P - \left(\frac{\partial \ln \eta}{\partial 1/T}\right)_V\right\}. \quad (3)$$

So far no inquiry has been made into the nature of either $\Delta H_{\ddagger}^{h}$ or $\Delta H_{\ddagger}^{j}$. It is here proposed to derive the two parameters as follows: From the model underlying the rate process theory of flow we can deduce that $\Delta H_{\ddagger}^{h}$ is the change in potential energy between neighboring molecules accompanying the displacement from their equilibrium position when forming a new hole. The displacement can be computed from the pressure coefficient of viscosity, as

$$\left(\frac{\partial \Delta F_{\ddagger}}{\partial p}\right)_T = \Delta V_{\ddagger}, \quad (4)$$

* Presented in part at the annual meeting of the Society of Rheology, New York, October 26, 1945.

[1] Glasstone, Laidler, and Eyring, *Theory of Rate Processes* (McGraw-Hill Book Company, New York, 1941). R. E. Powell, Ph.D. Thesis, Princeton (1943).

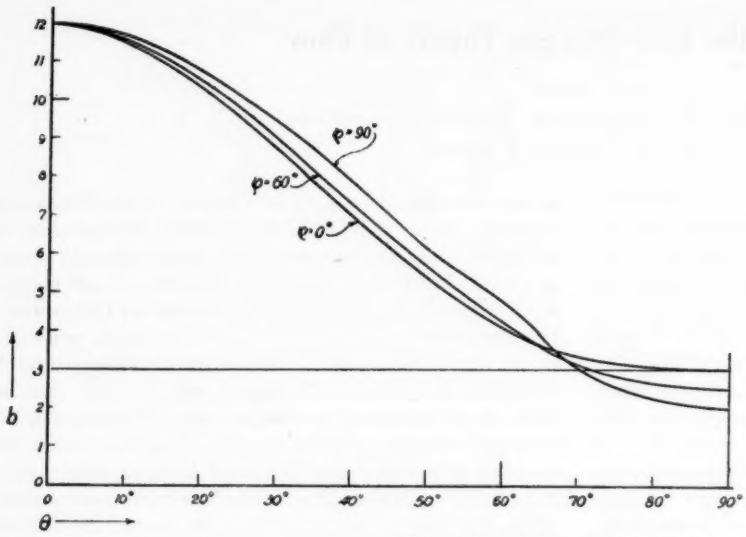

$b=6+2.0(3\cos^2\theta-1)+\{[(\sin\theta)^2\cos\varphi-2(\cos\theta)^2]^2-2\cos^2\theta\}$

for various values of θ and φ.

$$-E^{11}=\frac{b}{4}\frac{I_0\alpha^2}{r^6};\quad \text{for}\quad \alpha_{11}-\frac{\alpha_1}{a}=1.$$

FIG. 1. London's orientation function.

where $\Delta F_{\ddagger}$ = free energy of activation for viscous flow and $\Delta V_{\ddagger}$ = local volume change (increase) accompanying the process of activation. The linear displacement of the molecules forming a hole is, therefore, to a good approximation $(1/N^{\frac{1}{3}})[(V+\Delta V_{\ddagger})^{\frac{1}{3}}-V^{\frac{1}{3}}]$. Using Lennard-Jones'[2] equation for the potential energy between a central molecule and its nearest neighbors we obtain for $\Delta H_{\ddagger}^{h}$ the expression

$$\Delta H_{\ddagger}^{h}=\Lambda^*\left\{1.2\left[\left(\frac{V^*}{V}\right)^2-\left(\frac{V^*}{V_{\ddagger}}\right)^2\right]-0.5\left[\left(\frac{V^*}{V}\right)^4-\left(\frac{V^*}{V}\right)^4\right]\right\},\quad (5)$$

where $\Lambda^*=Z\epsilon^*$, the minimum value of the interaction energy ϵ at the equilibrium distance r^*, Z = number of nearest neighbors, $V^*=r^{*3}/\sqrt{2}$, $V_{\ddagger}=V+\Delta V_{\ddagger}$, $\Lambda^*\sim 1.2\Delta E_{\text{vap}}$ in many cases. Inasmuch as (5) is based *on London's* inverse sixth power law for molecular interaction[3] one can readily show that the magnitude of ϵ is determined by the factor $\frac{3}{4}I_0\alpha^2$ in the case of non-polar compounds and contains the additional term $(2/3)(\mu^4/kT)$ in the case of dipolemolecules, where I_0 = first ionization potential (also derivable from ultraviolet spectra[4]) and α = polarizability. One could argue that Eq. (5) is valid only for spherical molecules or at least only for those of spherical fields of force and that a more complicated expression is required to describe the potential energy field of linear polyatomic molecules. London's recent equation for the dispersion energy in systems composed of linear molecules[5] takes into consideration the difference in polarizability vertical to and in line with the bond axes. The potential energy between neighboring molecules becomes thus a function of their angle of approach. Figure 1 is a plot of the value of the numerical coefficient before $I_0\alpha^2$ as a function of the angles of approach. It is seen that the potential energy is at a minimum for parallel orientation of the bond axes, in agreement with the known x-ray diffraction patterns of *n*-paraffins and their derivatives. In calculating the potential energy along these curves, it becomes apparent that the difference in potential energy between the top and the bottom is of such magnitude that there should still be a finite concentration of molecules which are randomly oriented with respect to each other. This difference is often of the same order of magnitude as $\Delta F_{\ddagger}$. As $\Delta F_{\ddagger}$ is defined by

$$\Delta F_{\ddagger}=RT\ln\left(\frac{V\eta}{Nh}\right)=-RT\ln\frac{c_{\ddagger}}{c},\qquad (6)$$

[2] Lennard-Jones and Devonshire, Proc. Roy. Soc. **A163**, 53 (1937); **A165**, 1 (1930).
[3] F. London, Trans. Faraday Soc. **33**, 8 (1937).
[4] W. C. Price, *et al.* Nature **148**, 372 (1942); Proc. Roy. Soc. **A174**, 207 (1940).
[5] F. London, *Surface Chemistry* II (AAAS, 1943), p. 141.

where $c_\ddagger$ and c are the concentration of the activated and normal molecules, respectively, it appears reasonable to deduce that the activated molecules are (preferentially) recruited from the randomly oriented molecules whose numerical factor in front of $I_0\alpha^2$ is so nearly equal to $\frac{3}{4}$ that the use of the simple Eq. (5) is fully justified for molecules of any shape, provided

$$\langle E_{\max}'' \rangle - \langle E_{\min}'' \rangle \lesssim \Delta F_\ddagger .$$

The close agreement of the values of $\Delta H_\ddagger^h$ calculated by Eqs. (5) and (3) indicates the validity of the assumptions made in the derivation of (5).

If we remember that the energy of vaporization is the energy required to make a hole of molecular size, we should expect the ratio $\Delta H_\ddagger^h/\Delta E_{vap}$ to be of the order of (or equal to) $\Delta V_\ddagger/V$. The data on Table I show this indeed to be the case, what *cannot* be said of the ratio $\Delta H_\ddagger/\Delta E_{vap}$ as has been proposed by Eirich and Simha[6] and accepted by Eyring* and many subsequent workers. A number of cyclic-hydrocarbons and similarly constituted liquids show $\Delta H_\ddagger/\Delta E_{vap}$ values larger than 1,[7] but their $\Delta V_\ddagger/V$ and $\Delta H^h/\Delta E_{vap}$ values are of the usual order of magnitude, i.e., around 0.2.

As I_0, α, and V^* (and ΔH_V) can be determined independently of viscosity, $\Delta H_\ddagger^h$ of any liquid could be predicted if $\Delta V_\ddagger$ were also derived from first principles; this has, however, not yet been accomplished. But it is conceivable that one could achieve this aim on the basis of Alfrey's model of the flow process.[8] The peculiar temperature dependence of $\Delta H_\ddagger^h$ (it goes through a maximum as does $\Delta V_\ddagger$) is not immediately derivable from either Eqs. (5) or (7) and may well be connected with the anisotropic thermal expansion of the unit cells of a liquid, as observed by x-ray diffraction.[9] Some specific cases of relationships between structure changes of a liquid and $\Delta H_\ddagger$ will be discussed later on.**

The other component of $\Delta H_\ddagger$, the energy of motion $\Delta H_\ddagger^j$ has a number of interesting properties which point toward an understanding of its nature, and which have so far been entirely overlooked: (a) the strong temperature dependence and (b) the close relation between $\Delta H_\ddagger^j$ and the "non-ideal" portion of ΔE_{vap}.

The first named of these properties is peculiar to heats of activation connected with the activation of internal degrees of freedom.[10] The number $S/2$ of degrees of freedom activated is to (a not very good)† approximation

$$-\left(\frac{\partial \Delta H_\ddagger^j}{\partial T}\right)_p = R\left(\frac{S}{2}-1\right), \tag{8}$$

and the average characteristic frequency $\nu_\ddagger$ of these degrees of freedom could be given by

$$\Delta H_\ddagger^j = \frac{S}{2} N h \nu_\ddagger . \tag{9}$$

The values of $S/2$ and $\nu_\ddagger$ thus calculated are assembled in Table II. One sees that $S/2$ increases quite regularly with molecular weight, as would be expected, and that $\nu_\ddagger$ is of the order of Raman shifts and infra-red bands ascribed to external and internal rotation.[11] The motion of larger molecules past each other seems to require the activation of normally (at that temperature)

TABLE I. The heat of activation for hole formation $\Delta H_\ddagger^h$ (in kcal./mole) calculated by Eqs. (3) and (5), and its relation to the energy of vaporization.

	$\Delta H_\ddagger^h$ from equation			$\frac{\Delta V_\ddagger}{V}$	$\frac{\Delta H_\ddagger^h}{\Delta E_V{}^0}$ *	$\frac{\Delta H_\ddagger^h}{\Delta E_V}$	$\frac{\Delta H_\ddagger}{\Delta E_V}$
	t°C	(3)	(5)				
CCl_4	0/30	1.700	1.06	0.188	0.244	0.237	0.34
n-hexane	0/30	0.715	0.61	0.136	0.105	0.100	0.21
n-octane	0/30	0.860	0.66	0.100	0.101	0.090	0.20
n-decane	0/30	0.900	0.80	0.099	0.097	0.090	0.25
Toluene	0/30	1.352	1.00	0.135	0.165	0.155	0.23
n-propanol	0/30	0.970	1.60	0.209	0.130	0.090	0.38
n-pentanol	0/30	1.440	1.60	0.192	0.168	0.115	0.46
Oleic acid	0/30	2.99	2.80	0.106	——	0.125	0.24

* $\Delta E_V{}^0 = \Delta E_V - \Delta E_V{}^j$.

[6] Eirich and Simha, J. Chem. Phys. **7**, 116 (1939).

* Eyring's other relation $\Delta E_{vap}/\Delta F_\ddagger = 2.45$ was purely fortuitious as it was observed in the course of this work that $\Delta F_\ddagger$ passes often through a minimum and rises then constantly until T_{crit}; $\Delta E_{vap}/\Delta F_\ddagger$ taking on values ranging from 4 to 0.

[7] A. Bondi, ACS-Meeting in print, 1945, Petroleum Division, p. 315.

[8] T. Alfrey, Rheol. Bull. **16**, No. 1 (1945).

[9] E. W. Skinner, Phys. Rev. **36**, 1625 (1930).

** The anomalous increase of $\Delta H_\ddagger$ with temperature which has so far mostly been observed for low boiling liquids (see $h - c_5$ on Fig. 5a, and the lower alcohols on Fig. 7) may also be connected with the fact that the concentration $c_\ddagger$ of activated molecules starts in all of these cases to rise above about 1 percent in the same temperature range. Mutual interference of the activated zones may, therefore, be responsible for these peculiarities.

[10] D. D. Eley, Trans. Faraday Soc. **39**, 168 (1943) and private communications.

† See discussion between R. M. Barrer and D. D. Eley in Trans. Faraday Soc. **39** (1943).

[11] G. Herzberg, *Molecular Spectra* II (D. Van Nostrand Company, New York, 1945), p. 496 *seq.*

TABLE II. The internal energy contribution $\Delta H_{\ddagger}^{i}$ to the energy of activation for viscous flow.

	$\Delta H_{\ddagger}^{i}$ kcal./m	at °C	$\Delta H_{\ddagger}^{i}$ kcal./m	at °C	ΔE_V^{i} kcal./m	$S/2$	$\tilde{\nu}$ cm^{-1}
Neo-pentane	0.690	30/50	0.0	50/100	0.000	10.0	12
n-hexane	0.805	0/30	0.570	40/75	0.450	3.8	63
n-octane	1.060	0/30	0.670	40/75	1.040	5.6	54
n-decane	1.610	0/30	1.250	40/75	0.740	5.2	96
Benzene	0.462	0/30	0.0	50/75	0.355	5.3	30
O-xylene	0.695	0/30	0.115	60/75	—	6.5	23
Methyl alcohol	1.810	0/30	1.650	40/75	2.030	2.9	212
Ethyl alcohol	2.430	0/30	—		2.340	—	—
n-propyl alcohol	3.200	0/30	2.850	40/75	3.320	5.1	207
n-amyl alcohol	3.910	0/30	3.550	40/75	3.670	5.2	251
Acetone	0.570	0/30	0.400	40/75	0.730	2.0	85
Carbon tetrachloride	0.660	0/30	0.433	40/75	0.195	3.7	52
Ethyl iodide	0.780	0/30	0.635	40/75	0.870	2.7	92

TABLE IIA. Values of $\Delta H_{\ddagger}$, $\Delta H_{\ddagger}^{i}$, $\Delta H_{\ddagger}^{h}$ and $\Delta V_{\ddagger}/V$ of several petroleum-fraction (lubricating oils).

Oil	t °C	$\Delta H_{\ddagger}$ kcal.	$\Delta H_{\ddagger}^{i}$ kcal.	$S/2$	$\tilde{\nu}$ cm^{-1}	n	$\Delta H_{\ddagger}^{h}$ kcal.	$\frac{\Delta H_{\ddagger}^{h}}{\Delta E_V}$	$\frac{\Delta V_{\ddagger}}{V}$
A-285	38/54	8.0	4.0	26	43	21	4.0	0.180	0.181
	54/99	6.30	2.43				3.87	0.180	0.120
A-409	38/54	14.80	7.11	31	68	30	7.69	0.235	0.163
	54/99	11.30	5.22				6.08	0.190	0.145
N-364	38/54	7.90	3.93	18	64	26	3.97	0.145	0.160
	54/99	6.77	2.87				3.90	0.146	0.100
N-393	38/54	10.50	5.48	32	49	29	5.02	0.167	0.167
	54/99	7.80	3.54				5.21	0.185	0.109
N-435	38/54	11.63	5.82	24	78	32	5.81	0.177	0.169
	54/99	9.44	4.43				5.01	0.160	0.126
N-666	38/54	12.80	7.63	42	53	48	5.17	0.125	0.087
	54/99	10.30	5.18				5.14	0.130	0.079

Waterman analyses of oils used:	A-285	A-409	N-364	N-393	N-435	N-666
Rings per molecule	2.18	3.45	2.48	2.75	3.13	3.40
C-atoms in paraffin side chains	11	15	15	17	19	34

Notes: n = average number of C-atoms per molecule (note the fairly good proportionality between n and $S/2$). ΔE_V was estimated from the heat of evaporation data of "similar" pure hydrocarbons and corrected to the temperature of viscosity measurement using ΔC_p(liq-gas) = 0.2 C_p liq. which has been found a rather good approximation, for hydrocarbons of this molecular weight range.
The constants of this table have been computed from viscosity data by R. B. Dow, J. S. McCartney, and C. E. Fink, J. Inst. Petr. **27**, No. 213, 301 (1941).

still unexcited external rotation and sometimes even internal rotation, i.e., actual deformation of the molecule. There seems to be a way to differentiate between the two, and this involves the second of the properties of $\Delta H_{\ddagger}^{i}$ mentioned above, the relationship to the non-ideal portion of the energy of vaporization. According to Hildebrand[12] the ideal entropy of vaporization at a vapor concentration of 0.0202 mole/1 is 20.2 e.u. The excess entropy of vaporization ΔS_V^{i} leads to the non-ideal portion of the energy of vaporization ΔE_V^{i} by

$$\Delta E_V^{i} = T(\Delta S_{\text{vap}} - 20.2) = T\Delta S_V^{i}. \qquad (10)$$

Table II contains a number of ΔE_V^{i} values, compared—where the Hildebrand-temperature falls within the range of the viscosity measurements—with $\Delta H_{\ddagger}^{i}$. The close similarity between $\Delta H_{\ddagger}^{i}$ and ΔE_V^{i} is quite striking. Some of the inconsistencies in the homologous series are probably caused by inaccurate viscosity and/or vapor pressure data.

[12] J. H. Hildebrand, J. Chem. Phys. **7**, 233 (1939).

If we accept the suggestion by Halford[13] that ΔS_V^j is closely related to the length of free swing required for rotational motion in a liquid, we may say that whenever $\Delta H_\ddagger^j \leqslant \Delta E_V^j$ the activated rotation is a normally unexcited or restricted external rotation.* When $\Delta H_\ddagger^j > \Delta E_V^j$ as in the case of neo-pentane and other more complex hydrocarbons, we must assume $\Delta H_\ddagger^j$ to be caused by the activation of internal rotations, i.e., of the individual motion of molecule segments past (internal) potential energy barriers. As restricted internal rotation would hardly be affected by change from the liquid to the gaseous state, it would not contribute to ΔS_{vap}.

In either case $\Delta H_\ddagger^j$ arises from insufficiency of the available free volume for the molecule to execute free rotational motions. Considering that $\Delta H_\ddagger^j$ decreases to zero for non-polar substances at elevated temperatures, it appears reasonable to introduce the postulate that the molecules of a liquid will encounter no obstacles to free motion whever the effective free volume expanded to a certain fraction, V_f^0/V, of the molecular volume. It is here proposed to write, therefore

$$\Delta H_\ddagger^j = E_r\left\{1-\left(\frac{\delta_3 V_f}{V_f^0}\right)^{\frac{1}{3}}\right\}, \qquad (11)$$

where E_r = energy of the restricted rotator, δ_3 = free angle ratio, V_f = free volume. Discussion of this equation is beyond the scope of this paper and will appear at a later date, suffice it to say that no unreasonable assumptions are required to give a good fit of the experimental data.

To sum up: $\Delta H_\ddagger^j$ is more complicated to derive from first principles than $\Delta H_\ddagger^h$, and can in many (but not all) cases be predicted—for one temperature—from the excess entropy of vaporization. [Its temperature coefficient can in the case

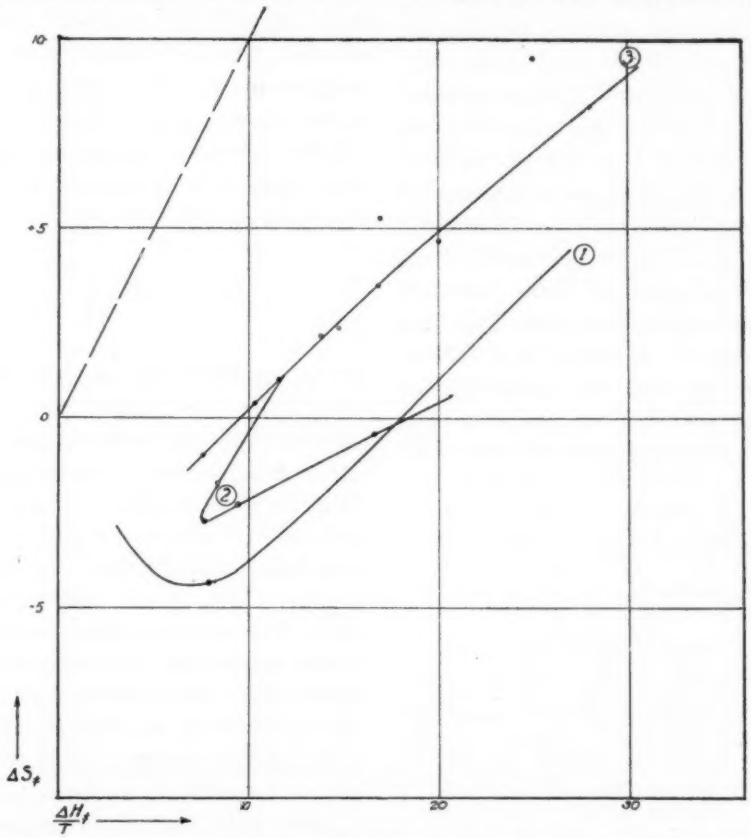

FIG. 2. Relation between $\Delta S_\ddagger$ and $\Delta H_l/T$ at $T = 303°K$ for aliphatic hydrocarbons ①, alcohols ③, and acids ②. Slope of broken line = 1.0.

[13] R. S. Halford, J. Chem. Phys. **8**, 496 (1940).

* In this case Eq. (8) would either have to be thought of as applying to more than one molecule, or to be abandoned entirely.

of hydrocarbons be very approximately computed from the number of C-atoms per molecule.] Where strong dipole forces are active $\Delta H_{\ddagger}^{i}$ changes but little with temperature.

2. THE ENTROPY OF ACTIVATION

In most previous investigations little attention has been paid to the entropy of activation for viscous flow $\Delta S_{\ddagger}$, since its numerical value deviates but little from zero for most of the "common" liquids. The more viscous materials which have been examined in the course of this study show, however, $\Delta S_{\ddagger}$ values of between -10 and $+100$ e.u. which cannot possibly be ignored. One can observe fluids of high $\Delta H_{\ddagger}$ to show also large $\Delta S_{\ddagger}$ values. There is, indeed, within any one group of compounds a degree of proportionality between $\Delta S_{\ddagger}$ and $\Delta H_{\ddagger}$ (Fig. 2) which reminds one of the Barclay-Butler rule[14] connecting the heat and entropy of vaporization. Frank suggested[15] that the Barclay-Butler rule has the following meaning: "When a vapor condenses, a molecule, so to speak, falls into a potential well, i.e., the greater the loss of energy on condensation, the narrower it is and the smaller the free volume, therefore the greater the loss of entropy. In addition, the deeper and narrower the well, the greater the interference tends to be, not only with moving back and forth, but also with squirming into different positions. This also means loss of entropy." Applying this to the process of activation for flow, we should expect the same partition function changes to contribute to $\Delta S_{\ddagger}$ which contributed to $\Delta H_{\ddagger}$. The greater group specificity of the $\Delta S_{\ddagger}$ *vs.* $\Delta H_{\ddagger}$ relationship points to the existence of a factor, which is specific for the flow process and does not affect vaporization, the cooperation of molecule pairs as depicted by Alfrey's[8] model of the flow (Fig. 3). The probability for two of the few molecules of extra energy content $\Delta H_{\ddagger}$ to collide and align "properly" for this minuet is certainly very small and bound to contribute a sizeable negative term to $\Delta S_{\ddagger}$. This term and the term for intramolecular cooperation lumped together as $\Delta S_{\ddagger}^{c}$ would be the only sources of entropy change once $\Delta H_{\ddagger}/T$ is zero. The intercept of the $\Delta S_{\ddagger}$ *vs.* $\Delta H_{\ddagger}/T$ curves with the $\Delta S_{\ddagger}$ axis would, therefore, be $\Delta S_{\ddagger}^{c}$.

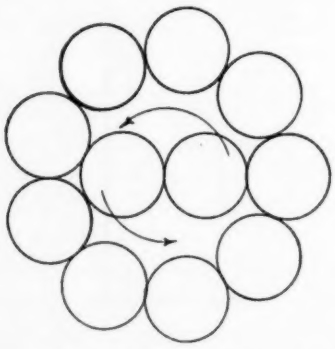

FIG. 3. Alfrey's model; rotational flow.

As would be expected, $\Delta S_{\ddagger}^{c}$ is constant at low temperatures but increases at high temperatures reaching relatively quickly another constant value, which is then identical with $\Delta S_{\ddagger}$, suggesting that at elevated temperatures, the entire entropy change is caused by cooperative factors. Relationship between $\Delta S_{\ddagger}^{c}$ and chemical constitution will be discussed later. Prediction of its magnitude by other than semi-empirical rules seems at present not possible.

Other terms contributing to $\Delta S_{\ddagger}$ are: $\Delta S_{\ddagger}^{tr}$ which can be derived from the change in effective free volume and would be

$$\Delta S_{\ddagger}^{tr} = R \ln \left(\frac{\delta_3 V_f + \Delta V_{\ddagger}}{\delta_3 V_f} \right);$$

$\Delta S_{\ddagger}^{tr}$ contributes about 1.5 to 10 e.u. The higher values are associated especially with liquids composed of spherically shaped molecules, whose free volume is usually small and $\Delta V_{\ddagger}$ quite large. Another term is $\Delta S_{\ddagger}^{rot}$, which is caused by the activation of external rotation. The origin of this rotational contribution, the lack of free swing, has been mentioned above in connection with $\Delta H_{\ddagger}^{i}$. The same considerations which led to the conclusion (in Eq. (11)) that only a fraction of the total energy of a rotator has to be supplied for the process of activation, depending on the available free volume, apply to the magnitude of $\Delta S_{\ddagger}^{rot}$. In addition we have to consider the possibility that the flow process might require rotation only around a single preferred axis. There is some experimental evidence for this hypothesis: If we compare the entropy of activation for dipole orientation $\Delta S_{\ddagger}(\epsilon)$ and for viscous

[14] I. M. Barclay and J. A. V. Butler, Trans. Faraday Soc. **34**, 1445 (1938).
[15] H. S. Frank, J. Chem. Phys. **13**, 793 (1945).

TABLE III. Comparison of the processes of activation for flow and for dipole orientation.

Substance	Process	t °C	$\Delta F\ddagger$ kcal.	$\Delta H\ddagger$ kcal.	$\Delta S\ddagger$ e.u.	$\Delta S\ddagger(\epsilon)-\Delta S\ddagger(\eta)$ e.u.	$S(\text{rot}-l)$** e.u.
n-propanol	Flow	25	3.52	4.53	3.4		
	Orientation	25	3.57	6.10	8.5	5.11	6.7
n-butanol	Flow	25	3.79	4.61	2.75		
	Orientation	25	3.90	6.40	8.4	5.65	8.2
Cocoanut oil	Flow	30	6.67	6.71	0.15		
	Orientation	30	2.26	8.16	19.4	19.25	22.7
Ethyl abietate	Flow*	10	8.24	23.84	55.0		
	Orientation	10	4.18	26.30	78.0	23	23.7
	Flow	20	7.85	19.15	38.6	12.4	
	Orientation	20	3.67	18.60	51.0		

* Extrapolated viscosity data used.
** Rotational entropy contribution calculated for rotation around longest axis of molecule.

flow $\Delta S\ddagger(\eta)$, we shall find $\Delta S\ddagger(\epsilon)-\Delta S\ddagger(\eta)$ often to equal just the rotational entropy contribution calculated for rotation of the dipole around the longer axis of the molecule (see Table III), a motion which is in accord with our present views of the rotation of dipoles in an alternating electric field. Had $\Delta S\ddagger(\eta)$ contained the complete ΔS^{rot}, $\Delta S\ddagger(\epsilon)$ would have been smaller than $\Delta S\ddagger(\eta)$ instead of larger, as is always observed. Which of the three possible external rotations contributes to $\Delta S\ddagger(\eta)$ will for the time being be a matter of trial calculations.** As our knowledge of the small (difficulty observed) temperature dependent rotational Raman-shifts of liquids increases we shall approach the possibility of predicting $\Delta S\ddagger^{\text{rot}}$ from such spectrographic data. Similar reasoning applies to the computing of the contribution $\Delta S\ddagger^{i}$ of activated internal rotation (or torsional oscillations).

From the relation

$$\Delta S\ddagger = R \ln \frac{F\ddagger}{F} + \frac{\Delta E\ddagger^{\text{internal}}}{T}$$

follows that the slope of the curves in Fig. 4 represents the ratio of the change in internal energy (during activation) to $\Delta H\ddagger$. It is in accordance with the views expressed above that —by these curves—$\Delta E^{\text{int}}/\Delta H\ddagger$ should tend to zero at high temperatures (high V_f/V ratios).

To sum up the results of this analysis of $\Delta S\ddagger$: It is found that of the many terms contributing to $\Delta S\ddagger$ only a few can be separated, let alone be predicted. By analysis of viscosimetrically determined data one can separate the contribution of cooperation factors $\Delta S\ddagger^{c}$, and the translational term $\Delta S\ddagger^{\text{tr}}$. In the future $\Delta S\ddagger^{\text{rot}}$ and $\Delta S\ddagger^{i}$ may become predictable from Raman or infra-red spectra in the 10 to 100 cm^{-1} range.

We must admit that the analysis of $\Delta H\ddagger$ and $\Delta S\ddagger$ which—it is believed—has here been tried for the first time has failed of its objective, the prediction of the absolute value of the viscosity of pure liquids from available physical property data, but the results obtained appear to provide sufficient new insight into the mechanism of the flow process to evaluate profitably the influence of molecular structure upon viscosity.

In the following paragraphs the influence of the two most prominent factors, molecular geometry and hydrogen bonding, upon $\Delta H\ddagger$, $\Delta S\ddagger$, and $\Delta V\ddagger$ will be discussed in some detail.

3. MOLECULAR GEOMETRY AND VISCOSITY

A number of investigators have tried to calculate the viscosity or the viscosity-temperature coefficient from atomic or bond increments in a manner similar to the molar volume, parachor, refraction, etc.[16] If it was not already obvious to a large number of workers in the field, the vast

** From the work of Kauzmann and Eyring [J. Am. Chem. Soc. **62**, 3113 (1940)] it could be concluded that $\Delta S\ddagger^{\text{rot}}$ of the moving segment of long linear molecules is of the order of 7 e.u.

[16] E. C. Bingham and collaborators, J. Rheol. **1**, 372 (1930); **3**, 113, 479 (1932). J. N. Friend, Phil. Mag. **34**, 643, 810 (1943); **35**, 57, 136 (1944). H. Umstatter, Kolloid Zeits. **102**, 232 (1943). Others reviewed in "1st and 2nd Report on Viscosity and Plasticity to the Amsterdam Acad. Sci.," Amsterdam, 1935 and 1938.

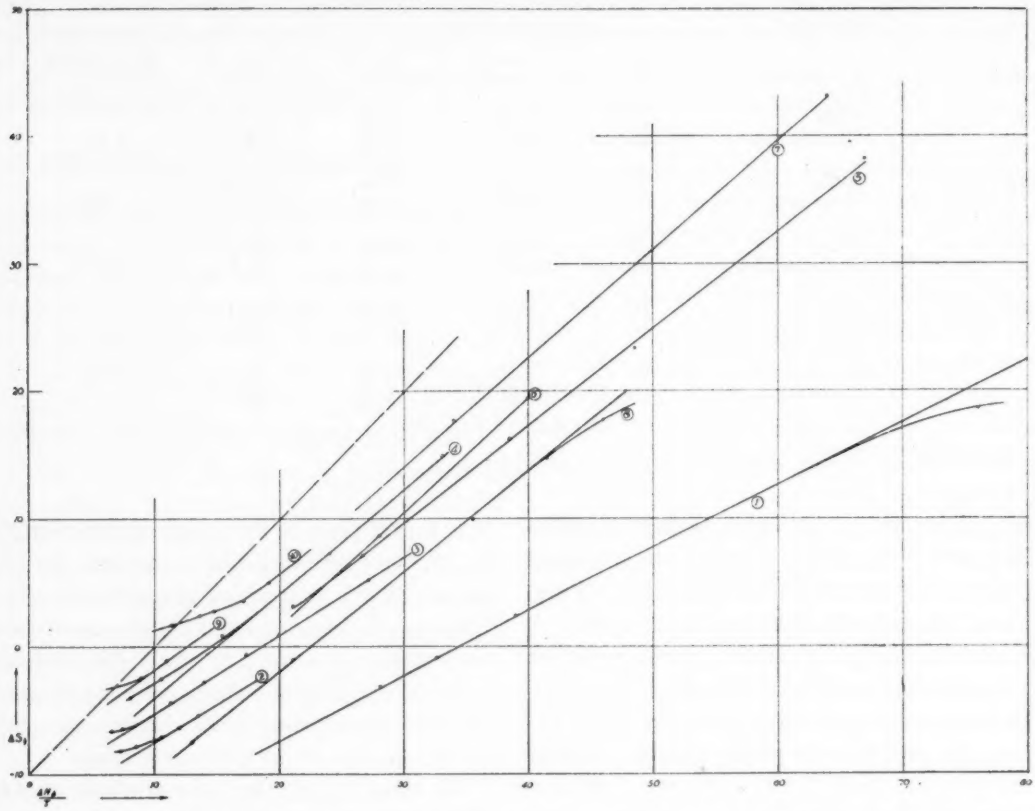

FIG. 4. Plot of $\Delta S_{\ddagger}$ *vs.* $\Delta H_{\ddagger}/T$ over a wide temperature range for a number of typical compounds. Slope of broken line = 1.0.

① Polyiso-butylene
② *n*-triatetracontane
③ 10-nonyl nonadecane
④ di-isobutyl-naphthalene
⑤ tri-(cyclohexyl-ethyl)-methane
⑥ tri cresyl phosphate
⑦ 2,2- di-pseudo cumente-propane
⑧ castor oil
⑨ cutyric acid
⑩ *n*-amyl alcohol

amount of viscosity data of pure hydrocarbons which have accumulated during the past decade[17] has made it quite clear that these attempts have been futile. The various isomers of the hydrocarbon differ often in viscosity to such an extent that bond additivity is ruled out entirely.

On examining the equations of the previous sections for the basic causes of this behavior of liquids, we find that there are, indeed, a number of bond or atom additive properties contained in a number of parameters: the polarizability α in $\Delta H_{\ddagger}^{h}$, the mass per molecule in the rotational energy and δ_3, of $\Delta H_{\ddagger}^{i}$ and $\Delta S_{\ddagger}^{rot}$ and lastly the molar volume in the quotient Nh/V. There are, however, a number of decisive factors which are

[17] See in M. P. Doss, *Physical Constants of the Principal Hydrocarbons* (Texaco, New York, 1943).

TABLE IV. Relationship between the volume requirement $\Delta V_{\ddagger}$ of the activated molecule and molecular structure (all from viscosity/pressure data below 1000 atmospheres).

Substance	t °C	$\Delta V_{\ddagger}$ cm³	$\frac{\Delta V_{\ddagger}}{V}$	t °C	$\Delta V_{\ddagger}$ cm³	$\frac{\Delta V_{\ddagger}}{V}$
(a) *Flexible structures*						
n-decane	30	18.4	0.094	75	14.3	0.072
di-*n*-amyl ether	30	21.7	0.106	75	21.7	0.102
n-octadecyl alcohol	70	29.2	0.087	150	33.3	0.092
Oleic acid	30	33.0	0.106	75	29.0	0.092
Oleyl oleate	20	38.6	0.064	—	—	—
Linseed oil	20	25	0.026	50	23	0.024
Castor oil	25	26	0.027	100	23.6	0.024
*Petroleum fractions**						
N-393	38	72	0.167	99	49	0.114
N-670	38	65	0.087	99	61	0.079
(b) *Rigid structures*						
Neo-pentane	31	34.4	0.285	101	43.4	0.312
Cyclohexane	30	—	—	75	26.6	0.230
Chlorobenzene	30	13.2	0.128	75	14.8	0.138
Tetrachlorodiphenyl	54	116	0.582	99	44	0.218
Pentachlorodiphenyl	54	226	1.090!	99	70	0.330

TABLE V. Effect of spatial configuration on viscosity of hydrocarbons and organo silicone derivatives.

	T °C	η poise	$\Delta H\ddagger$ kcal.	$\Delta S\ddagger$ e.u.	$\Delta V\ddagger$ cm³	$\frac{\Delta V\ddagger}{V}$
n-pentane	30	0.0022	1.30	−4.0	15.3	0.132
($\Delta S_f = 14.0$ e.u.)	75	0.00148	1.10	−4.6	17.5	0.138
Neo-pentane	30	0.0023	2.20	−1.2	34.4	0.285
($\Delta S_f = 2.4$ e.u.)	100	0.0011	1.80	−2.5	43.4	0.312
n-hexane	30	0.0029	1.50	−4.2	17.3	0.131
($\Delta S_f = 17.5$ e.u.)	75	0.0019	1.48	−4.2	20.3	0.144
Neo-hexane	20	0.00375	1.70	−3.8	—	—
Ethyl-trimethyl-Silane*	20	0.00334	1.63	−4.0	—	—!
Cyclo-hexane	30	0.0082	∼2.68	∼−2.0	—	—
($\Delta S_f = 2.2$ e.u.)	75	0.0043	∼2.68	∼−2.0	26.6	0.230
n-decane	30	0.00783	2.52	−3.5	18.4	0.094
($\Delta S_f = 28.3$ e.u.)	60	0.0054	2.96	−4.3	—	—
Cyclodecane	20	0.0448	4.71	+1.1	—	—
	60	0.0176	4.01	−1.1	—	—
Decamethyl tetrasiloxane**	25	0.0131	2.25	−6.5	—	—
	99	0.00541	2.45	−5.9	—	—
Octamethyl cyclo tetrasiloxane**	25	0.0220	3.18	−4.1	—	—
	99	0.0070	3.25	−4.0	—	—
n-C_{26}	60	0.0656(S)	4.32	−4.3	—	—
$C_2-C(C_2)-C_{21}$	20	0.20(S)	5.50	0	—	—
	60	0.066(S)	4.43	−4.0	—	—
$C_8-C(C_8)-C_8$	20	0.160(S)	5.87	1.0	—	—
	60	0.050(S)	4.42	−3.34	—	—
$[C_6H_5-C_2]_3\cdot C$	20	7.30(S)	19.01	38.4	—	—
	60	0.45(S)	9.35	7.2	—	—
$n-C_{32}$	80	0.099(S)	4.37	−6.1	—	—
$(C_{10})_3\cdot C$	20	0.291(S)	6.56	1.8	—	—
	80	0.055(S)	5.06	−3.03	—	—
$C_6-C(C_2)-C(C_6)-C(C_6)-C-C-C(C_2)-C_6$	20	0.484(S)	7.87	5.2	—	—
	80	0.063(S)	6.00	−0.6	—	—
	245	0.0079(S)	3.89	−5.9	—	—

* Viscosity data from: F. C. Whitmore *et al.*, J. Am. Chem. Soc. **68**, 475 (1946).
** Viscosity data from: C. B. Hurd, J. Am. Chem. Soc. **68**, 364 (1946), and D. F. Wilcock, ibid. **68**, 691 (1946).

not at all bond additive: $\Delta V\ddagger$, which determines the magnitude of $\Delta H\ddagger^h$, depends upon the flexibility of the molecule, and is the smaller *a* fraction of the total molecular volume the more flexible a molecule, that is, the smaller a molecular segment can move freely and act as unit of flow. Table IV gives a number of typical examples for the relationship between molecular structure and the value of $\Delta V\ddagger$. Attention is called to the extreme values for rigid spherical structures like the chlorinated diphenyls on the one hand and the uniformly small $\Delta V\ddagger$ of the linear molecules such as the fixed oils on the other. A remarkable feature of the important ratio $\Delta V\ddagger/V$ is its independence from the constituent atoms of the molecule, being a function only of the relative distribution in space (*Raumerfuellung*) and—as mentioned above—of the flexibility of a molecule's structure. The non-additive elements of $\Delta H\ddagger^i$ are E_r and δ_3, which

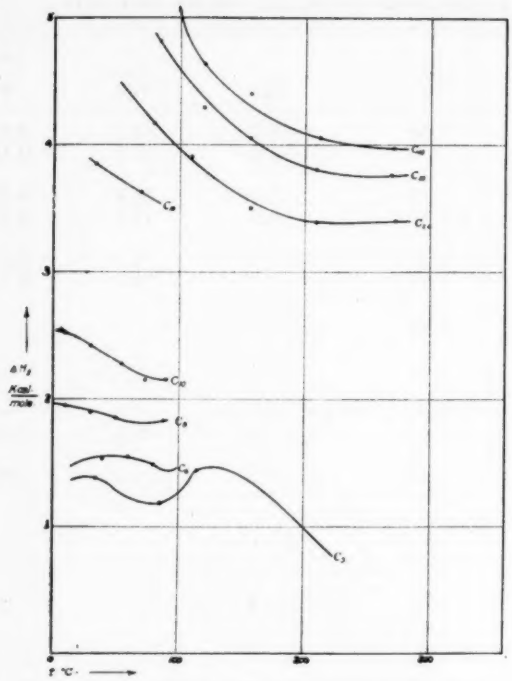

FIG. 5a. *n*-paraffins. $\Delta H\ddagger$ *vs.* temperature curves.

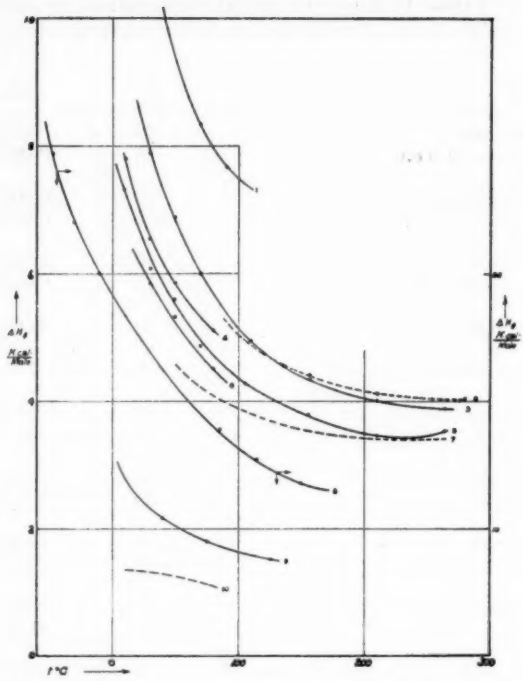

FIG. 5b. $\Delta H\ddagger$ *vs.* temperature curves of iso-paraffins. (Broken lines = *n*-paraffins for comparison.)

① 7, 17 dimethyl, 9, 11, 13, 15 tetra hexyl eicosane
② 7, 12 dymethyl, 9, 10 dihexyl octadecane
③ *n*-tritetracontane
④ 11 decyl-heneicosane
④ 10-nonyl-nonadecane
⑤ 9-octyl-heptadecane
⑦ *n*-tetracosane
⑧ polyisobutylene
⑨ neopentane
⑩ *n*-pentane

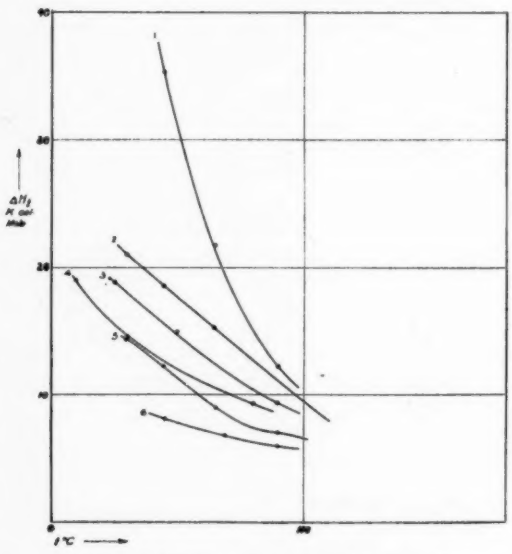

FIG. 5c. $\Delta H\ddagger$ *vs.* temperature curves of polycyclic hydrocarbons.

① 2, 2 dipseudo cumene propane
② β-dihydro diamyl anthracene
③ β-dihydro dioctyl anthracene
④ tri(ethyl cyclohezane) methane
⑤ β-dihydro diethyl anthracene
⑥ tri-octadecyl-benzene (for comparison)

FIG. 5. The temperature curves of the heat of activation $\Delta H\ddagger$. These curves show quite well the dependence of the temperature sensitive component of $\Delta H\ddagger$; namely, $\Delta H\ddagger^i$, upon molecule size and structural complexity.

TABLE V(A). Effect of position of ring on viscosity.

	t °C	Viscosity stokes	$\Delta H\ddagger$ kcal.	$\Delta S\ddagger$ e.u.
n-octadecane (for comparison)	20	0.0579	3.84	−3.0
	80	0.0184	3.64	−3.8
1-phenyl dodecane	20	0.0629	4.36	−1.6
	80	0.0197	3.52	−4.1
2-phenyl dodecane	20	0.0688	4.74	−0.4
	80	0.0197	3.82	−3.2
4-phenyl dodecane	20	0.0782	5.40	+1.0
	80	0.0196	3.85	−3.2
6-phenyl dodecane	20	0.0880	5.94	+3.5
	80	0.0197	4.30	−1.9

contain the moments of inertia—and their product—being clearly determined by the relative distribution of the molecular structure in space, and the free volume V_f "which is due to the thermal displacements of the center of gravity of the molecule from its equilibrium position." [18] The free volume is thus directly related to the expansion at the melting point; the curious relationship between viscosity functions and the entropy of fusion ΔS_f becomes thereby somewhat clarified. The data on Table V show that whenever ΔS_f is large, $\Delta H\ddagger$ and $\Delta S\ddagger$ are small and *vice versa*. The behavior of the spherical molecules neo-pentane and cyclohexane —whose ΔS_f has nearly the theoretical value R —is quite characteristic of this general trend. In other words V_f is—by ΔS_f and ΔV_f—also essentially a function of molecular geometry and not of chemical character.† The temperature coefficient of $\Delta H\ddagger^i$—and thereby of $\Delta H\ddagger$—is according to Eq. (11) determined by the expansion coefficient and V_f. The former is within any one group of compounds proportional to the reciprocal molecular weight, and varies quite generally inversely as the cohesive energy E''.

These relationships are well recognizable in Figs. 5a–c.

The effect of most dipoles, excepting OH and NH, on $\Delta H\ddagger$ and on viscosity in general, is quite small. This is not at all surprising for the size of the dipole interaction terms occurring in both $\Delta H\ddagger^h$ and $\Delta H\ddagger^i$ depends very strongly on the distance between the dipoles. With the exception of those dipoles which contain hydrogen this distance of closest approach is so large as to reduce the magnitude of the dipole interaction contribution to but a few hundred cal./mole, as is readily seen on Table VI, where polar molecules and structurally similar hydrocarbons are compared with each other.* It appears from these data that one need not consider chemical characteristics at all if one wants to synthesize

TABLE VI. Demonstrating the relative independence of viscosity function from chemical composition and the dominating effect of molecular structure.

Substance	M	t °C	η poise	$\Delta F\ddagger$ kcal.	$\Delta H\ddagger$ kcal.	$\Delta S\ddagger$ e.u.	$\mu\dagger$ d.u.	$N\mu^2/r^3$ kcal.
Di-n-amyl ether	158	20	0.0108	3.66	2.87	−2.7	1.2	0.3
n-undecane	156	20	0.0117	3.74	2.94	−2.8	0	
Methyl stearate	298	50	0.039	5.23	4.11	−3.5	1.8	0.6
n-heneicosane	296	50	0.037	5.25	4.00	−3.8	0	
di-ethylhexyl sebacate	428	38	0.115	5.87	5.10	−2.4	3.6	2.4
9-octyldocasane	422	38	0.115	5.95	5.15	−2.6	0	
Tricresyl phosphate	368	60	0.135	6.15	9.03	8.7	(4.3)	2.3
Tri(ethylbenzene) methane	329	60	0.106	5.97	8.73	8.3	0	
Ethylabietate*	330	40	1.41	7.26	15.30	25.6	1.8	0.6
Di-isoamyl dihydro-anthracene*	322	40	4.20	7.82	18.7	36	0.5	

* These two compounds differ somewhat in structure. A better hydrocarbon analog of ethylabietate could, however, not be found in the literature. The relatively close numerical vlues of their viscosity constant demonstrate quite well the material effect of rigid condensed tricyclic structures.
† The dipole moments are estimated values.

[18] Kincaid and Eyring, J. Chem. Phys. **6**, 620 (1938).

† The relation between ΔH_f and *Raumerfuellung*, i.e., the three-dimensionality of molecular structure, has first been discovered by J. Pirsch, Ber. **70**, 12 (1937).

* It should also be noted that μ^2/r^3 is the negative value of the orientation energy contribution to E'' at full parallel orientation of the dipoles. This interaction term will tend to zero with increasing angle of mutual orientation. As there is obviously always a finite (and quite sizeable) concentration of non-oriented dipole molecules from which $c_\ddagger$ would be recruited, the influence of dipoles on viscosity is, as a rule, quite small; as is brought out by the figures above.

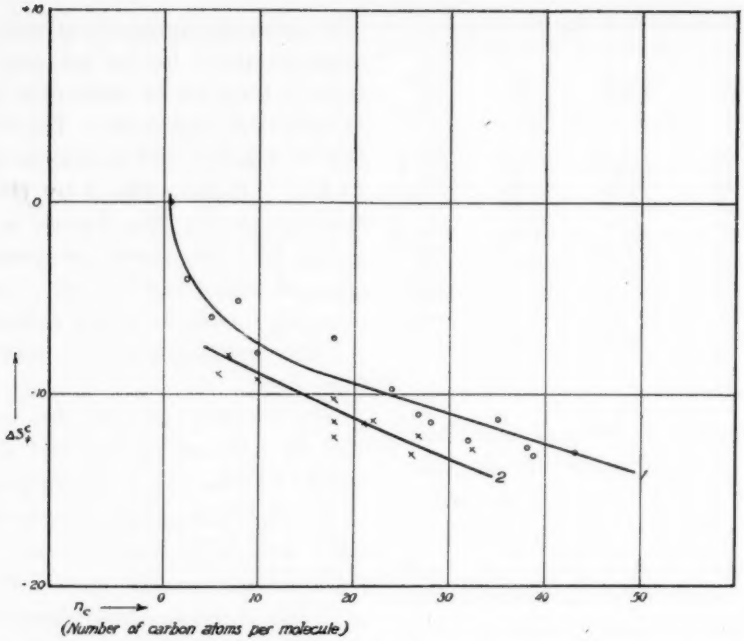

FIG. 6. Relationship between $\Delta S_\ddagger^c$ (from $\Delta S_\ddagger$ *vs.* $\Delta H_\ddagger/T$ intercept) and molecule size for long chain hydrocarbons (1) and cyclic hydrocarbons (2).

a substance of given viscosity characteristics but only the stereometric arrangement of molecular structure (provided there are no OH groups and not too many cumulative dipoles in the molecule).

The cooperative entropy factor $\Delta S_\ddagger^c$ is seemingly directly proportional to the size of the unit of flow (OH compounds excepted). Fig. 6. The balance of the entropy terms depend on the same factors as the corresponding energy contribution.

4. HYDROGEN BONDED LIQUIDS

The well-known anomalies caused by hydroxyl groups, which have been quite conclusively ascribed to hydrogen bonds[19] are naturally also reflected in the viscosity function. The simplest case is represented by the fatty acids. Electron diffraction and vapor pressure data[20,21] have now well established that the hydrogen bond, coupling two carboxylic acids to a dimer unit, is so well stabilized (by resonance) that the double molecules exist not only in the liquid but even in the vapor state, at least for the lower members of the fatty acid series. It is, therefore, but an additional confirmation of the reality of the double molecule to find that the viscosity parameters of fatty acids correspond remarkably well to those of hydrocarbons of the structure and molecular weight of the fatty acid double molecule, as seen from Table VII. Because of the relatively large accumulation of dipoles in the double molecule of the lower members of the series, the viscosity, $\Delta H_\ddagger$, and $\Delta S_\ddagger$ of the latter are somewhat higher than would otherwise be expected. The consequently more pronounced contribution of the dipole interaction terms to $\Delta H_\ddagger^h$ and $\Delta H_\ddagger^j$ cause the quite small temperature coefficient of $\Delta H_\ddagger$

TABLE VII. Evidence for the existence of fatty acids as double molecules by comparison of viscosity data with those of hydrocarbons and esters.

	M	t °C	η poise	$\Delta F_\ddagger$ kcal.	$\Delta H_\ddagger$ kcal.	$\Delta S_\ddagger$ e.u.
Propionic acid	(148)	20	0.011	(3.60)	2.45	(−3.8)
Propionic anhydride	130	20	0.011	3.51	2.66	−2.8
n-decane	142	20	0.0091	3.54	2.52	−3.5
Valeric acid	(204)	20	0.022	(4.28)	3.90	(−2.9)
n-tetradecane	198	20	0.022	4.22	3.44	−2.6
n-heptylic acid	(260)	20	0.043	(4.88)	4.04	(−2.9)
n-octadecane	254	20	0.045	4.78	3.95	−2.8
Oleic acid	(564)	20	0.318	(6.60)	5.90	(−2.3)
Oleyl oleate	532	20	0.330	6.30	5.30	−3.4

Data in parentheses are calculated for the double molecule.

[19] S. Gladstone, *Textbook of Physical Chemistry* (D. Van Nostand Company, New York, 1943), p. 114.

[20] J. Karle and L. O. Brockway, J. Am. Chem. Soc. **66**, 574 (1944).

[21] H. L. R. Ritter and J. H. Simons, J. Am. Chem. Soc. **67**, 757 (1945).

TABLE VIII. Energies and entropies of activation of aliphatic alcohols.

	t °C	$\Delta H\ddagger$ kcal.	$\Delta H\ddagger^h$ kcal.	$\Delta H\ddagger^j$ kcal.	ΔEv^j kcal.	$S/2$	$\Delta S\ddagger$ e.u.	$\frac{\Delta V\ddagger}{V}$	$\frac{\Delta H\ddagger^h}{\Delta Ev^0}$
Methyl OH	15	2.20	0.40	1.80	2.03	2.9	−1.0	0.199	0.063
	60	2.28	0.63	1.65			0.0	0.204	0.095
Ethyl OH	15	2.97	0.61	2.43	2.34		0	0.185	0.082
	60	3.29							
n-propyl OH	15	4.16	0.97	3.20	3.32	5.1	2.2	0.209	0.129
	60	4.05	1.25	2.85			2.2	0.219	0.178
i-propyl-OH	15	5.00	1.12	3.88	—	3.4	3.5	0.256	
	60	4.95	1.18	3.67			4.7	0.266	
n-butyl-OH	15	4.60	1.37	3.29	4.30?	1.4	2.3	0.202	0.158
	60	4.45	1.20	3.25			2.3	0.185	
i-butyl-OH	15	5.46					5.0	0.225	
	60	5.21					4.0	0.219	
tri methyl carbinol*	35	8.68			3.00		15.0		
	70	6.15					7.5		
n-amyl-OH	15	5.35	1.44	3.91	3.67	5.2	4.7	0.192	0.182
	60	5.01	1.45	3.55			3.1	0.199	
n-heptyl-OH	10	5.4			3.30		2.5		
	70	4.7					1.5		
tri-ethyl carbinol*	10	12.3					26.5		
	70	5.5					4.5		
n-octanol†	10	6.48					5.9		
	90	5.05					1.4		
4-methyl-heptanol-3†	10	3.50					0		
	90	2.56					−3.3		
1-octadecanol	85	6.92	2.79	4.13		14	2.8	0.087 at 70°C	
	140	4.78	2.41	2.37			−2.7	0.092 at 150°C	

Notes: ΔEv^j refers to temperature at which vapor conc. =0.0202 mole/1 $\Delta V\ddagger/V$ is always taken at 30 and 75°C, respectively, except where noted otherwise $\Delta Ev^0 = \Delta Ev - \Delta Ev^j$.

* The extremely high values of $\Delta H\ddagger$ and $\Delta S\ddagger$ for the symmetrical trialkyl carbinols seem readily ascribed to the spherical shape of these compounds. But only viscosity pressure data—which are still sadly missing—will provide through $\Delta V\ddagger$, $\Delta H\ddagger^j$ and $\Delta H\ddagger^h$ values a full understanding of the mechanism of flow of such fluids.

† The data of these two isomers were inserted to show the interference of hydrocarbon radical structure with OH-network formation.

and thereby the bent $\Delta S\ddagger$ *vs.* $\Delta H\ddagger/T$ curves shown in Fig. 9. Progressive dissociation of the dimer with increasing temperature would affect those parameters in the same direction.

The state of molecular aggregation of alcohols is less well defined than that of the fatty acids. At ordinary temperatures the bond between hydroxyl groups is not strong enough to form distinguishable double molecules. They rather form a continuous network structure throughout the liquid phase. Contrary to ordinary dipole systems, for which the potential energy difference between the fully oriented and random configuration is usually less than 2 kcal., the hydroxyl group *network* is more probable than randomness by a potential energy difference of more than 10 kcal.[22]

The motion of *any* alcohol molecule involves, therefore, passage of OH-groups past each other. Since the displacement per jump is not larger than with other molecules, $\Delta V\ddagger$ and $\Delta H\ddagger^h$ are of normal magnitude, Table VIII, but the motion in the strong fields requires a $\Delta H\ddagger^j$ considerably greater than that of molecules of comparable size. As "the jumping pairs" now have a predetermined configuration, $\Delta S\ddagger^c$ of (the lower) alcohols is not very important, and $\Delta S\ddagger$ becomes relatively high, compensating the large $\Delta H\ddagger$ value somewhat. The viscosity of alcohols is

[22] H. Harms, Zeits. f. physik. Chemie **B43**, 257 (1939).

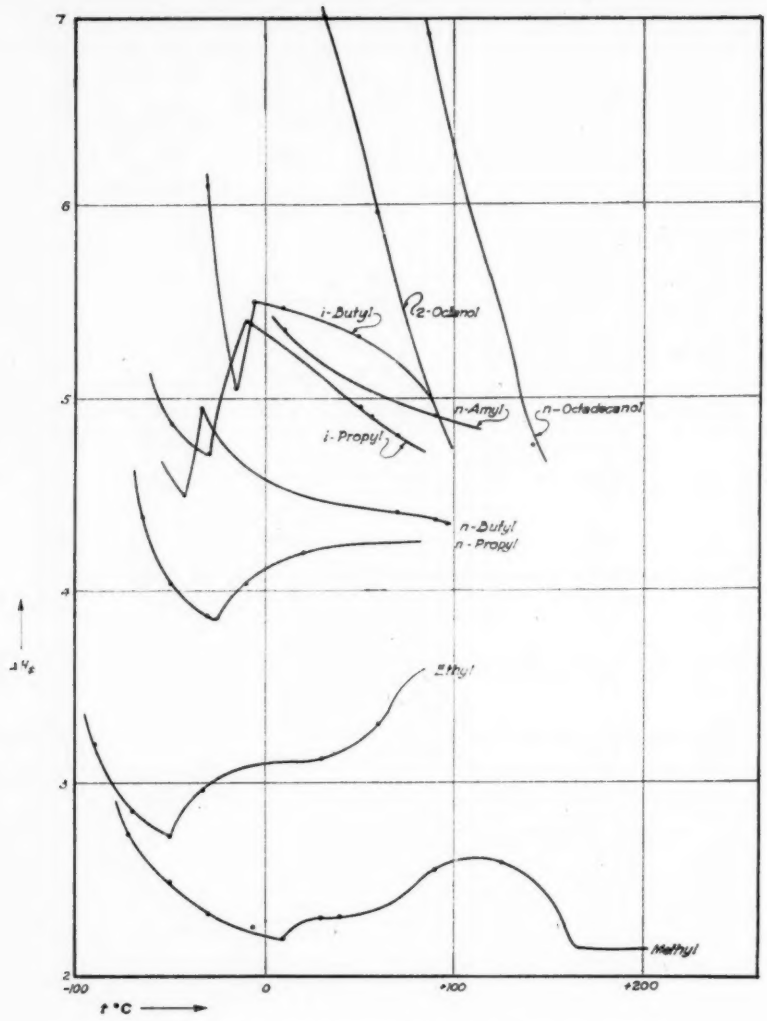

FIG. 7. $\Delta H\ddagger$ *vs.* temperature curves of aliphatic alcohols.

nevertheless quite a bit higher than of other compounds of similar structure and molecular weight. Low temperature (at -75°C) x-ray diffraction data[23] indicate the presence of true hydrogen bridges (as in fatty acids) of 2.7 to 2.9A O$-$H$-$O distance in methyl and ethyl alcohols. At room temperature these are no longer observable. If this should mean that alcohols form distinguishable double or otherwise multiple molecules at low temperatures, whose motion would not involve mutual passage of OH-groups, one would expect $\Delta H\ddagger$ to decrease at the same low temperature instead of increase. Calculation of $\Delta H\ddagger$ from the careful viscosity measurements of Tonomura[24] down to -98°C shows this actually to be the case, as depicted on Fig. 7. Much more revealing, indeed surprising, are the $\Delta S\ddagger$ *vs.* $\Delta H\ddagger/T$ curves of these alcohols, shown in Fig. 8. They show the regular linear behavior at lowest temperatures until they reach a sudden inflection point, where within a fractional unit of $\Delta H\ddagger/T$, $\Delta S\ddagger$ increases by 1.6 to 3.0 e.u. Remembering that $\Delta S\ddagger$ is in the form $e^{\Delta S/R}$ a measure of the population of a given energy state, we compute from these entropy changes that at the inflection point the number of units of flow (but not $c\ddagger/c$!) increases (by

[23] G. G. Harvey, Phys. Rev. **55**, 1115 (1939).

[24] T. Tonomura, Sci. Rep. Tohoku Imp. Univ. [1] 22, 104 (1932).

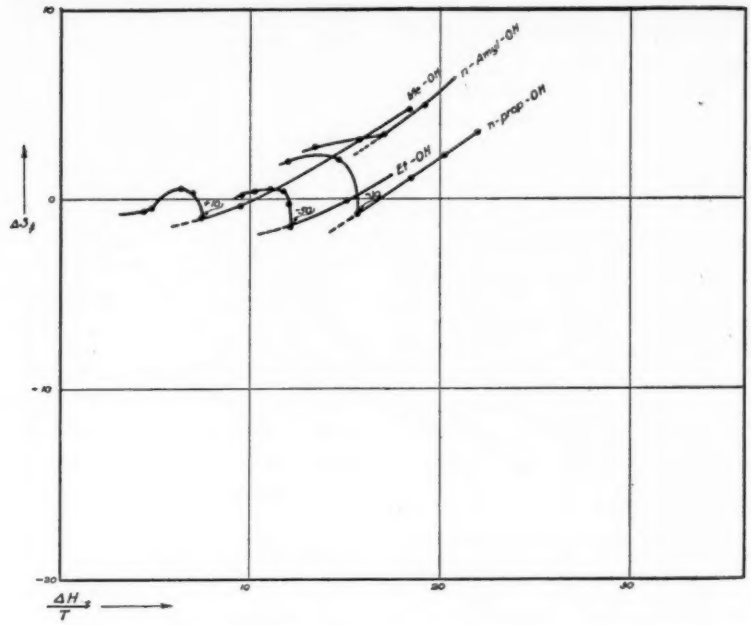

FIG. 8. Alcohols $\Delta S\ddagger$ *vs.* $\Delta H\ddagger/T$ curves.

increasing the temperature) by a factor of 2.2 for methyl-alcohol, 2.4 for ethyl alcohol, and 4.5 for *n*-propyl alcohol. The inflection temperatures are at about 10°C, −50°C and −30°C, respectively. The inflection of the butyl and amyl alcohol curves are more gradual, and less well defined. If the interpretation of the behavior of alcohols is correct, we should expect to observe similar effects of the dissociation of fatty acids upon $\Delta S\ddagger$ and $\Delta H\ddagger$ at elevated temperatures. There are but few high temperature viscosity data of fatty acids available, and dissociation of these in the liquid state takes place at temperatures at which the increase of $\Delta S\ddagger^e$ starts already to flatten out the $\Delta S\ddagger$ curves, but nevertheless the curves on Fig. 9 indicate the general trend to be as expected. Viscosity data of compounds containing more than one OH-group per molecule are very scarce. The most peculiar of these is castor oil. The $\Delta H\ddagger^i$ values of this liquid, calculated from the viscosity data of Hersey and Shore[25] are presented on Table IX. The stepwise decrease of $\Delta H\ddagger^i$ with increasing temperatures suggests successive disengagement of the hydroxyl groups with increasing disorder in the liquid.

[25] Hersey and Shore, Mech. Eng. **50**, 221 (1928).

5. VISCOSITY AND LIQUID STRUCTURE

The structure of liquids, which by x-ray diffraction and their theoretical interpretation has acquired the status of a reality today, has hardly been referred to in the quantitative discussion. It is, however, not accidental that the rate process theory of flow should be able to give a good account of the relationship between molecular structure and viscosity without explicit consideration of the structure of the liquid. The reason for this lies in the basic premise of the theory: the proportionality between fluidity and the concentration of activated molecules $c\ddagger$. The smallness of $c\ddagger$ has never before been sufficiently emphasized. We have mentioned in Section 1 that $c\ddagger$ is small enough to be entirely recruited out of the small random oriented population even in such liquids, which are otherwise known as well-ordered systems, such as *n*-paraffins, fatty acids, etc. at ordinary temperatures. The activated molecules have since the inception of the theory been thought to occur only in the immediate neighborhood of lattice disturbances, the "holes." Just as the frequency of lattice imperfections in crystals is not *a priori* connected with the geometry of the lattice, such condition should

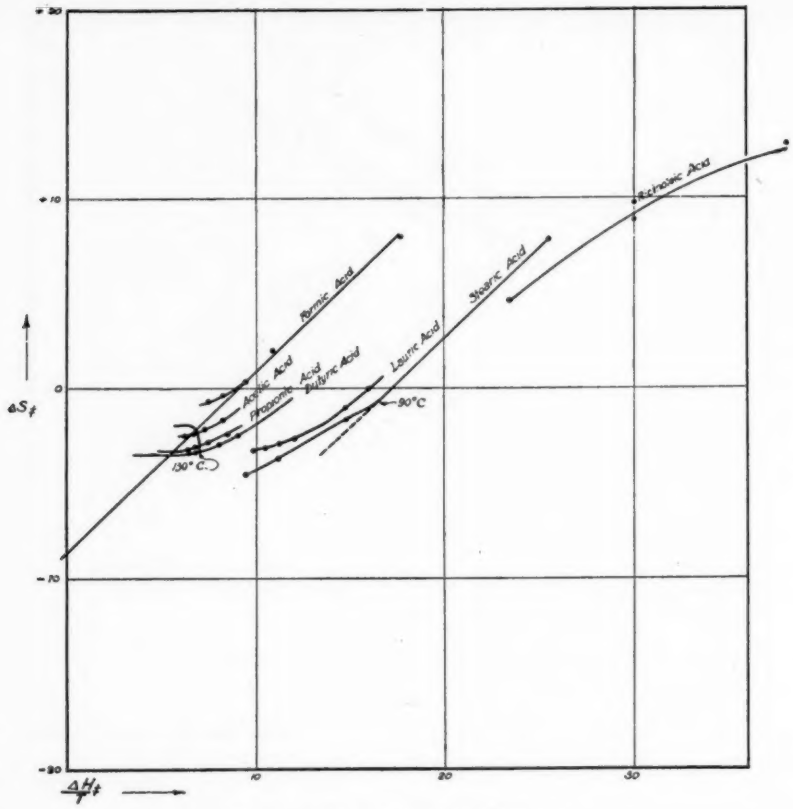

FIG. 9. Acids $\Delta S_{\ddagger}$ *vs.* $\Delta H_{\ddagger}/T$ curves.

not be expected to exist in liquids. An indirect connection does exist through the proportionality between the number of holes in the lattice and $\exp[(-\zeta^h+\zeta^i)/kT]$, where ζ^h is the energy of hole formation and ζ^i the potential energy of a molecule on an interlattice position, both of which are affected by the number of nearest neighbors and thereby the lattice arrangement. We shall similarly expect $\Delta V_{\ddagger}$ (and by it $\Delta H_{\ddagger}^h$ and $\Delta S_{\ddagger}^{tr}$) to be affected by the number and arrangement of the nearest neighbors. Further refinement of the theory, designed to predict $\Delta V_{\ddagger}$ and its temperature and pressure function will, therefore, have to take the details of the liquid structure into account.

SUMMARY

1. The energy of activation for viscous flow consists of two independent terms: the energy of hole formation $\Delta H_{\ddagger}^h$ and the energy of motion into the hole $\Delta H_{\ddagger}^j$. $\Delta H_{\ddagger}^h$ has here been derived as the change in potential energy between one molecule and its nearest neighbors, which accompanies the displacement from equilibrium position incident to the formation of a hole. With the displacement given by the pressure coefficient of the free energy of activation $(\partial \Delta F_{\ddagger}/\partial p)_T = \Delta V_{\ddagger}$ London's interaction energy law is shown to predict $\Delta H_{\ddagger}^h$ values of the right order of magnitude. $\Delta H_{\ddagger}^j$, the heat of activation of the viscosity isochore is shown to be often of the same magnitude as $T \times$ Hildebrand's excess entropy of vaporization, a parameter which might also be called the non-ideal portion of ΔE_{vap}. Both may be considered as a measure of restricted external rotation in the liquid state. Where $\Delta H_{\ddagger}^j$ is materially larger than ΔE_{vap}^j, the molecular structure as well as the temperature coefficient of $\Delta H_{\ddagger}^j$ suggest that the process of motion requires deformation of the molecule against internal potential energy barriers.

2. The entropy of activation $\Delta S_{\ddagger}$ is separated into a cooperative term $\Delta S_{\ddagger}^e$ which is derived graphically from the $\Delta S_{\ddagger}$ *vs.* $\Delta H_{\ddagger}/T$ curve, a

translational term $\Delta S_{\ddagger}^{tr}$ which is calculated from the volume increase $\Delta V_{\ddagger}$ and the free volume, and a rotational term $\Delta S_{\ddagger}^{rot}$, which represents the entropy counterpart of $\Delta H_{\ddagger}^{i}$.

3. Numerical examples are provided to show that the viscosity of liquids depends largely on the stereometric arrangement of molecular structure and only secondarily on the nature of the constituent atoms and resulting dipole moments (OH groups excepted). This result is shown to be caused by the determining influence of the purely geometrical factor $\Delta V_{\ddagger}$ upon $\Delta H_{\ddagger}^{h}$ and $\Delta S_{\ddagger}^{tr}$, and the presence of the product of the moments of inertia in $\Delta H_{\ddagger}^{i}$ and $\Delta S_{\ddagger}^{rot}$. These findings are believed to be significant for the planning of the syntheses of substances with given viscosity characteristics.

4. Viscosity data confirm the existence of fatty acids as double molecules in the liquid state at room temperature. The viscosity behavior of alcohols suggests the presence of distinguishable multiple molecules at low temperatures (below $-50°C$), and quite well-defined transition from this form to the continuous OH-bond network structure which prevails at ordinary temperatures.

5. It is pointed out that in all ordinary liquids the concentration $c_{\ddagger}/c$ of activated molecules is so small (10^{-6} to 10^{-2}) that the random oriented portion of otherwise well-ordered liquids can usually provide their entire number. This causes—contrary to expectation—the structure of a liquid, i.e., its state of order, to play only a minor role in the calculation of viscosity.

TABLE IX. $\Delta H_{\ddagger}^{i}$ values of castor oil.

t °C:	20/40	40/60	60/80	80/100	100/133
$\Delta H_{\ddagger}^{i}$ kcal./mole:	8.75	8.28	5.33	5.34	2.60

BIBLIOGRAPHY OF DATA

Where not noted otherwise, the constants inserted into the tables and figures of this paper have been computed from viscosity data by:

E. C. Bingham and L. C. Spooner, Physics **9**, 387 (1933).
P. W. Bridgman, *Physics of High Pressure* (1931).
R. B. Dow, Physics **6**, 71 (1935).
S. Kiesskalt, *VD1-Forchungsarbeiten H.* **291** (1927).
W. R. Mazee, T.O.M.-Reel No. 79, p. 2504 *et seq.*
R. W. Schiessler *et al.* Proc. A.P.I. **23**, 15 (1942); **24**, 49 (1943). [Also from reference 17.]
V. Wijk and Seeder, Physica **7**, 40 (1940).
Also from compressibility data by P. W. Bridgman, *Physics of High Pressure.*
R. B. Dow and C. E. Fink, J. App. Phys. **11**, 353 (1940).

THE JOURNAL OF CHEMICAL PHYSICS VOLUME 14, NUMBER 10 OCTOBER, 1946

Ultrasonic Propagation in Liquids: I. Application of Pulse Technique to Velocity and Absorption Measurements at 15 Megacycles*

J. R. PELLAM AND J. K. GALT
Research Laboratory of Electronics, Massachusetts Institute of Technology, Cambridge, Massachusetts
(Received July 8, 1946)

Equipment developed by the Massachusetts Institute of Technology Radiation Laboratory has been applied to the measurement of sound velocity and absorption in liquids at 15 mc/sec. Pulses of one microsecond duration are generated by a transducer, which also picks up the resultant echoes from a plane reflector. Velocity measurements are made by determining the distance the transducer must be moved to delay the received echoes by a specified increment. Absorption measurements are made by determining the attenuation necessary to keep the receiver signal constant as the transducer is moved. The attenuation factor can be measured to an accuracy of about 5 percent and sound velocity to about 0.05 percent. Measurements in homologous series of organic liquids are reported.

I. INTRODUCTION

THE electronic pulsed-circuit techniques and equipments developed during the war are adaptable to the measurement of velocity and absorption of sound in liquids.[1] Preliminary work of this nature took place at the M.I.T. Radiation Laboratory,[2] and the pulse principle has also been applied[3] to the examination of mechanical flaws in metals. For velocity determination in liquids the pulse method is at least as accurate as optical diffraction and acoustic interferometer methods previously employed,[4] and considerably more accurate for absorption measurements. It is direct and convenient and therefore particularly adapted to investigations involving large numbers of liquids. The present paper reports measurements of sound velocity and absorption in selected organic liquids at 15 mc/sec. and at several temperatures.

The scheme is essentially to use the liquid sample as a "storage medium" for short sound pulses and to measure the time delay and attenuation undergone by the sound in traversing a known path within the liquid. The acoustical pulses are generated from electrical pulses by means of a crystal transducer and are converted back to electrical form upon completing a transit through liquid; the effects of changing the acoustical path length can be compensated for electrically. Hence the increased delay produced by an increase in path length gives a measure of sound velocity; the attenuation which must be removed from the electrical circuit to balance acoustical losses in the additional distance provide a measure of absorption.

The variation in acoustic path length is accomplished by mounting the crystal transducer on a movable support riding within a tank containing a sample of the liquid. The 15 mc/sec. sound pulses, after being generated from electrical pulses by the transducer, travel through the liquid to a plane reflector and back again to re-excite the crystal at a later time. The resulting delayed electrical signal passes through a calibrated attenuator to a receiver, the output of which is fed to an oscilloscope equipped with a special sweep indicating time delays; the start of this sweep is synchronized with the generation of the original pulse, and calibrated accurately with respect to time. The change of the signal position on the screen as the transducer mount is moved with respect to the reflector is a direct measure of the corresponding delay; simultaneously, attenuation is inserted or removed by means of the calibrated attenuator to keep the receiver input signal constant.

Velocity is obtained directly from the slope of *distance traveled* plotted *vs. pulse delay*, and absorption is obtained from the slope of *compen-*

* This paper is based on work done for the Office of Scientific Research and Development under Contract OEMsr-262.

[1] This has been reported at the April 1946 meeting of the American Physical Society: J. R. Pellam and J. K. Galt, abstract A12.

[2] M. Cefola, M. E. Droz, S. Frankel, E. M. Jones, G. Maslach, and C. E. Teeter, Jr. Radiation Laboratory, M.I.T. Report 963, March, 1946.

[3] F. A. Firestone, Metal Progress **48**, 505 (1945). E. N. Simon, Metal Progress **48**, 513 (1945).

[4] L. Bergmann, *Der Ultrashall* (Edwards Brothers Reprint, Ann Arbor, Michigan, 1944).

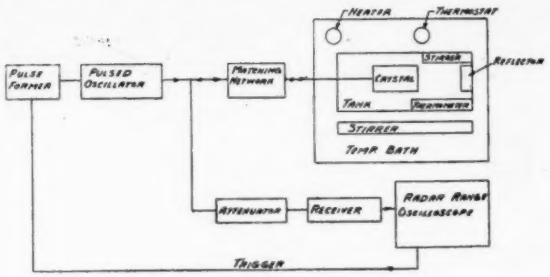

FIG. 1. Block diagram.

sating electrical attenuation vs. distance. Since the method depends only upon observing the effects of differences in acoustical path length, knowledge of exact distance traveled by the sound is unnecessary.

Results obtained in this manner may be regarded as physically equivalent to those obtained by continuous wave methods, since it may be shown that differences in behavior between pulsed sound and continuous sound in liquids should produce negligible effects. For example, no significant dispersion in liquids has been detected at these frequencies[4] (nor any pulse distortion during these measurements) so that the group velocities measured by pulsing should not differ measurably from the phase velocities ordinarily dealt with. Similarly, although attenuation of sound in liquids varies as the square of the frequency, the band width associated with the pulses used is small enough to prevent appreciable effect on absorption measurements.*

II. EQUIPMENT

(a) Electrical Equipment and Circuits

Figure 1 is a block diagram of the equipment and Fig. 2 is a photograph of the assembled apparatus. The timing sequence is as follows:

A crystal controlled circuit in the oscilloscope starts the scope sweep and simultaneously sends a trigger to the pulse generator. The pulse formed by the generator passes through a simple impedance matching network to the transducer; when the resulting sound pulse returns to the transducer after its round-trip within the liquid, the delayed electrical pulse is formed which passes back through the matching network. Since the transmitter is off when the echo signal arrives, very little leakage loss occurs and the main portion travels through the attenuator to the receiver.

All triggering and time measurements are accomplished by the crystal-controlled circuit in the oscilloscope (DuMont Type 256B A/R Range Scope), so that synchronization occurs automatically. In addition to setting off the pulse generator and starting the sweep, this circuit also provides marker pips spaced accurately every 12.192 microseconds thereafter (corresponding to 2000 yards radar range). Minute examination of the front edge of the echo signal is possible by means of an expanded sweep with variable delay and a speed of 1 inch per microsecond. Crystal control is necessary primarily for timing the marker pips accurately; one pip is developed for each oscillation, and since the crystal frequency is accurate to better than 1 part in 10,000 the same is true for the range marker positions.

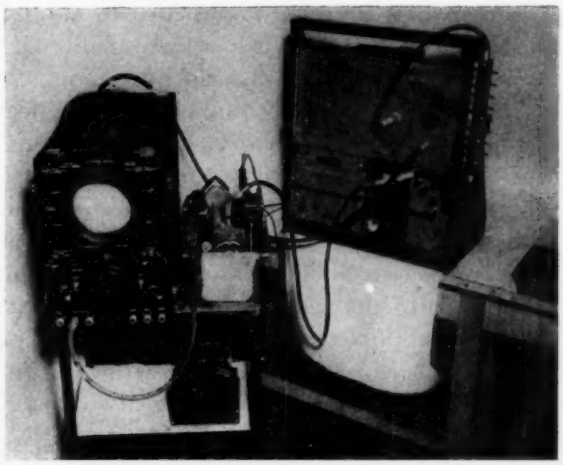

FIG. 2. Apparatus. Left: *A/R* range scope; center: liquid delay tank; and right: pulse forming network, oscillator, attenuator, and receiver.

* The exponential pressure attenuation coefficient (α), defined by

$$p = p_0 e^{-\alpha x}$$

will have a fractional error given by

$$\frac{\Delta\alpha}{\alpha} = \left(\frac{\Delta\nu}{\nu}\right)^2 \frac{\partial^2\alpha}{\alpha\partial\nu^2} = \left(\frac{\Delta\nu}{2\nu}\right)^2$$

if measured over a frequency range of width ($\Delta\nu$). The last term results from placing (α) proportional to frequency squared, as is frequently the case. It may be shown that, for pulses of much longer duration than the period of a single oscillation, $\Delta\nu/2\nu$ is just the reciprocal of the number of cycles per pulse. The pulses employed in the measurements reported here contained about 15 oscillations, corresponding to an error of roughly one part in 250.

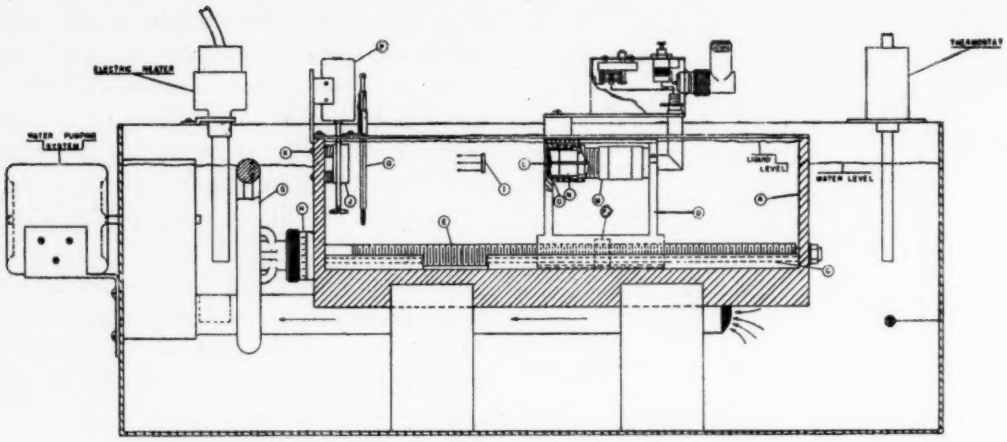

FIG. 3. Liquid delay tank.

The detailed discussion of the design of the pulse generator circuit has been given elsewhere.[5] The trigger from the oscilloscope passes through a stage of amplification to excite the second stage, a blocking oscillator. The output of the blocking oscillator, after being clipped to form a video pulse, is applied through a switch tube to the 15 mc/sec. r-f oscillator. The latter is driven into oscillation for the duration of the pulse, and the resultant r-f pulsed signal feeds through two stages of amplification. The final signal level put out to the transducer may be controlled by means of a variable power supply to the amplifier.

Since the electrical impedance presented by the crystal is very different from the 70-ohm characteristic impedance of the transmission line leading from the pulse generator, an impedance matching network[6] is provided to improve the response of the transducer. A small coil is used both as an autotransformer to match the line and as a means for tuning out the dead capacity of the crystal to give a purely resistive load (see Fig. 3). A coil of about 3 microhenries total inductance with a 6 to 1 turns ratio fulfills both requirements.

The receiver includes: (1) four stages of amplification at 15 mc/sec.; (2) a 15 mc/sec. local oscillator and mixer; (3) two stages of amplification at 30 mc/sec. (each stage consisting of three tubes with circuits tuned to slightly different frequencies for broad banding); (4) a detector; (5) two stages of video amplification; (6) a video amplifier in the oscilloscope. The 30 mc/sec. stages were used only because of equipment availability; a receiver operating at 15 mc/sec. throughout is now under construction.

The calibrated attenuator has steps of 1 db and up. Shielding is adequate to prevent leakage from introducing appreciable errors, even though attenuations as high as 110 db are inserted.

(b) Sound Delay Tank for Liquids

A sample of the liquid being investigated is placed in a sturdy brass tank (*A*) (see Fig. 3) within a constant temperature bath (*B*). The bottom of the tank is sufficiently thick ($\frac{1}{2}''$) to accommodate a milled track (*C*), with adjustable side plate for tightening, and upon which the transducer mount (*D*) travels. Motion is produced by turning the phosphor bronze micrometer screw (*E*) which threads through a stainless steel nut (*F*) set in the transducer mount. A hand-wheel (*G*) is provided and a dial (*H*) which indicates travel in thousandths of an inch. Calibration of the screw against size blocks makes it possible to read the transducer position significantly to 0.0001″.

The sound pulse (*I*) is reflected at the end of the tank by a disk (*J*) of stainless steel, ground and lapped optically flat. This reflector is supported by three adjustment screws (*K*), and may thereby be set perpendicular to the sound beam by aligning for maximum returned signal strength.

[5] S. Frankel, M.I.T. Radiation Laboratory Report 645–8.

[6] The authors are grateful to Messrs. Jones and Frankel of the Radiation Laboratory for the design constants used in this network.

The transducer element (L) is an X-cut 15 mc/sec. quartz crystal plate, $\frac{1}{2}''$ in diameter and gold plated on both sides. This crystal is held in place within a cartridge (M) by a Lucite bead (N) so that a diameter of about 1 cm is exposed to the liquid. A metal foil (O) between the bead and the quartz establishes electrical contact with the back surface.

(c) Temperature Control

Temperature equilibrium is maintained by balancing the effects of dry ice in the bath against the warming action of a thermostatically controlled electric heater. A water pumping system improves temperature uniformity outside the measuring tank, and a motor-driven stirrer (P) maintains constant temperature within the liquid sample itself. Temperature is read by thermometer (Q) and must be maintained to within less than 0.03°C for velocity measurements accurate to 0.01 percent.

III. MEASUREMENT TECHNIQUES

The velocity of sound within most organic liquids is of the order of 1.5×10^5 cm/sec. which corresponds at this frequency to about 100 wave-lengths per cm. Hence the crystal radiating surface is about 100 wave-lengths across, so that the pulses travel out within a very sharp beam (0.7° to the first minimum). It may be shown that this spread produces less than $\frac{1}{2}$ db of geometrical attenuation over the range employed; therefore readings of attenuation are suitable, without corrections, for computing liquid absorption coefficients directly.

Velocity readings are taken at 2000-yard (radar) range intervals by placing the returned signal pip at definite positions with respect to successive scope range markers, and recording the setting of the micrometer screw. By properly adjusting the scope these markers appear as very short (dark) breaks in the sweep, and if consistent positioning criteria are adopted, accurate range difference readings result. It turns out that careful adjustment of attenuation is necessary for consistent velocity readings. Consequently simultaneous readings for velocity and attenuation are preferable.

This interdependence between measurements exists because the signal pulses never build up instantaneously, even though they are sharp; as a result the front edge of the pulse may actually be shifted with respect to the range marker by varying the attenuation level. Therefore by adjusting attenuation to bring the signal peak always to the same arbitrary height on the screen (chosen within the linear range of scope amplification), the identical portion of the signal may be obscured by successive range markers Once this condition is satisfied, the crystal position may be set more precisely if a predetermined attenuation is then arbitrarily removed; this allows setting on a lower, and therefore steeper, portion of the pulse front. Consistent results are obtained in this manner providing the same quantity is removed for each range reading, and a value of 10 db was found convenient.

It is evident that if this adjustment of the returned signal to a pre-determined level is attained by means of the attenuator leading to the receiver (see Fig. 1) without disturbing the gain of the remainder of the system, absorption data follow as a by-product of the velocity measurements.

For accurate absorption readings the sharpness of the beam requires that (1) the reflector disk be adjusted carefully, and (2) temperature gradients within the liquid sample be avoided. *The proper operation of the stirrer* (P) *is absolutely*

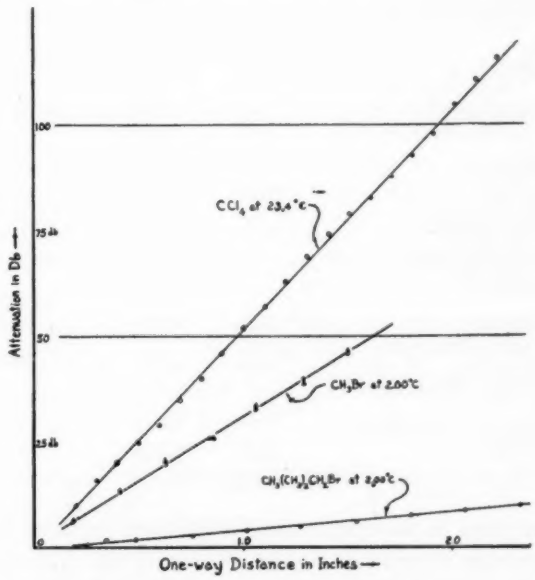

FIG. 4. Plot of sound attenuation *vs.* distance.

TABLE I. Experimental values of the pressure attenuation and velocity in liquids. Frequency $f=15$ mc/sec. $p=p_0 \exp[-\alpha x]$.

Substance	(1) Temp. °C	(2) Velocity cm/sec.	(3) Attenuation cm^{-1}	(4) $(\alpha/f^2)\times10^{17}$ sec²/cm experimental	(5) classical	(6) $\alpha^{-1}(\partial\alpha/\partial T)_p$ exper. $°C^{-1}$	(7) $c^{-1}(\partial c/\partial T)_p$ exper. $°C^{-1}$
Methyl bromide CH_3Br	2.0	0.905×10^5	0.684 (±1%)	304	—	—	
Ethyl bromide CH_3CH_2Br	2.0	0.959	0.136 (±5%)	61	10		
	10.0	0.932	0.14	62	—	+0.010	−0.0036
	20.0	—	0.14	62	10		
	30.0	—	0.18	80	—		
n-propyl bromide $CH_3CH_2CH_2Br$	2.0	1.0326	0.088 (±5%)	39	11	—	
n-butyl bromide $CH_3(CH_2)_2CH_2Br$	2.0	1.083	0.11 (±10%)	49	13	—	
Methyl iodine CH_3I	2.0	0.888	0.555 (±1%)	247	10		
	6.5	—	0.588	262	—		−0.0031
	20.0	—	0.711	316	—		
	30.0	0.815	0.751	334	—	+0.0087	
	35.0	—	0.765	340	—		
	40.0	—	0.776	345	—		
Ethyl iodide CH_3CH_2I	2.0	0.9235	0.09 (±10%)	40	12	—	
n-propyl iodide $CH_3CH_2CH_2I$	2.0	0.982	0.122 (±5%)	54	14	—	
n-butyl iodide $CH_3(CH_2)_2CH_2I$	2.0	1.022	0.109 (±5%)	48	17	—	
n-propyl chloride $CH_3CH_2CH_2Cl$	2.0	1.158	0.095 (±10%)	42	8	—	
n-butyl chloride $CH_3(CH_2)_2CH_2Cl$	2.0	1.213	0.242 (±2%)	108	10	—	
Methyl acetate (Pract) CH_3COCH_3	19.0	1.195	0.16 (±3%)	71	6	—	
Ethyl acetate (Pract) $CH_3COC_2H_5$	24.3	1.145	0.163 (±3%)	72	8	—	
Amyl acetate (Pract) $CH_3COC_5H_{11}$	29.2	1.173	0.167 (±7%)	74	14	—	
Methyl alcohol CH_3OH	2.0	1.186	0.10 (±15%)	45	15	−0.011	−0.0032
	19.3	1.123	0.084 (±10%)	37	14		
Ethyl alcohol CH_3CH_2OH	2.0	1.246	0.052 (±10%)	23	29		
n-propyl alcohol $CH_3CH_2CH_2OH$	2.0	1.288	0.195 (±2%)	87	55		−0.0028
	27.5	1.1976	0.157 (±3%)	70	36	−0.0086	
n-butyl alcohol $CH_3(CH_2)_2CH_2OH$	2.0	1.324	0.240 (±5%)	54	65		
n-amyl alcohol $CH_3(CH_2)_3CH_2OH$	2.8	1.320	0.348 (±2%)	155	113		
	28.6	1.224	0.231	106	58	−0.014	−0.0029
Benzene C_6H_6	7.5	1.382	1.52 (±3%)	680	9		
	21.8	1.3116	1.79 (±1%)	800	8	+0.011	−0.0036
Nitrobenzene $NO_2C_6H_5$	7.5	1.518	0.165 (±5%)	73	16		
	23.8	1.462	0.178 (±4%)	79	14	+0.0048	−0.0023
Chlorobenzene C_6H_5Cl	7.5	1.333	0.276 (±1%)	123	10		
n-hexane $CH_3(CH_2)_4CH_3$	21.2	1.085	0.174 (±5%)	77	10		
n-heptane $CH_3(CH_2)_5CH_3$	22.4	1.150	0.18 (±10%)	80	10		
Carbon tetrachloride CCl_4	23.5	0.924	1.20 (±1%)	533	20		

essential to the temperature uniformity required for accurate absorption measurements. If the stirrer is stopped there is an immediate change in signal level and non-linear absorption curves result. The heat developed by attenuation within the beam contributes to these refraction effects.

IV. RESULTS

(a) Linearity of Absorption Curves

Curves of attenuation *vs.* range are given in Fig. 4 for three sample liquids, indicating the degree of linearity found (over a range exceeding 100 db for CCl_4). No effects attributable to geometrical divergence of the beam are evident; the limit of accuracy appears to depend upon the smallest attenuation increment used (1 db) as suggested by the small systematic variation about a straight line.

(b) Summary of Measurements

Part I of this paper is concerned only with the presentation of measurements in the form of raw data, interpretation being reserved for Part II. However, these results are given in terms of quantities or parameters possessing physical significance in view of Part II.

Table I is a summary of measurements obtained for the various series of related organic compounds investigated. The velocity is given in column (2) in units of cm/sec. and the absorption coefficients (α) in column (3) in units of cm^{-1}. (α) is the exponential pressure attenuation coefficient defined by

$$p = p_0 e^{-\alpha x}. \tag{1}$$

Since for a number of liquids (α) varies nearly as the frequency squared, a convenient form for comparing measured results with those computed from classical (viscosity) theory is given in column (4). The classical absorption values were calculated considering viscosity effects alone; heat conduction will increase these values by about 5 percent. Columns (6) and (7) give the experimental temperature coefficients for (α) and velocity, respectively.

These particular series of homologous compounds were chosen with a view to observing the gross effects of substitutions within molecules (such as the revelation for example that replacing an $-H$ in benzene by a $-Cl$ cuts absorption by a factor of 5, and that an $-NO_2$ cuts it by 9). The most complete array examined was the alkyl halide group, of which 10 members were included (the 2°C was chosen just below the boiling point of methyl bromide).

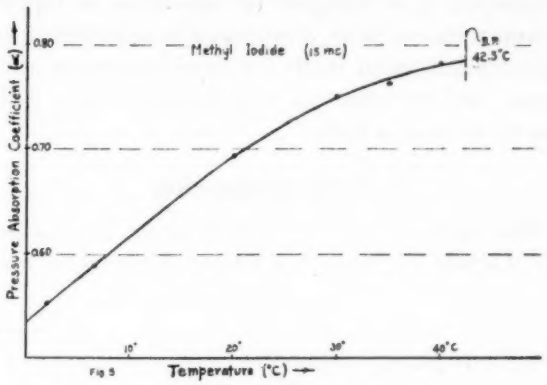

FIG. 5. Sound pressure absorption coefficient α *vs.* temperature.

(c) Accuracy

Velocity results are given here to an accuracy of about 1 part in 1000. It is believed, however, that the pulse method is inherently capable of yielding as high accuracy for velocity measurements as the best diffraction techniques. On the other hand, whereas previous techniques were often incapable of exceeding 25 percent accuracy in absorption measurements, the absorption is given here to about 5 percent on the average. Since the limit of this accuracy is set by the smallest attenuation increment, best results occur for highly absorbing liquids since they provide a greater attenuation range. Thus for liquids such as CCl_4 (α) is given to about 1 percent, but is accurate only to about 10 percent for liquids exhibiting low absorption.

(d) Temperature Dependance of Absorption

The pulse method for measuring (α) is sufficiently accurate for investigating the effects of temperature. For example Fig. 5 shows the absorption coefficient for methyl iodide plotted against temperature (for values up to the boiling point). Temperature coefficients may be obtained from such curves and, as shown in Part II of this paper, have considerable significance with regard to the mechanism of sound propagation.

V. REMARKS

(a) Anticipated Measurements

A new apparatus for measuring velocity and attenuation by the pulse technique has just been

completed. It is designed for operation at liquid helium temperatures. Preliminary measurements have already been made for liquid nitrogen and argon, and measurements in liquid helium will shortly be under way.

(b) Acknowledgments

The authors wish to express their thanks to Mr. Gerald Holton of Harvard University for aid with the measurement runs and to Miss Ruth Roman and Mr. J. E. Krasinski, Electronics Laboratory, for technical assistance. The ultrasonic measurement program was arranged through the cooperation of Professor J. A. Stratton, Director of the Research Laboratory of Electronics, and Professor R. H. Bolt, Director of the Acoustics Laboratory. The encouragement and advice of Professor P. M. Morse is gratefully acknowledged.

THE JOURNAL OF CHEMICAL PHYSICS VOLUME 14, NUMBER 10 OCTOBER, 1946

Ultrasonic Propagation in Liquids. II. Theoretical Study of the Free Volume Model of the Liquid State*

CHARLES KITTEL
Research Laboratory of Electronics, Massachusetts Institute of Technology, Cambridge, Massachusetts
(Received July 8, 1946)

The free volume theory of liquids is applied to problems connected with sound propagation. The equation of state derived by Tonks for assemblies of hard elastic spheres may be written $pV_a \cong 3NkT$, where the *available volume* V_a is the difference between the actual volume and the volume corresponding to the closest possible packing. It is shown that the molar available volume is approximately given by the increase in molar volume of a substance on heating from 0°K to the temperature considered, so that the pictorial concept of the available volume has a real physical basis. Using the Tonks equation, expressions are derived for the sound velocity, and the temperature and pressure coefficients of sound velocity. These expressions are compared with experimental results. Expressions are also given for the cubic expansion coefficient and the difference of the specific heats on the free volume model. The Herzfeld-Rice derivation of the sound absorption caused by phase shifts in the vibrational specific heat is carried through for the Tonks equation of state. The temperature and pressure coefficients of sound absorption are discussed. Remarks are made on the relation of molecular structure to sound absorption.

I. INTRODUCTION

THE purpose of this paper is to describe the velocity and absorption of ultrasonic waves in liquids in terms of the free volume theory of liquids and the relaxation theory of absorption processes. It is emphasized at the beginning that simple models of liquids may not be expected to give close numerical agreement with observation. We should, however, require that the model give the correct order of magnitude of physical quantities and their variations. This test we propose to apply to the free volume theory of liquids. The implications of the theory with respect to the mechanical properties of liquids have not previously been considered, to the author's knowledge.

The important experimental facts regarding ultrasonic propagation in liquids are summarized below:

(a) The velocity of sound in a liquid is commonly of the order of five to ten times the velocity in the vapor at the same temperature. For example, the velocity of sound in liquid oxygen[1] at 90°K is 910 m/sec., while the velocity in oxygen vapor[2] at the same temperature is 180 m/sec.

(b) The temperature coefficient of sound velocity $c^{-1}(\partial c/\partial T)_p$ is of the order of -3×10^{-3} °C^{-1}; in gases the temperature coefficient is of the same order but is positive.

(c) The pressure coefficient of sound velocity $c^{-1}(\partial c/\partial p)_T$ is of the order of $+5\times10^{-10}$ cm^2/dyne.

(d) The absorption of sound waves in liquids usually exceeds the classical value calculated on the basis of

* This paper is based on work done for the Office of Scientific Research and Development under Contract OEMsr-262.

[1] H. W. Liepmann, Helv. Phys. Acta **9**, 507 (1936).
[2] A. van Itterbeek and P. Mariëns, Physica **4**, 207 (1937).

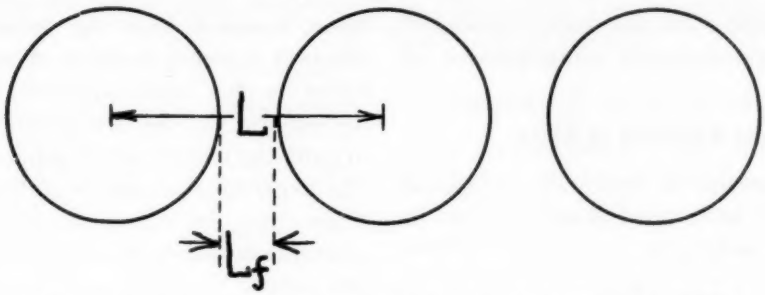

FIG. 1. Intermolecular separation L and free length L_f on Eyring model.

ordinary viscosity losses; in the case of CS_2, for example, the observed value is several thousand times greater than the classical value.

(e) The temperature coefficient of sound absorption $\alpha^{-1}(\partial\alpha/\partial T)_p$ is of the order of ± 0.01 °C^{-1}. Both positive and negative signs occur, whereas on classical theory the sign is always negative, as the viscosity has a negative temperature coefficient.

(f) The pressure coefficient of sound absorption $\alpha^{-1}(\partial\alpha/\partial p)_T$ is -6×10^{-10} cm^2/dyne for toluene, the only liquid for which a determination has been reported.

The two traditional concepts of the liquid state regard a liquid as either a very dense gas or else as a solid in which the long range order between the molecules has broken down. Both of these concepts account qualitatively for the two distinguishing properties of liquids; namely, that a liquid combines the small shear modulus characteristic of gases with the small compressibility characteristic of solids. To explain in a convenient and natural manner the origin of other physical properties of liquids, such as fusion, viscosity, dielectric constant, density, and solution effects, sometimes the gas and sometimes the solid point of view is used.

In understanding the propagation of sound in liquids the gas model is particularly suitable. It turns out that sound velocities can be predicted qualitatively from this model; and, further, the absorption of sound in liquids can be related to the absorption processes in gases, which are fairly well understood. On the other hand, the absorption processes in solids are poorly explained at the present time.

II. SOUND VELOCITY

The relationship between the velocity of sound in the liquid and gaseous states has been made plausible by the work of Eyring and his collaborators,[3] who have given a simple and useful explanation of the relation in terms of the gas model. The relation is derived by Eyring in a qualitative way and is not quite correct; later on we shall consider a rigorous equation of state for this model from which the sound velocity can be calculated unambiguously.

Eyring pictures the sound wave as traveling with infinite velocity within a molecule and with gas kinetic velocities through the space between the molecules of the liquid (Fig. 1). This space is termed the "available volume." The molecules effectively short-circuit a part of the path of the sound wave. If the intermolecular separation is L and the "free length" L_f, the molecules short-circuit all but the fraction L_f/L of the path. The sound velocity in the liquid is then given by

$$c_{\text{liq}} = (L/L_f)c_{\text{gas}}, \tag{1}$$

where kinetic theory gives

$$c_{\text{gas}}^2 = \gamma_{\text{gas}}(RT/M), \tag{2}$$

with $\gamma_{\text{gas}} = C_p/C_v$, the ratio of specific heats in the gas.

The reasoning leading to Eq. (1) from the specified properties of the model is not rigorous. It is possible to derive a rigorous equation of state for the free volume model, and this has been done by Tonks[4] in a paper on the statistical mechanics of assemblies of hard elastic spheres. Recently, Rice[5] and Frank[6] have drawn attention to the importance of Tonks' work in relation to

[3] H. Eyring and J. O. Hirschfelder, J. Phys. Chem. **41**, 249 (1937); J. F. Kincaid and H. Eyring, J. Chem. Phys. **5**, 587 (1937), **6**, 620 (1938); J. O. Hirschfelder, D. P. Stevenson, and H. Eyring, J. Chem. Phys. **5**, 896 (1937).

[4] L. Tonks, Phys. Rev. **50**, 955 (1936).

[5] O. K. Rice, J. Chem. Phys. **10**, 653 (1942); **12**, 1 (1944); **14**, 335 (1946).

[6] H. S. Frank, J. Chem. Phys. **13**, 478 (1945).

theories of the liquid state and have considered some of the thermodynamic consequences of the model.

The Tonks Equation of State

The Tonks equation of state for a classical three-dimensional gas of hard elastic spheres in the limit of close packing is

$$pV(1-\theta^{\frac{1}{3}})=NkT, \tag{3}$$

where θ is the packing fraction with respect to the closest possible packing. We have $\theta=V_0/V=1-(V_a/V)$, where V_0 is the minimum possible volume and V_a, the *available volume*, is defined as $V-V_0$. For close packing as in a liquid

$$1-\theta^{\frac{1}{3}}\cong V_a/3V. \tag{4}$$

In this approximation the equation of state becomes

$$pV_a=3NkT. \tag{5}$$

The form

$$p=(3RT/M)\rho_1, \tag{6}$$

where

$$\frac{1}{\rho_1}=\frac{1}{\rho}-\frac{1}{\rho_0} \tag{7}$$

is also useful. Here ρ_0 is the density corresponding to the closest possible packing.

The remarkable and simple form Eq. (5) which the equation of state assumes makes it easy to deduce various properties of the model. This form does not appear to have been stated explicitly before.

Before using Eq. (5) we shall consider its physical significance as applied to actual liquids. The pressure p is understood to be made up of two terms, one representing the effect of the attractive intermolecular forces and the other representing the external applied pressure. Let us imagine the intermolecular potential energy to be altered by removing the attractive part of the potential while leaving the repulsive part; the "internal pressure" may then be regarded as that pressure which would compress the system to the volume actually occupied. The implied relationship between internal pressure and temperature is plausible on the free volume model, since the internal pressure does balance the kinetic pressure of the molecules regarded as moving freely within the volume. It is not obvious, however, that the thermal expansion at constant external pressure should be given correctly by the Tonks equation. This amounts to the assumption that the balancing pressure due to potential energy is independent of the volume. The experimental checks of Eqs. (10) and (15) below may be taken as justification of this assumption within the generous limits of error of this paper.

It is important to note that what is called the *available volume* V_a in this paper is not identical with the *free volume* V_f as customarily defined, although the same model is used. The available volume is the difference between the actual volume and the minimum possible volume and is given by $V(1-\theta)$; the free volume is defined[3-5] as the volume of possible motion of the center of a single molecule, and is given, per mole, by $V(1-\theta^{\frac{1}{3}})^3$. For close packing $V_f\cong V_a(V_a^2/27V^2)$. The available volume is a natural quantity to use in the equation of state; the free volume is a natural quantity to use in the partition function. The numerical values of the free volume given by Kincaid and Eyring are defined in terms of an approximate equation for sound velocity in liquids; the use of the more exact equation below will necessitate small changes in the numerical values.

The velocity of sound is given in the usual way by $c^2=(\partial p/\partial\rho)_S=(\rho_1/\rho)^2(\partial p/\partial\rho_1)_S$, so that

$$c_{\text{liq}}=\left(\frac{V}{V_a}\right)\left(\frac{C_v+3R}{C_v}\right)^{\frac{1}{2}}\left(\frac{3RT}{M}\right)^{\frac{1}{2}}=\left(\frac{V}{V_a}\right)\left(\frac{3\gamma_{\text{liq}}}{\gamma_{\text{gas}}}\right)^{\frac{1}{2}}c_{\text{gas}}, \tag{8}$$

where γ_{liq} has been set equal to $(C_v+3R)/C_v$, in accordance with Eq. (16). It may be noted that c_{liq} and c_{gas} are to be taken at the same temperature.

Calculation of Sound Velocity

It is not practical to give a direct comparison of Eq. (8) with measurements of sound velocity in liquids since there is no really accurate independent method for determining the available or the free volume (see, however, Kincaid and Eyring[3]). We may, however, make an estimate of the available volume by considering the

TABLE I. Comparison of available volume as calculated from thermal expansion and sound velocity data for 300°K.

Substance	Available volume increments cc/mole V_1 0°K to melting point	V_2 fusion volume change	V_3 melting point to 300°K	Calculated available volume in cc/mole derived from thermal expansion [Eq. (10)]	sound velocity [Eq. (8)]
$CHBr_3$	8	10	(2)	20	19
CCl_4	11	4	5	20	28
Benzene	10	10.3	2.5	23	25

Notes: Thermal expansion and fusion volume change data are from the Landolt-Börnstein tables. V_1 is based on a linear extrapolation of measured values obtaining between 80°K and 200°K; this overestimates the change at low temperatures (since by the Nernst theorem the expansion coefficient must vanish at 0°K) and underestimates the change at high temperatures. No allowance has been made for any effective "zero-point" available volume.

increase in volume between absolute zero and the temperature concerned.

If we are to take the free volume picture seriously there should exist some correlation between the *molar available volume* as calculated using Eq. (8) from sound velocity measurements at room temperature and the actual *increase in molar volume* of the material between 0°K and room temperature. Such a relationship does in fact exist.

We write

$$V = V_0 + V_a, \tag{9}$$

where V_0 is the molar volume corresponding to the closest possible packing in a geometrical sense, and V_a is the molar available volume. Let

$$V_a = V_1 + V_2 + V_3, \tag{10}$$

where

V_1 = molar volume change on heating solid from 0°K to the melting point;
V_2 = molar volume change on fusion; and
V_3 = molar volume change on heating liquid from melting point to the temperature concerned.

Unfortunately the expansion data from which the V's can be calculated are inadequate, and a certain amount of guesswork enters into any estimate of the available volume based on thermal expansion data. A comparison of available volumes as calculated from sound velocity and thermal expansion data is given in Table I. The agreement is as good as can be expected.

This evidence shows that the pictorial concept of the available volume has a real physical basis. It is in principle possible to give an approximate calculation of sound velocities from thermal expansion data alone.

Temperature Coefficient of Sound Velocity

We may determine the available volume from the sound velocity at one temperature and using this value compare the calculated with the experimental value of the temperature coefficient of sound velocity $c^{-1}(\partial c/\partial T)_p$. The velocity of sound in liquids has usually a *negative* temperature coefficient; that is, the velocity decreases with increasing temperature. This is contrary to the position with gases, which show a positive temperature coefficient. In terms of the free volume picture of a liquid the effect of the increased distance the molecules have to travel, owing to thermal expansion, dominates the increase in molecular velocity.

We may derive an expression for the temperature coefficient of sound velocity on the free volume model. From Eqs. (2) and (8),

$$c^{-1}(\partial c/\partial T)_p = V^{-1}(\partial V/\partial T)_p - V_a^{-1}(\partial V_a/\partial T)_p + (2T)^{-1} + (2\gamma_{\text{liq}})^{-1}(\partial \gamma_{\text{liq}}/\partial T), \tag{11}$$

where the variation in γ_{gas} is neglected. Now ΔV is essentially equal to ΔV_a, since the expansion of the molecules themselves may be neglected in comparison with the expansion of the available volume. Writing A for the temperature coefficient of cubic expansion,[7] we have

$$c^{-1}(\partial c/\partial T)_p = (2T)^{-1} - A[(V/V_a) - 1] + (2\gamma_{\text{liq}})^{-1}(\partial \gamma_{\text{liq}}/\partial T)_p; \tag{12}$$

this equation may be written in terms of observables by using Eq. (8):

$$c^{-1}(\partial c/\partial T)_p = (2T)^{-1} - A\left\{\left(\frac{\gamma_{\text{gas}}}{3\gamma_{\text{liq}}}\right)^{\frac{1}{3}}\left(\frac{c_{\text{liq}}}{c_{\text{gas}}}\right) - 1\right\} + (2\gamma_{\text{liq}})^{-1}(\partial \gamma_{\text{liq}}/\partial T)_p. \tag{13}$$

A detailed comparison of experimental values of the temperature coefficient with calculated values from Eq. (13) is given in Table II. The purpose in giving this and other tables is not in

[7] The conventional symbol for both the cubic expansion coefficient and the pressure attenuation coefficient is α; in this paper, A is used for the cubic expansion coefficient to avoid confusion.

TABLE II. Temperature coefficient of sound velocity $c^{-1}(\partial c/\partial T)_p$—comparison of Eq. (13) deduced from the Tonks equation with experimental values (data for $T=300°K$).

Substance	C_p/C_v gas	C_p/C_v liq.	Cubic exp. coef. °C^{-1}	c_{liq}/c_{gas}	V/V_a	$\gamma_{liq}^{-1}(\partial\gamma_{liq}/\partial T)_p$	Temp. coef. of sound vel. °C^{-1} exper.	calc.
Amyl acetate	(1.2)	1.33	1.16×10^{-3}	7.47	4.1	?	-4.8×10^{-3}	-1.9×10^{-3}
Benzene	1.08	1.44	1.24	7.00	3.5	-0.6×10^{-3}	−3.6	−1.7
Carbon disulfide	1.24	1.56	1.20	5.54	2.8	+1.2	−2.8	−0.0
Carbon tetrachloride	1.08	1.46	1.23	6.93	3.4	−0.6	−3.4	−1.6
Chlorobenzene	(1.2)	1.35	0.98	7.42	4.0	−0.8	−2.9	−1.7
Ethyl alcohol	1.11	1.18	1.10	6.12	3.4	−0.2	−3.0	−1.1
Heptane	(1.2)	1.19	1.24	6.35	3.6	?	−3.7	−1.6
Methyl iodide	(1.2)	(1.3)	1.24	5.40	3.1	?	−3.1	−0.9
Nitrobenzene	(1.2)	(1.3)	0.83	8.96	5.0	?	−2.3	−1.6
Toluene	(1.2)	1.34	1.1	6.92	3.8	−1.5	−3.3	−2.1
Water	1.32	1.00	0.117	3.50	2.3	?	+1.7	+1.5

Notes: Values of C_p/C_v in parentheses are assigned arbitrarily; other values from E. Hiedemann *Ultraschallforschung* (Walter de Gruyter and Company, Berlin, 1939). Cubic expansion coefficients are from the Landolt-Börnstein tables. Temperature variation of γ_{liq} from E. B. Freyer, J. C. Hubbard, and D. H. Andrews, J. Am. Chem. Soc. 51, 759 (1929). Experimental values of the temperature coefficient of sound velocity are taken from Hiedemann's book and from the preceding paper by J. R. Pellam and J. K. Galt. The values used for c_{gas} are calculated from Eq. (2).

order to emphasize specific cases of agreement or disagreement, but rather to exhibit the consequences of the free volume equation of state. It seems likely that Eq. (5) will find wide use in problems of the liquid state, so that it is well to understand some of the limitations and capabilities of the equation.

It is seen that the calculated values are in order of magnitude agreement with the measurements, but that the calculated values underestimate the value somewhat. It is significant that the order of magnitude of the results derived from the simple model of hard elastic spheres is correct, and that the existence of an "anomalous" positive temperature coefficient for water is correctly indicated by the theory. This agreement is attributed to the use of experimental values of the thermal expansion coefficient, rather than the theoretical values given by Eq. (15) below.

Pressure Coefficient of Sound Velocity

It is of interest to consider the pressure coefficient of sound velocity $c^{-1}(\partial c/\partial p)_T$. Using the Tonks equation we find

$$c^{-1}(\partial c/\partial p)_T=\beta_T[(V/V_a)-1]$$

$$=\beta_T\left\{\left(\frac{\gamma_{gas}}{3\gamma_{liq}}\right)^{\frac{1}{2}}\left(\frac{c_{liq}}{c_{gas}}\right)-1\right\}, \qquad (14)$$

where β_T is the isothermal compressibility and is equal to γ_{liq} times the adiabatic compressibility. The variation of γ_{liq} with pressure should probably be considered, but relevant data could not be found. A comparison of experimental with theoretical values is given in Table III, from which it appears that the predictions of the theory are slightly low. The positive sign of the pressure coefficient arises because the sound path through the available volume is shortened by compressing the volume.

The fact that both the temperature and pressure coefficients of velocity as calculated are somewhat low suggests that the available volume is overestimated by the sound velocity equation.

III. DISCUSSION OF FREE VOLUME THEORY

It is appropriate at this point to discuss the basis for the application of the Tonks equation of state to actual liquids. Five main assumptions underlie this application:

(a) It is assumed that the internal structure of the molecule is "hard"—that is, the internal compressibility of a molecule is neglected in comparison with the compressibility of the system as a whole. This assumption is justifiable.*

(b) It is assumed that the molecules are spherical. It should be possible to generalize the derivation of the equation of state to describe other shapes.

(c) It is assumed that the compressibility of the molecules with respect to each other—that is, the inter-

* The internal compressibility of a molecule β_{mole} is of the order of L/k, where L is the length of the molecule and k is the force constant. The force constant is given by $k=(2\pi f)^2 m$, where the frequency f is a fundamental vibration frequency of the molecule and is of the order of 1000 cm^{-1} or 3×10^{13} c.p.s.; m is the reduced mass of the molecule and is of the order of 3×10^{-23} g for a light molecule. With these values $k\sim10^6$ dynes/cm, so that $\beta_{mole}\sim10^{-14}$ cm^2/dyne, which is to be compared with $\beta_{gas}\sim10^{-10}$ cm^2/dyne under the equivalent pressures obtaining in a liquid.

molecular compressibility—is purely kinetic in origin. The repulsive forces are imagined to rise sharply at the boundary of the hard sphere. This is quite a drastic assumption.

(d) It is assumed that the internal pressure arising from the attractive intermolecular forces is approximately independent of volume. This is also a drastic assumption.

(e) The Tonks derivation is based on classical mechanics, and no account is given of quantum effects. It is almost certain that quantum effects are of considerable importance in liquids, since the spacing between the energy levels of a molecule confined within its own free volume is of the order of kT for room temperature.[8]

In the light of the assumptions which have been made it is of interest to consider further consequences of the Tonks equation. We have already seen that the equation leads to values of the temperature and pressure coefficients of sound velocity which are correct to within an order of magnitude at least.

Thermal Expansion Coefficient

The measure of agreement with experiment attained by the calculated values of the temperature coefficient of velocity may be attributed in part to the use of experimental values of the cubic expansion coefficient when substituting in Eq. (13) to obtain the results displayed in Table II; this is particularly true with respect to water. We may, however, calculate the cubic expansion coefficient from the Tonks equation of state, obtaining

$$A = V^{-1}(\partial V/\partial T)_p = (V_a/V)(1/T). \qquad (15)$$

TABLE III. Pressure coefficient of sound velocity $c^{-1}(\partial c/\partial p)_T$—comparison of calculated values from Eq. (14) with experimental values.

Substance	Adiabatic compressibility cm²/dyne	Pressure coefficient of sound velocity cm²/dyne experimental	calculated
Carbon disulfide	59.0×10^{-12}	3.7×10^{-10}	1.7×10^{-10}
Carbon tetrachloride	74.5	4.7	2.7
Ether	138.7	7.7	3.1
Ethyl bromide	88.1	5.7	2.1
Methyl acetate	80.9	2.7	2.0
Benzene	64.9	3.1	2.3
Toluene	68.2	3.2	2.7

Notes: Values of the adiabatic compressibility are from Hiedemann's book. Experimental values of the pressure coefficient of sound velocity are from J. C. Swanson, J. Chem. Phys. **2**, 689 (1934), except for the value for methyl acetate, which is from P. Biquard, Comptes rendus (Paris) **206**, 897 (1938).

[8] E. Bartholomé and A. Eucken, Trans. Faraday Soc. **33**, 45 (1937).

TABLE IV. Cubic expansion coefficient—comparison of calculated values from Eq. (15) with experimental values $-V^{-1}(\partial V/\partial T)_p$ in °C⁻¹.

Substance	V/V_a	Cubic expansion coefficient experimental	calculated
Benzene	3.5	1.24×10^{-3}	0.95×10^{-3}
Carbon disulfide	2.8	1.20	1.19
Carbon tetrachloride	3.4	1.23	0.98
Chlorobenzene	4.0	0.98	0.84
Ethyl alcohol	3.4	1.10	0.98
Mercury	6.4	0.18	0.52
Methyl iodide	3.1	1.24	1.07
Water	2.3	0.12	1.45
Water (400°K)	(2.3)	0.97	(1.1)

Notes: The data are for $T=300$°K. The values of the ratio of the volume to the free volume (V/V_a) are from Table II.

A comparison of experimental with theoretical values is given in Table IV. The agreement is excellent for the organic liquids, but is poor for water and mercury, as might be expected. We have neglected entirely the role of the metallic electrons, so that the present discussion is often inapplicable to liquid metals. Water is anomalous in general behavior at room temperature and below, but near the boiling point the calculated value of the cubic expansion coefficient is in good agreement with experiment.

Difference of Specific Heats ($C_p - C_v$)

Using Eq. (5) we may compute the difference $(C_p - C_v)$ for the Tonks equation, finding

$$C_p - C_v = p(\partial V_a/\partial T)_p = 3R \qquad (16)$$

instead of simply R which obtains for an ideal gas. A comparison is given in Table V of experimental with theoretical values of the difference $(C_p - C_v)$. The agreement in the case of the liquefied gases is good except for the case of hydrogen, where quantum effects are of importance. For the organic liquids the calculated $(C_p - C_v)$ of 6 cal./mole/°C is generally low. With regard to C_v, one might expect on the basis of the free volume model that C_v would be equal in the liquid and gaseous states at the same temperature. It is well known,[8] however, that C_v is greater in the liquid state.

IV. SOUND ABSORPTION

The two principal mechanisms responsible for the absorption of sound in liquids are the ordinary shearing viscosity and the energy loss associated

with incomplete excitation of vibrational energy states of the molecules. In many liquids the latter mechanism is the dominant cause of attenuation. A detailed bibliography of the literature concerned with incomplete vibrational excitation in gases has been given by Richards.[9] The theory developed for gases was first applied to liquids by Mandelstam and Leontovic,[10] and later extended by Kneser.[11] Herzfeld[12] has given an interesting discussion of absorption in liquids, while Tisza[13] has considered the important implications of the subject with respect to the hydrodynamical equations.

The program of this section is to give a physical order-of-magnitude estimate of the maximum absorption expected from relaxation processes; to go through a detailed calculation of absorption for the Tonks equation of state; to consider the temperature and pressure coefficients of absorption; and, finally, to discuss the relation between sound absorption and molecular structure.

It is possible to make a simple estimate of the maximum absorption caused by relaxation of a vibrational mode. The average value of the energy in a sound wave is of the order of $\Delta p \Delta V$. Now $\Delta p/p = -\Delta V/V + \Delta T/T$ for an ideal gas, where the first term on the right represents "mechanical" effects and the second term "thermal" effects of the pressure. For an adiabatic process the ratio of the thermal term to the mechanical term is $(\gamma-1)$, where γ is the ratio of the specific heats. Let C_i be the specific heat associated with the relaxing degree of freedom; then C_i/C_v represents the fraction of thermal energy in the mode concerned, and $(C_i/C_v)(\gamma-1)/\gamma$ is an approximate upper limit to the fraction of the total energy of the sound wave dissipated in one cycle. We should of course find absorptions of this order of magnitude only in the neighborhood of the relaxation frequency characterizing the exchange of energy between translational and vibrational degrees of freedom.

Let us compare this estimate of the peak absorption with some experimental values. For CO_2 gas we have $(\gamma-1)/\gamma \sim 0.23$, and $C_i/C_v \sim 0.3$, so that about 0.07 of the energy is dissipated per cycle. This means that the intensity is down $1/e$ in about 14 wave-lengths; using data for high frequencies we should estimate 8 wave-lengths. Measurements by Fricke[14] show that at the relaxation frequency of 20 kc/sec. the intensity is down by $1/e$ in about 4 wave-lengths, indicating that our order of magnitude estimate is generally correct. The famous example of a highly absorbing low viscosity liquid is CS_2, for which the measured absorption[15] at 1 mc/sec. is about 2000 times the classical value as calculated from viscosity and heat conduction losses alone; yet at this frequency the intensity is only down by $1/e$ in 50 wave-lengths. At 7 mc/sec. the intensity[16] is down by $1/e$ in about 12 wave-lengths; this value appears quite reasonable in the light of the above estimates.

TABLE V. Comparison of experimental values of $(C_p - C_v)$ with calculated values from Eq. (16).

Substance	C_p expt.	C_p/C_v expt.	(C_p-C_v) cal./mole/°C expt.	calc.
Argon (87°K)	10.0	2.2	5.5	6
Oxygen (90°K)	13.0	1.7	5.3	6
Nitrogen (76°K)	13.6	2.0	6.6	6
Hydrogen (20°K)	6.9	1.5	2.5	6
Benzene	31.6	1.44	9.7	6
Carbon tetrachloride	30.7	1.46	9.7	6
Ether	40.6	1.33	10.0	6
Ethyl alcohol	27.	1.18	4.2	6
n-heptane	49.	1.19	7.8	6
n-propyl alcohol	35.6	1.16	5.0	6
Toluene	37.8	1.34	10.0	6

Notes: The data are for 300°K unless otherwise specified. Experimental values of C_p/C_v are from L. Bergmann, *Der Ultraschall* (Edwards Brothers reprint, Ann Arbor, 1944).

Absorption in Liquids on Free Volume Model

It is instructive to calculate the absorption in detail for the free volume model of the liquid state, applying the method of Herzfeld and Rice[17] to the Tonks equation of state, Eq. (5). In a sense the calculation is but a formal extension of the treatment of absorption in gases developed by Herzfeld and Rice, and others. Let C_i be the specific heat of the relaxing mode of vibration,

[9] W. T. Richards, Rev. Mod. Phys. **11**, 36 (1939).
[10] L. Mandelstam and M. Leontovic, Comptes rendus (Doklady) Acad. Sci. U.S.S.R. **3**, 111 (1936).
[11] H. O. Kneser, Ann. d. Physik **32**, 277 (1938).
[12] K. F. Herzfeld, J. Acous. Soc. Am. **13**, 33 (1941).
[13] L. Tisza, Phys. Rev. **61**, 531 (1942).
[14] E. F. Fricke, J. Acous. Soc. Am. **12**, 245 (1940).
[15] J. Claeys, J. Errera, and H. Sack, Trans. Faraday Soc. **33**, 136 (1937).
[16] S. Parthasarathy, Current Sci. **6**, 501 (1938).
[17] K. F. Herzfeld and F. O. Rice, Phys. Rev. **31**, 691 (1928).

and C_e the specific heat of all the other degrees of freedom of the molecule. Let T' denote the effective temperature of the energy associated with C_i, and T the temperature associated with C_e. Losses owing to ordinary viscosity and heat conduction are not considered; it can be shown that these are additive to the first approximation.

From the Tonks equation of state,

$$p=3RT\rho_1/M; \quad (1/\rho_1)=(1/\rho)-(1/\rho_0). \quad (17)$$

The force equation gives the particle acceleration

$$\partial u/\partial t=-(1/\rho)(\partial p/\partial x) =-(3RT/M)(\rho_1/\rho)[(\partial \ln T/\partial x) +(\partial \ln \rho_1/\partial x)], \quad (18)$$

while the conservation equation is

$$\partial \ln \rho/\partial t=-\partial u/\partial x=(\rho/\rho_1)(\partial \ln \rho_1/\partial t). \quad (19)$$

From the first law of thermodynamics

$$C_e(\partial T/\partial t)+C_i(\partial T'/\partial t)=(pM/\rho_1^2)(\partial \rho_1/\partial t). \quad (20)$$

The relaxation time constant τ' is introduced* through the equation

$$C_i(\partial T'/\partial t)=C_i(T-T')/\tau'. \quad (21)$$

We consider small changes in ρ_1, T and T', and suppose that the small changes are of the form $\exp[j(\omega t-kx)]$, where $k=k_1-jk_2$. On substituting in Eqs. (17) through (21) we find an expression for k^2. For the technique of the calculation Herzfeld and Rice many be consulted. The imaginary part of k^2 is $-2k_1k_2$, where

$$2k_1k_2=\omega^2(M/3RT)(\rho/\rho_1)^2 \times\left\{\frac{\omega\tau}{1+(\omega\tau)^2}\cdot\frac{\gamma^\infty-\gamma^0}{\gamma^0\gamma^\infty}\right\}. \quad (22)$$

Here

$$\tau=\tau'(C_i/C_v^0)(\gamma^\infty/\gamma^0); \quad \gamma^0=C_p^0/C_v^0; \quad \gamma^\infty=C_p^\infty/C_v^\infty.$$

The low frequency specific heat C_v^0 is given by C_i+C_e, while the high frequency specific heat C_v^∞ is simply C_e.

Now $k_1\cong\omega/c_{liq}$, where the sound velocity c_{liq} is given by Eq. (8). Also, $k_2=\alpha$, where α is the ordinary pressure attenuation coefficient in the expression $p=p_0\exp[-\alpha x]$ for the damping of a plane wave. We have finally

$$\alpha=(\pi f^2/c_{liq})\left\{\frac{3R}{C_p^\infty}\frac{C_i}{C_v^0}\frac{f_0}{f^2+f_0^2}\right\}, \quad (23)$$

where $f=\omega/2\pi$ and $f_0=1/2\pi\tau$; here $C_p-C_v=3R$ from Eq. (16).

The maximum absorption per wave-length occurs when $f=f_0$ and is given by

$$(c_{liq}/f)\alpha_{max}=\frac{\pi}{2}\frac{C_p-C_v}{C_p^\infty}\frac{C_i}{C_v^0}, \quad (24)$$

which is of the same form as the previous estimate reached by a qualitative argument.

At low frequencies ($f\ll f_0$) we have

$$\alpha=f^2(\pi/f_0c_{liq})\frac{C_p-C_v}{C_p^\infty}\frac{C_i}{C_v^0}, \quad (25)$$

so that at low frequencies α/f^2 is constant for the attenuation caused by the relaxation mechanism, just as for viscosity and heat conduction. These results are in agreement with those of Kneser and Herzfeld, when slight differences in definitions are taken into account.

Temperature Coefficient of Sound Attenuation

Experimental determinations of the temperature coefficient of attenuation in different liquids show both positive and negative values. Where relaxation is a minor factor, a negative coefficient is found owing to the decrease in viscosity with increasing temperature. Where relaxation is the predominant factor, a positive coefficient is expected when the frequency is above the relaxation frequency, and a negative coefficient when the frequency is below the relaxation frequency. This is because a rise in temperature increases the probability of energy transfer and thus increases the relaxation frequency. If $f>f_0$, an increase in f_0 brings the region of maximum absorption nearer to the measurement frequency; the opposite holds if $f<f_0$. The actual situation, however, may be more complicated.

Considering only relaxation losses we find from Eq. (23):

$$\alpha^{-1}(\partial\alpha/\partial T)_p\cong\pm f_0^{-1}(\partial f_0/\partial T)_p +C_i^{-1}(\partial C_i/\partial T)_p-2C_v^{-1}(\partial C_v/\partial T)_p -c_{liq}^{-1}(\partial c_{liq}/\partial T)_p, \quad (26)$$

* For simplicity all of the modes of internal motion are supposed to relax at the same frequency, in which case C_i includes the whole of the vibrational specific heat.

TABLE VI. Temperature coefficient of sound absorption—interpretation of results in terms of Eq. (26)—frequency 15 mc/sec.

Substance	Temp. coef. $\alpha^{-1}(\partial\alpha/\partial T)_p$ °C^{-1}	$\alpha_{\text{exper}}+\alpha_{\text{classical}}$	Tentative interpretation
Ethyl bromide	+0.010	7	Dominant factor is change in f_0, the relaxation frequency. $f_0<15$ mc/sec.
Methyl iodide	+0.0087	30	Fundamental vibrational frequency of CH_3I molecule is fairly low (534 cm^{-1}), so that specific heat change is not important; f_0 is dominant factor. $f_0<15$ mc/sec.
Methyl alcohol	−0.011	3	Change in viscosity contributes only −0.004; velocity contributes +0.003; specific heat term is positive, so that at least −0.010 must be accounted for by f_0 change. $f_0\gg 15$ mc/sec., in agreement with Herzfeld,[a] who concludes on other grounds that $f_0\sim 3\times 10^4$ mc/sec.
n-propyl alcohol	−0.0086	2	As for methyl alcohol, $f_0\gg 15$ mc/sec.
n-amyl alcohol	−0.014	1.5	Changes in both viscosity and f_0 are probably effective here. The absorption is nearly classical. $f_0\gg 15$ mc/sec.
Benzene	+0.011	90.	The evidence of the temperature coefficient of absorption is that $f_0<15$ mc/sec., yet Herzfeld indicates that $f_0\sim 2000$ mc/sec. It is possible that these figures represent two different relaxation modes, the mode with a weak absorption peak near 10 mc/sec. having a predominant effect on the temperature coefficient. Such a peak is suggested by a plot of α *vs.* f based on collected results. Kneser[b] gives $f_0>55$ mc/sec.

[a] See reference 12 in text.
[b] See reference 11 in text.

where the plus sign before the term $f_0^{-1}(\partial f_0/\partial T)_p$ applies to the case $f\gg f_0$, and the minus sign applies when $f\ll f_0$. The intermediate case is more complicated. Consider now the magnitude of the term arising from f_0: Landau and Teller[18] show that under certain assumptions

$$f_0 \propto \exp\left[-3(\pi a\nu)^{2/3}(M/2kT)^{1/3}\right], \qquad (27)$$

where a is the atomic radius, M the mass of the molecule, and ν the frequency of the vibrational mode. The exponential factor gives essentially the probability of exchange of vibrational and translational energy in a collision, and comes out to be of the order of 10^{-4} to 10^{-6}, in agreement with the experimental results for gases, where a collision frequency of the order of 10^{10} collisions per second is associated with relaxation frequencies of the order of 10^5 cycles per second. From Eq. (27) we have

$$f_0^{-1}(\partial f_0/\partial T)_p = q/3T, \qquad (28)$$

where q is the argument of the exponential factor in the above equation. Since q is of the order of 10, we have $f_0^{-1}(\partial f_0/\partial T)_p\sim 10^{-2}$.

Let us consider the order of magnitude of the other terms in Eq. (26). The term arising from c_{liq} is of the order of 3×10^{-3} and may usually be neglected. The two terms in the specific heat may be combined in one, since $\Delta C_v\cong\Delta C_i$, giving $(\partial C_i/\partial T)_p(C_i^{-1}-2C_v^{-1})$. Since the specific heat C_i usually corresponds to a vibration, it is given by an Einstein function. The relative slope of an Einstein function varies from very steep at low temperatures to flat at high temperatures. For molecules containing at least two non-hydrogen atoms we are up near the flat part of the curve at room temperature, and the contribution of the change in specific heat to $\alpha^{-1}(\partial\alpha/\partial T)_p$ will be of the order of 5×10^{-3} or less. It therefore appears that the term arising from f_0 often may be the most important single contribution; in some cases, however, the term in the specific heat may be significant.

In liquids for which the viscosity η is a major factor contributing to the attenuation a term arising from η of the order of 10^{-2} must be considered. Including viscosity, the attenuation α as given by Eq. (23) is increased by the additive Stokes term $8\pi^2 f^2\eta/3c^3\rho$.

Measurements of the temperature coefficient of absorption have been reported by Pellam and Galt,[19] Bazulin,[20] Sörenson,[21] Baumgardt,[22] and

[18] L. Landau and E. Teller, Physik. Zeits. Sowjetunion **10**, 34 (1936); cf. C. Zener, Phys. Rev. **38**, 277 (1931).

[19] J. R. Pellam and J. K. Galt, "Ultrasonic propagation in liquids. I. Application of pulse technique to velocity and absorption measurements at 15 megacycles," J. Chem. Phys. **14**, 608 (1946).

[20] P. Bazulin, Comptes rendus (Doklady) Acad. Sci. U.S.S.R. **14**, 273 (1937).

[21] C. Sörenson, Ann. d. Physik **27**, 70 (1936).

[22] E. Baumgardt, Comptes rendus (Paris) **202**, 203 (1936).

Hunter.[23] An interpretation of the results of Pellam and Galt is given in Table VI.

Study of the table suggests that the temperature coefficient of sound absorption is a useful quantity in the study of molecular relaxation times. The indications are not always unambiguous, but in the absence of more complete experimental knowledge of the acoustic absorption spectrum of liquids the temperature coefficient provides pertinent information.

Pressure Coefficient of Sound Attenuation

The pressure coefficient of sound attenuation in toluene has been determined by Biquard[24] who measured the absorption at 7 mc/sec. between pressures of 1 to 500 atmos., giving $\alpha^{-1}(\partial\alpha/\partial p)_T = -6\times10^{-10}$ cm^2/dyne. At one atmosphere $\alpha/f^2 = 80\times10^{-17}$ sec.^{2} cm^{-1}, as compared with the classical value 8×10^{-17}, suggesting that the principal part of the absorption may be ascribed to relaxation processes. On the assumption that $f \ll f_0$ and that changes in specific heat may be neglected, we have from Eq. (25)

$$\alpha^{-1}(\partial\alpha/\partial p)_T = -f_0^{-1}(\partial f_0/\partial p)_T - c^{-1}(\partial c/\partial p)_T. \quad (29)$$

Now f_0 at constant temperature is proportional to the collision frequency, so that

$$-f_0^{-1}(\partial f_0/\partial p)_T = L_f^{-1}(\partial L_f/\partial p)_T = -(V/3V_a)\beta_T, \quad (30)$$

where L_f is the free length as in Fig. 1. The magnitude of the term in f_0 is 1×10^{-10}, while the term in the sound velocity c is 3×10^{-10}. The calculated value of $\alpha^{-1}(\partial\alpha/\partial p)_T$ comes out to be -4×10^{-10} cm^2/dyne, in fair agreement with the experimental value -6×10^{-10} cm^2/dyne.

The physical interpretation of the result is that the molecules are brought closer together by the application of pressure, thus increasing the collision and relaxation frequencies. If $f<f_0$ an increase in f_0 moves the region of maximum absorption away from the working frequency. Also, the wave-length is increased by pressure, so that the absorption per unit length will decrease even if the absorption per wave-length is constant.

[23] J. L. Hunter, J. Acous. Soc. Am. **13**, 36 (1941).
[24] P. Biquard, Rev. d'Acoustique **8**, 130 (1939).

Sound Absorption and Molecular Structure

According to present ideas the magnitude of the non-classical part of the attenuation is determined by the position and magnitude of the relaxation frequencies of the molecule. It is difficult to calculate these frequencies since they are dependent upon the detailed coupling between different modes of motion. In gases it is well-confirmed experimentally that the relaxation mechanism accounts for most of the non-classical absorption. Relaxation frequencies in pure gases are of the order of 10^3-10^5 c.p.s.; since "collisions" in liquids are at least 10^3 more frequent than in gases we would expect relaxation frequencies in liquids to be of the order of 10^7 c.p.s. The indication of the present evidence is that the actual frequencies are of this order or higher. The existence of well-defined vibrational states in liquid molecules is known from infra-red and Raman spectra evidence.

A review of the absorption of sound in various liquids at 15 mc/sec. shows several regularities with regard to molecular structure.

(a) The three most absorbing liquids of low viscosity are *non-polar*—CS_2, CCl_4, benzene.

Substance	$\alpha_{exper}/\alpha_{classical}$
CS_2 (7 mc/sec.)	~600
CCl_4	25
Benzene	90

Other non-polar liquids are highly absorbing—heptane, hexane, toluene. This tendency suggests that the coupling of translational and vibrational motion is small in molecules with small electrostatic interactions, giving a long lifetime to the vibrational state and a low relaxation frequency.

(b) Highly associated liquids tend to show low, near-classical absorption at 15 mc/sec. The alcohols and water are good examples of associated liquids, and they show the following values:

Substance	$\alpha_{exper}/\alpha_{classical}$
Methyl alcohol	3
Ethyl alcohol	1
Propyl alcohol	2
Butyl alcohol	1
Amyl alcohol	1.5
Water	3

This tendency suggests that the formation of molecular groups is conducive to the transfer of

vibrational energy and therefore leads to high relaxation frequencies. This is expected. In the limiting case of a solid there is little distinction between translational energy of molecules with respect to one another and vibrational energy internal to a molecule. In solids we have relaxation times of the order of 10^{-12} sec., as estimated from heat conductivity data.

CONCLUSIONS

It is found that the Tonks equation of state as applied to liquids is a suitable framework for making close order-of-magnitude estimates concerning quantities involved in sound propagation. The detailed numerical agreement is usually unsatisfactory, thus indicating the limitations of the model. In particular the temperature and pressure dependence of the compressibility is given only roughly by this model. On the other hand, the thermal expansion coefficient is given quite accurately; also, it is possible to attach physical significance to the concept of the available volume.

ACKNOWLEDGMENTS

It is a pleasure to thank Professor George Kimball of Columbia University and Professor L. Tisza for suggestions on the manuscript. The ultrasonics research program was arranged through the cooperation of Professor J. A. Stratton, Director of the Research Laboratory of Electronics, and Professor R. H. Bolt, Director of the Acoustics Laboratory. The encouragement and advice of Professor P. M. Morse is gratefully acknowledged.

THE JOURNAL OF CHEMICAL PHYSICS VOLUME 14, NUMBER 10 OCTOBER, 1946

A Theoretical Evaluation of Normal Frequencies of Vibration of the Isomeric Octanes[1]

CHARLES O. AHONEN
Lehigh University, Bethlehem, Pennsylvania
(Received June 26, 1946)

A theoretical evaluation of some of the normal frequencies of vibration of the isomeric octanes has been made. This report gives the skeletal frequencies for those of the eighteen isomeric octanes which lead to representations having 7 or fewer frequencies. The forces are assumed to be valence forces. The force constants used are 4.12×10^5 dynes per cm for the C−C bond stretching, and 0.37×10^5 dynes per cm for the bending between two C−C bonds, the values being based on computations by the author for *n*-propane, using the experimental data of E. F. Barker and Violet L. Wu. The angle between two C−C bonds was taken as 107° whenever possible. The results of this investigation are summarized by means of charts, showing the location of bands calculated. For the molecules reported all normal skeletal frequencies for a valence force model were evaluated, and attempts at correlation between experimental and theoretical bands have been made.

INTRODUCTION

IT has been shown[2] that for small oscillations which are assumed to be simple harmonic the frequencies obtained on the basis of classical mechanics are identical with those obtained by quantum mechanics. For this reason, it is still customary to use classical theory of small oscillations to obtain the normal frequencies of vibration of molecules.

In obtaining the frequencies belonging to normal modes of vibration, it is assumed that the potential energy is a function of the displacement coordinates, and, in order to express this function explicitly, it is necessary to make use of a definite force model. The earliest model used was the central force model, in which the potential energy depends only on the changes in the distances which separate the atoms of the molecule. It was found, however, that such a model is not adequate to represent the force field, as far as the study of vibration spectra is concerned. In the valence force model the atoms are connected by valence bonds, and it is assumed that a change in angle between two bonds, as well as a change in the length of a bond, results in an increase in potential energy. The valence force model has been more successful in the treatment of vibration spectra, though it is still, at best, an approximation, and the results obtained with it cannot be expected to be identical with experimental values. It is found, for example, that in many cases zero frequencies arise, caused by the fact that, for the force field chosen, the displacements of the atoms from the equilibrium positions give rise only to terms of third or higher order in the potential function. If additional forces, such as those restricting free rotation about bonds, were introduced these zero frequencies might be removed. The actual frequencies, though not exactly zero, should, if the valence force model is any good at all, be very small. The frequencies obtained are to be regarded as approximations, the force model being too crude to obtain exact results.

In the following discussion, a molecule is assumed to consist of n atoms bound to equilibrium positions by valence forces. The atoms are bound together in such a way that a change in length of a valence bond by an amount ΔL gives rise to an increase in potential energy of $\frac{1}{2}Kcc|\Delta L|^2$, and a change $\Delta\theta$ in the angle between two valence bonds meeting at a single atom results in an increase in potential energy of $\frac{1}{2}K_\theta(\Delta\theta)^2$. Hence, the total increase in potential energy, because of an arbitrary change, is

$$V=\tfrac{1}{2}\sum Kcc|\Delta L|^2+\tfrac{1}{2}\sum K_\theta(\Delta\theta)^2,$$

where the summation extends over all valence bonds in the first term and over all valence angles in the second term.

[1] This research was completed at the Harrison M. Randall Laboratory of Physics, University of Michigan, Ann Arbor, Michigan, 1945.
[2] D. M. Dennison, "Infrared spectra of polyatomic molecules," Rev. Mod. Phys. **3**, No. 2 (April, 1931).

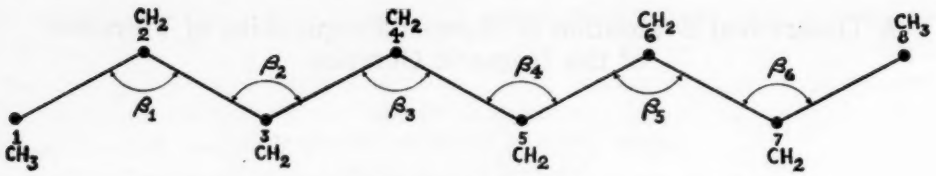

FIG. 1. Skeletal form of *n*-octane. $\beta_1°=\beta_2°=\beta_3°=\beta_4°=\beta_5°=\beta_6°=107°$.

The isomeric octanes constitute a group of saturated hydrocarbons, each possessing 8 carbon and 18 hydrogen atoms. The direct application of the above theory to a molecule of that type would lead to a secular determinant of order 72, and, even with the aid of group theory, a complete determination of the frequencies would present a task too formidable to be attempted. It has been found, however, that the skeletal frequencies obtained by considering the hydrogen atoms frozen to the carbon atoms are not much changed. In the present discussion, all hydrogen atoms are considered frozen to the carbon atoms, thus reducing the original system in each case to a system of 8 mass points, made up of the combined masses of 1 carbon and 3 or fewer hydrogen atoms. The present paper gives the skeletal frequencies of those isomeric octanes which belong to point groups of higher symmetry than the C_s. For the C_s group, the frequencies belonging to the lower ordered representations have also been worked out, but will not be reported here.

In general, the atoms constituting a hydrocarbon tend to stretch out and form a rather symmetric pattern, as has been indicated by measurement on oil films. The molecules are assumed to consist of zigzag chains arranged as symmetrically as possible, and since the effect of the C−H bonds is eliminated, the distinction between optical isomers is ignored. No systematic experimental spectra are available which distinguish the optical isomers, and it is felt that significant information is obtained about the skeletal frequencies with the forms chosen. The angles in the main chains of the molecules are taken as 107° in the equilibrium position, though in some cases this had to be altered because of symmetry considerations. Values for the angles between valence bonds ranging from 99° to 116° have been used by other investigators for various molecules involving CH_3 groups.[3] Although the angle would vary with position, 107° was chosen, somewhat arbitrarily, as representative, this value having been used with some success as the tetrahedral angle for certain hydrocarbons. Four types of masses occur, representing the masses of C, CH, CH_2, and CH_3 groups, respectively. The values for these masses were determined from the masses of the hydrogen and carbon atoms given by R. T. Birge.[4] The values used are

$$\begin{aligned}
&C = 19.93\times10^{-24}\text{ g},\\
&CH = (19.93+1.673)\times10^{-24}\text{ g} = 21.6\times10^{-24}\text{ g},\\
&CH_2 = (19.93+2\times1.673)\times10^{-24}\text{ g}\\
&\qquad = 23.3\times10^{-24}\text{ g},\\
&CH_3 = (19.93+3\times1.673)\times10^{-24}\text{ g}\\
&\qquad = 24.9\times10^{-24}\text{ g}.
\end{aligned}$$

The force constants used are based on computations by the author on *n*-propane, using the experimental data of E. F. Barker and Violet L. Wu.[5] The values chosen as best suited for the octanes are

For C—C stretching, $Kcc = 4.12\times10^5$ dynes/cm.

For $\begin{matrix}C\\ \diagdown\\ C\\ \diagup\\ C\end{matrix}$ bending, $K_\theta = .37\times10^5$ dynes/cm.

TABLE I. Table of characters.

C_{2h}	E	C_2	σ_h	i	Raman	Infra-red	No.
$\Gamma^{(1)}\sim A_G$	1	1	1	1	P	IA	7
$\Gamma^{(2)}\sim B_G$	1	−1	−1	1	DP	IA	2
$\Gamma^{(3)}\sim A_u$	1	1	−1	−1	F	A	3
$\Gamma^{(4)}\sim B_u$	1	−1	1	−1	F	A	6
ϕ_R	0	π	0	π			
U_R	8	0	8	0			
$\pm1+2\cos\phi_R$	3	−1	1	−3			
$\chi(R)$	24	0	8	0			
Ξ	18	2	8	0			

[3] K. W. F. Kohlrausch, *Der Smekal-Raman Effekt* (Verlagsbuchhandlung, Julius Springer, Berlin, 1938).

[4] Raymond T. Birge, "A new table of values of the general physical constants," Rev. Mod. Phys. **13**, 233 (1941).

[5] E. F. Barker and Violet L. Wu, "The infra-red absorption spectrum of propane," J. Chem. Phys. **9**, No. 7, 490 (July, 1941).

MOLECULES BELONGING TO THE POINT GROUP C_{2h}

N-Octane[6] (Table I, Fig. 1)

Representation $\Gamma^{(1)}$: The values obtained for the 7 bands belonging to this representation are

$$\frac{1}{\lambda_1}=200.0\ \text{cm}^{-1},\quad \frac{1}{\lambda_4}=955.7\ \text{cm}^{-1},$$

$$\frac{1}{\lambda_2}=224.3\ \text{cm}^{-1},\quad \frac{1}{\lambda_5}=1053\ \text{cm}^{-1},$$

$$\frac{1}{\lambda_3}=443.4\ \text{cm}^{-1},\quad \frac{1}{\lambda_6}=1054\ \text{cm}^{-1},$$

$$\frac{1}{\lambda_7}=1127\ \text{cm}^{-1}.$$

Representation $\Gamma^{(2)}$: Because of the choice of potential function, the values obtained for the 2 bands belonging to this representation are

$$\frac{1}{\lambda_1}=0\ \text{cm}^{-1},\quad \frac{1}{\lambda_2}=0\ \text{cm}^{-1}.$$

Representation $\Gamma^{(3)}$: Because of the choice of potential function, the values obtained for the 3 bands belonging to this representation are

$$\frac{1}{\lambda_1}=0\ \text{cm}^{-1},\quad \frac{1}{\lambda_2}=0\ \text{cm}^{-1},\quad \frac{1}{\lambda_3}=0\ \text{cm}^{-1}.$$

Representation $\Gamma^{(4)}$: The values obtained for the 6 bands belonging to this representation

TABLE II. Table of characters.

C_{2h}	E	C_2	σ_h	i	Raman	Infrared	No.
$\Gamma^{(1)}\sim A_G$	1	1	1	1	P	IA	6
$\Gamma^{(2)}\sim B_G$	1	−1	−1	1	DP	IA	3
$\Gamma^{(3)}\sim A_u$	1	1	−1	−1	F	A	4
$\Gamma^{(4)}\sim B_u$	1	−1	1	−1	F	A	5
ϕ_R	0	π	0	π			
U_R	8	0	4	0			
$\pm 1+2\cos\phi_R$	3	−1	1	−3			
$\chi(R)$	24	0	4	0			
Ξ	18	2	4	0			

[6] Details of the calculation for this, as well as for the other molecules are given in a thesis submitted by the author to the Horace H. Rackham School of Graduate Studies, University of Michigan, 1945.

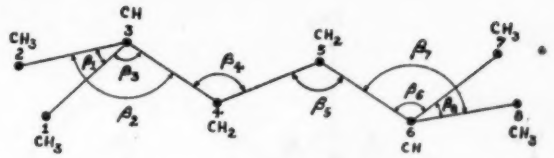

FIG. 2. Skeletal form of 2-5-dimethylhexane. $\beta_1^\circ=\beta_2^\circ=\beta_3^\circ=\beta_4^\circ=\beta_5^\circ=\beta_6^\circ=\beta_7^\circ=\beta_8^\circ=107°$.

are

$$\frac{1}{\lambda_1}=86.16\ \text{cm}^{-1},\quad \frac{1}{\lambda_4}=986.3\ \text{cm}^{-1},$$

$$\frac{1}{\lambda_2}=344.0\ \text{cm}^{-1},\quad \frac{1}{\lambda_5}=996.7\ \text{cm}^{-1},$$

$$\frac{1}{\lambda_3}=396.6\ \text{cm}^{-1},\quad \frac{1}{\lambda_6}=1104\ \text{cm}^{-1}.$$

2-5-Dimethylhexane (Table II, Fig. 2)

Representation $\Gamma^{(1)}$: The values obtained for the 6 bands belonging to this representation are

$$\frac{1}{\lambda_1}=0\ \text{cm}^{-1},\quad \frac{1}{\lambda_4}=851.3\ \text{cm}^{-1},$$

$$\frac{1}{\lambda_2}=217.9\ \text{cm}^{-1},\quad \frac{1}{\lambda_5}=1032\ \text{cm}^{-1},$$

$$\frac{1}{\lambda_3}=367.1\ \text{cm}^{-1},\quad \frac{1}{\lambda_6}=1146\ \text{cm}^{-1}.$$

Representation $\Gamma^{(2)}$: The values obtained for the 3 bands belonging to this representation are

$$\frac{1}{\lambda_1}=0\ \text{cm}^{-1},\quad \frac{1}{\lambda_2}=376.0\ \text{cm}^{-1},\quad \frac{1}{\lambda_3}=1113\ \text{cm}^{-1}.$$

Representation $\Gamma^{(3)}$: The values obtained for the 4 bands belonging to this representation are

$$\frac{1}{\lambda_1}=0\ \text{cm}^{-1},\quad \frac{1}{\lambda_4}=257.9\ \text{cm}^{-1},$$

$$\frac{1}{\lambda_2}=0\ \text{cm}^{-1},\quad \frac{1}{\lambda_5}=1061\ \text{cm}^{-1}.$$

Representation $\Gamma^{(4)}$: The values obtained for the 5 bands belonging to this representation

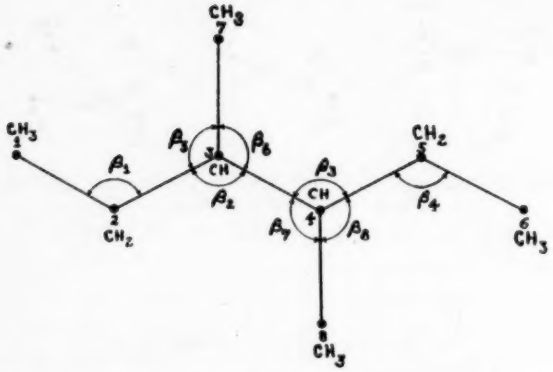

FIG. 3. Skeletal form of 3-4-dimethylhexane. $\beta_1^\circ=\beta_2^\circ=\beta_3^\circ=\beta_4^\circ=107^\circ$. $\beta_5^\circ=\beta_6^\circ=\beta_7^\circ=\beta_8^\circ=126.5^\circ$

are

$$\frac{1}{\lambda_1}=152.6\ \text{cm}^{-1},\quad \frac{1}{\lambda_4}=883.7\ \text{cm}^{-1},$$

$$\frac{1}{\lambda_2}=372.6\ \text{cm}^{-1},\quad \frac{1}{\lambda_5}=1124\ \text{cm}^{-1}.$$

$$\frac{1}{\lambda_3}=426.8\ \text{cm}^{-1},$$

3-4-Dimethylhexane (Table III, Fig. 3)

Representation $\Gamma^{(1)}$: The values obtained for the 7 bands belonging to this representation are

$$\frac{1}{\lambda_1}=222.2\ \text{cm}^{-1},\quad \frac{1}{\lambda_4}=670.9\ \text{cm}^{-1},$$

$$\frac{1}{\lambda_2}=276.4\ \text{cm}^{-1},\quad \frac{1}{\lambda_5}=1005\ \text{cm}^{-1},$$

$$\frac{1}{\lambda_3}=429.7\ \text{cm}^{-1},\quad \frac{1}{\lambda_6}=1274\ \text{cm}^{-1},$$

$$\frac{1}{\lambda_7}=1369\ \text{cm}^{-1}.$$

Representation $\Gamma^{(2)}$: Because of the choice of potential function, the values obtained for the 2 bands belonging to this representation are

$$\frac{1}{\lambda_1}=0\ \text{cm}^{-1},\quad \frac{1}{\lambda_2}=0\ \text{cm}^{-1}.$$

Representation $\Gamma^{(3)}$: Because of the choice of potential function, the values obtained for the 3 bands belonging to this representation are

$$\frac{1}{\lambda_1}=0\ \text{cm}^{-1},\quad \frac{1}{\lambda_2}=0\ \text{cm}^{-1},\quad \frac{1}{\lambda_3}=0\ \text{cm}^{-1}.$$

Representation $\Gamma^{(4)}$: The values obtained for the 6 bands belonging to this representation are

$$\frac{1}{\lambda_1}=146.1\ \text{cm}^{-1},\quad \frac{1}{\lambda_4}=856.5\ \text{cm}^{-1},$$

$$\frac{1}{\lambda_2}=255.9\ \text{cm}^{-1},\quad \frac{1}{\lambda_5}=1031\ \text{cm}^{-1},$$

$$\frac{1}{\lambda_3}=554.9\ \text{cm}^{-1},\quad \frac{1}{\lambda_6}=1208\ \text{cm}^{-1}.$$

MOLECULES BELONGING TO THE POINT GROUP C_{2v}

4-Methylheptane (Table IV, Fig. 4)

Representation $\Gamma^{(1)}$: The values obtained for the 7 bands belonging to this representation are

$$\frac{1}{\lambda_1}=109.6\ \text{cm}^{-1},\quad \frac{1}{\lambda_4}=743.6\ \text{cm}^{-1},$$

$$\frac{1}{\lambda_2}=239.2\ \text{cm}^{-1},\quad \frac{1}{\lambda_5}=984.2\ \text{cm}^{-1},$$

$$\frac{1}{\lambda_3}=410.5\ \text{cm}^{-1},\quad \frac{1}{\lambda_6}=1089\ \text{cm}^{-1},$$

$$\frac{1}{\lambda_7}=1288\ \text{cm}^{-1}.$$

Representation $\Gamma^{(2)}$: The values obtained for the 6 bands belonging to this representation

TABLE III. Table of characters.

C_{2h}	E	C_2	σ_h	i	Raman	Infra-red	No.
$\Gamma^{(1)}\sim A_G$	1	1	1	1	P	IA	7
$\Gamma^{(2)}\sim B_G$	1	−1	−1	1	DP	IA	2
$\Gamma^{(3)}\sim A_u$	1	1	−1	−1	F	A	3
$\Gamma^{(4)}\sim B_u$	1	−1	1	−1	F	A	6
ϕ_R	0	π	0	π			
U_R	8	0	8	0			
$\pm1+2\cos\phi_R$	3	−1	1	−3			
$\chi(R)$	24	0	8	0			
Ξ	18	2	8	0			

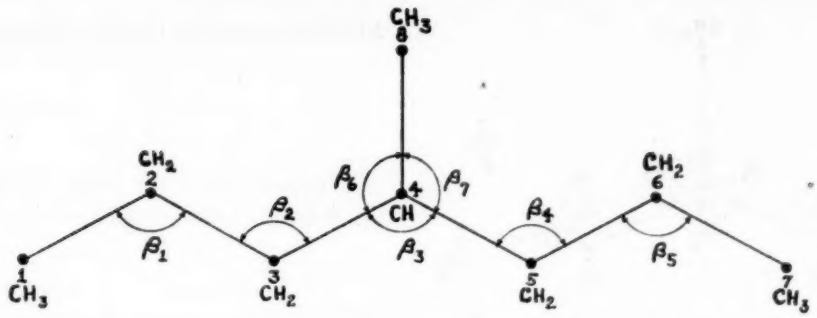

FIG. 4. Skeletal form of 4-methylheptane. $\beta_1^\circ=\beta_2^\circ=\beta_3^\circ=\beta_4^\circ=\beta_5^\circ=107°$. $\beta_6^\circ=\beta_7^\circ=126.5°$.

are

$$\frac{1}{\lambda_1}=245.5\ \text{cm}^{-1},\quad \frac{1}{\lambda_4}=898.6\ \text{cm}^{-1},$$

$$\frac{1}{\lambda_2}=288.5\ \text{cm}^{-1},\quad \frac{1}{\lambda_5}=1034\ \text{cm}^{-1},$$

$$\frac{1}{\lambda_3}=475.3\ \text{cm}^{-1},\quad \frac{1}{\lambda_6}=1280\ \text{cm}^{-1}.$$

Representation $\Gamma^{(3)}$: Because of the choice of potential function, the values obtained for the 2 bands belonging to this representation are

$$\frac{1}{\lambda_1}=0\ \text{cm}^{-1},\quad \frac{1}{\lambda_2}=0\ \text{cm}^{-1}.$$

Representation $\Gamma^{(4)}$: Because of the choice of potential function, the values obtained for the 3 bands belonging to this representation are

$$\frac{1}{\lambda_1}=0\ \text{cm}^{-1},\quad \frac{1}{\lambda_2}=0\ \text{cm}^{-1},\quad \frac{1}{\lambda_3}=0\ \text{cm}^{-1}.$$

TABLE IV. Table of characters.

C_{2v}	E	C_2	σ_x	σ_y	Raman	Infra-red	No.
$\Gamma^{(1)}\sim A_1$	1	1	1	1	P	A	7
$\Gamma^{(2)}\sim B_1$	1	−1	−1	1	DP	A	6
$\Gamma^{(3)}\sim A_2$	1	1	−1	−1	DP	IA	2
$\Gamma^{(4)}\sim B_2$	1	−1	1	−1	DP	A	3
ϕ_R	0	π	0	0			
U_R	8	2	2	8			
$\pm1+2\cos\phi_R$	3	−1	1	1			
$\chi(R)$	24	−2	2	8			
Ξ	18	0	2	8			

2-3-4-Trimethylpentane (Table V, Fig. 5)

Representation $\Gamma^{(1)}$: The values obtained for the 6 bands belonging to this representation are

$$\frac{1}{\lambda_1}=202.0\ \text{cm}^{-1},\quad \frac{1}{\lambda_4}=722.4\ \text{cm}^{-1},$$

$$\frac{1}{\lambda_2}=251.3\ \text{cm}^{-1},\quad \frac{1}{\lambda_5}=1027\ \text{cm}^{-1},$$

$$\frac{1}{\lambda_3}=427.3\ \text{cm}^{-1},\quad \frac{1}{\lambda_6}=1288\ \text{cm}^{-1}.$$

Representation $\Gamma^{(2)}$: The values obtained for the 5 bands belonging to this representation are

$$\frac{1}{\lambda_1}=231.3\ \text{cm}^{-1},\quad \frac{1}{\lambda_4}=889.3\ \text{cm}^{-1},$$

$$\frac{1}{\lambda_2}=374.3\ \text{cm}^{-1},\quad \frac{1}{\lambda_5}=1238\ \text{cm}^{-1}.$$

$$\frac{1}{\lambda_3}=587.9\ \text{cm}^{-1},$$

Representation $\Gamma^{(3)}$: The values obtained for the 3 bands belonging to this representation are

$$\frac{1}{\lambda_1}=0\ \text{cm}^{-1},\quad \frac{1}{\lambda_3}=1111\ \text{cm}^{-1}.$$

$$\frac{1}{\lambda_2}=286.9\ \text{cm}^{-1},$$

Representation $\Gamma^{(4)}$: The values obtained for the 4 bands belonging to this representation

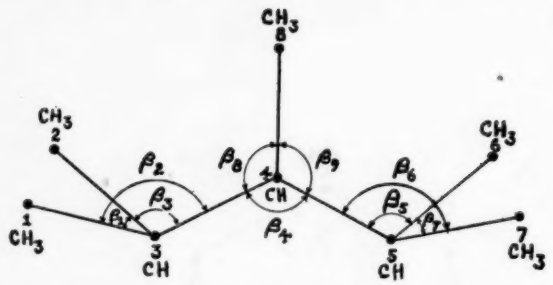

FIG. 5. Skeletal form of 2-3-4-trimethylpentane. $\beta_1°=\beta_2°=\beta_3°=\beta_4°=\beta_5°=\beta_6°=\beta_7°=107°$. $\beta_8°=\beta_9°=126.5°$.

are

$$\frac{1}{\lambda_1}=0\text{ cm}^{-1},\quad \frac{1}{\lambda_3}=457.2\text{ cm}^{-1},$$

$$\frac{1}{\lambda_2}=0\text{ cm}^{-1},\quad \frac{1}{\lambda_4}=1115\text{ cm}^{-1}.$$

2-Methyl-3-Ethylpentane (Table VI, Fig. 6)

Representation $\Gamma^{(1)}$: The values obtained for the 7 bands belonging to this representation are

$$\frac{1}{\lambda_1}=175.8\text{ cm}^{-1},\quad \frac{1}{\lambda_4}=584.1\text{ cm}^{-1},$$

$$\frac{1}{\lambda_2}=311.2\text{ cm}^{-1},\quad \frac{1}{\lambda_5}=1017\text{ cm}^{-1},$$

$$\frac{1}{\lambda_3}=410.2\text{ cm}^{-1},\quad \frac{1}{\lambda_6}=1043\text{ cm}^{-1},$$

$$\frac{1}{\lambda_7}=1364\text{ cm}^{-1}.$$

Representation $\Gamma^{(2)}$: The values obtained for the 5 bands belonging to this representation are

$$\frac{1}{\lambda_1}=0\text{ cm}^{-1},\quad \frac{1}{\lambda_4}=957.1\text{ cm}^{-1},$$

$$\frac{1}{\lambda_2}=252.4\text{ cm}^{-1},\quad \frac{1}{\lambda_5}=1206\text{ cm}^{-1}.$$

$$\frac{1}{\lambda_3}=549.5\text{ cm}^{-1},$$

Representation $\Gamma^{(3)}$: Because of the choice of potential function, the values obtained for the 2 bands belonging to this representation are

$$\frac{1}{\lambda_1}=0\text{ cm}^{-1},\quad \frac{1}{\lambda_2}=0\text{ cm}^{-1}.$$

Representation $\Gamma^{(4)}$: The values obtained for the 4 bands belonging to this representation are

$$\frac{1}{\lambda_1}=0\text{ cm}^{-1},\quad \frac{1}{\lambda_3}=450.5\text{ cm}^{-1},$$

$$\frac{1}{\lambda_2}=0\text{ cm}^{-1},\quad \frac{1}{\lambda_4}=1103\text{ cm}^{-1}.$$

MOLECULES BELONGING TO THE POINT GROUP D_{3h}

2-2-3-3-Tetramethylbutane (Table VII, Fig. 7)

Representation $\Gamma^{(1)}$: The values obtained for the 3 bands belonging to this representation are

$$\frac{1}{\lambda_1}=247.4\text{ cm}^{-1},\quad \frac{1}{\lambda_3}=1284\text{ cm}^{-1}.$$

$$\frac{1}{\lambda_2}=639.4\text{ cm}^{-1},$$

Representation $\Gamma^{(3)}$: Because of the choice of potential function, the value obtained for the 1 band belonging to this representation is

$$\frac{1}{\lambda_1}=0\text{ cm}^{-1}.$$

Representation $\Gamma^{(4)}$: The values obtained for the 2 bands belonging to this representation are

$$\frac{1}{\lambda_1}=484.1\text{ cm}^{-1},\quad \frac{1}{\lambda_2}=847.0\text{ cm}^{-1}.$$

TABLE V. Table of characters.

C_{2v}	E	C_2	σ_x	σ_y	Raman	Infra-red	No.
$\Gamma^{(1)}\sim A_1$	1	1	1	1	*P*	*A*	6
$\Gamma^{(2)}\sim B_1$	1	−1	−1	1	*DP*	*A*	5
$\Gamma^{(3)}\sim A_2$	1	1	−1	−1	*DP*	*IA*	3
$\Gamma^{(4)}\sim B_2$	1	−1	1	−1	*DP*	*A*	4
ϕ_R	0	π	0	0			
U_R	8	2	2	4			
$\pm1+2\cos\phi_R$	3	−1	1	1			
$\chi(R)$	24	−2	2	4			
Ξ	18	0	2	4			

Representation $\Gamma^{(5)}$ (doubly degenerate): The values obtained for the 3 bands belonging to this representation are

$$\frac{1}{\lambda_1}=353.6\ \text{cm}^{-1},\quad \frac{1}{\lambda_3}=1270\ \text{cm}^{-1}.$$

$$\frac{1}{\lambda_2}=570.7\ \text{cm}^{-1},$$

Representation $\Gamma^{(6)}$ (doubly degenerate): The values obtained for the 3 bands belonging to this representation are

$$\frac{1}{\lambda_1}=209.5\ \text{cm}^{-1},\quad \frac{1}{\lambda_3}=1123\ \text{cm}^{-1}.$$

$$\frac{1}{\lambda_2}=657.4\ \text{cm}^{-1},$$

SUPPLEMENTARY EVALUATIONS

The frequencies for *n*-butane and *n*-hexane were evaluated by the method described for the octanes for the purpose of determining how these bands merge with those of *n*-octane.

N-Butane (Table VIII, Fig. 8)

Representation $\Gamma^{(1)}$: The values obtained for the 3 bands belonging to this representation are

$$\frac{1}{\lambda_1}=359.6\ \text{cm}^{-1},\quad \frac{1}{\lambda_3}=1092\ \text{cm}^{-1}.$$

$$\frac{1}{\lambda_2}=979.7\ \text{cm}^{-1},$$

TABLE VI. Table of characters.

C_{2v}	E	C_2	σ_x	σ_y	Raman	Infra-red	No.
$\Gamma^{(1)}\sim A_1$	1	1	1	1	P	A	7
$\Gamma^{(2)}\sim B_1$	1	−1	−1	1	DP	A	5
$\Gamma^{(3)}\sim A_2$	1	1	−1	−1	DP	IA	2
$\Gamma^{(4)}\sim B_2$	1	−1	1	−1	DP	A	4
ϕ_R	0	π	0	0			
U_R	8	2	4	6			
$\pm 1+2\cos\phi_R$	3	−1	1	1			
$\chi(R)$	24	−2	4	6			
Ξ	18	0	4	6			

Representation $\Gamma^{(3)}$: Because of the choice of potential function, the value obtained for the 1 band belonging to this representation is

$$\frac{1}{\lambda_1}=0\ \text{cm}^{-1}.$$

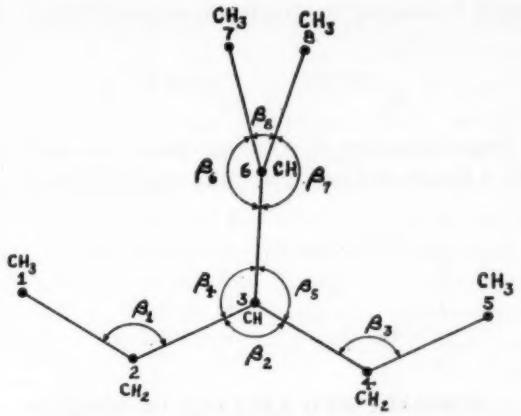

FIG. 6. Skeletal form of 2-methyl-3-ethylpentane. $\beta_1°=\beta_2°=\beta_3°=\beta_5°=107°$. $\beta_4°=\beta_6°=\beta_6°=\beta_7°=126.5°$.

Representation $\Gamma^{(4)}$: The values obtained for the 2 bands belonging to this representation are

$$\frac{1}{\lambda_1}=294.3\ \text{cm}^{-1},\quad \frac{1}{\lambda_2}=982.1\ \text{cm}^{-1}.$$

N-Hexane (Table IX, Fig. 9)

Representation $\Gamma^{(1)}$: The values obtained for the 5 bands belonging to this representation are

$$\frac{1}{\lambda_1}=261.6\ \text{cm}^{-1},\quad \frac{1}{\lambda_4}=1034\ \text{cm}^{-1},$$

$$\frac{1}{\lambda_2}=348.0\ \text{cm}^{-1},\quad \frac{1}{\lambda_5}=1119\ \text{cm}^{-1}.$$

$$\frac{1}{\lambda_3}=987.4\ \text{cm}^{-1},$$

Representation $\Gamma^{(2)}$: Because of the choice of potential function, the value obtained for the 1 band belonging to this representation is

$$\frac{1}{\lambda_1}=0\ \text{cm}^{-1}.$$

Representation $\Gamma^{(3)}$: Because of the choice of potential function, the values obtained for the 2

bands belonging to this representation are

$$\frac{1}{\lambda_1}=0\ \text{cm}^{-1},\quad \frac{1}{\lambda_2}=0\ \text{cm}^{-1}.$$

Representation $\Gamma^{(4)}$: The values obtained for the 4 bands belonging to this representation are

$$\frac{1}{\lambda_1}=149.1\ \text{cm}^{-1},\quad \frac{1}{\lambda_3}=972.4\ \text{cm}^{-1},$$

$$\frac{1}{\lambda_2}=427.0\ \text{cm}^{-1},\quad \frac{1}{\lambda_4}=1092\ \text{cm}^{-1}.$$

SUMMARY AND ANALYSIS OF RESULTS

Internal Consistency of the Theoretical Spectra

The calculated bands for all the molecules fall, roughly, into two main regions, one below 500 cm^{-1} and the other between 800 cm^{-1} and 1300 cm^{-1}, although there is some intermixture as well. The bands in the higher region may be assigned to modes in which the motions of the masses are mainly along the valence bonds, resulting in changes in the lengths of these bonds, while the bands in the lower region may be assigned to modes in which the motions of the masses are mainly perpendicular to the valence bonds, resulting in changes in the valence angles. This is borne out by the evaluation by the discussed method of the skeletal frequencies of the ethane and *n*-propane molecules. In the case of ethane, the motion for the frequency is a pure stretching of the valence bond, and gives rise to a band at 965 cm^{-1}, and, for *n*-propane the motion in which the angle between the valence bonds is changed gives rise to a band at 375 cm^{-1}. On the whole, the calculated spectra show no very distinct systematic displacement of the bands. (See Chart I.)

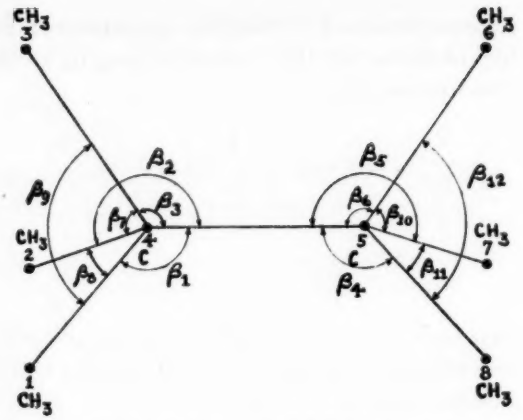

FIG. 7. Skeletal form of 2-2-3-3-tetramethylbutane. $\beta_1{}^\circ=\beta_2{}^\circ=\beta_3{}^\circ=\beta_4{}^\circ=\beta_5{}^\circ=\beta_6{}^\circ=107°$. $\beta_7{}^\circ=\beta_8{}^\circ=\beta_9{}^\circ=\beta_{10}{}^\circ=\beta_{11}{}^\circ=\beta_{12}{}^\circ=111°50'$.

From the spectra of the plane zigzag chain molecules, *n*-butane, *n*-hexane, and *n*-octane, may be seen the types of shift that result when new members are added to the chain of carbons. The single band at 965 cm^{-1} in the spectrum of ethane, corresponding to a stretching motion of the valence bond, becomes multiple in the others in a somewhat irregular fashion, and, starting with *n*-butane, bending vibrations appear at lower frequencies, which again spread out into several more bands in the spectra of the longer chains. These results are to be expected from general considerations, the additional bands resulting from the addition of more elements to the chain.

The main conclusion to be drawn is that small changes in form, and possibly also small changes in the potential function constants, result in large variations in the positions of the bands. Theory would lead us to expect no very systematic pattern for the bands in the spectra of the

TABLE VII. Table of characters.

D_{3h}	E	σ_h	$2C_3$	$2S_3$	$3C_2$	$3\sigma_v$	Raman	Infra-red	No.
$\Gamma^{(1)}\sim A_1'$	1	1	1	1	1	1	*P*	*IA*	3
$\Gamma^{(2)}\sim A_2'$	1	1	1	1	−1	−1	*F*	*IA*	0
$\Gamma^{(3)}\sim A_1''$	1	−1	1	−1	1	−1	*F*	*IA*	1
$\Gamma^{(4)}\sim A_2''$	1	−1	1	−1	−1	1	*F*	*A*	2
$\Gamma^{(5)}\sim E'$	2	2	−1	−1	0	0	*DP*	*A*	3
$\Gamma^{(6)}\sim E''$	2	−2	−1	1	0	0	*DP*	*IA*	3
ϕ_R	0	0	$2\pi/3$	$2\pi/3$	π	0			
U_R	8	0	2	0	0	4			
$\pm1+2\cos\phi_R$	3	1	0	−1	−1	1			
$\chi(R)$	24	0	0	0	0	4			
Ξ	18	0	0	0	2	4			

TABLE VIII. Table of characters.

C_{2h}	E	C_2	σ_h	i	Raman	Infra-red	No.
$\Gamma^{(1)}\sim A_G$	1	1	1	1	P	IA	3
$\Gamma^{(2)}\sim B_G$	1	−1	−1	1	DP	IA	0
$\Gamma^{(3)}\sim A_u$	1	1	−1	−1	F	A	1
$\Gamma^{(4)}\sim B_u$	1	−1	1	−1	F	A	2
ϕ_R	0	π	0	π			
U_R	4	0	4	0			
$\pm 1+2\cos\phi_R$	3	−1	1	−3			
$\chi(R)$	12	0	4	0			
Ξ	6	2	4	0			

octanes. It becomes evident that comparison of experimental with theoretical spectra will be difficult, and that for the most part only qualitative correspondence may be expected. An exact agreement with experiment would, of course, be extremely unlikely, since the exact forms of the molecules are not known, the forms used having been somewhat arbitrarily chosen to give the most symmetry possible consistent with chemical evidence. Also, the valence force model is itself an approximation.

Correlation with Experimental Spectra[7]

Any attempt to establish correlation of the theoretical spectra with spectra found experimentally meets with certain difficulties. The observed Raman and infra-red spectra are far from complete. The infra-red spectra do not include frequencies much below 700 cm^{-1}, and the Raman spectra, although somewhat more complete as to range covered, are available only for a few molecules. The purity of the experimental material is often questionable, especially in the case of the Raman spectra, so that extraneous bands due to impurities may be present. Both the Raman and the infra-red spectra show, besides the fundamental vibrations, many harmonics and overtones, as well as combination bands. Usually the fundamental bands should be stronger than the overtones or harmonics, but exceptions have been known. Acetylene is an example of a case in which the harmonic is very pronounced, being stronger than the fundamental. In addition, the observed spectra show not only the skeletal frequencies (i.e., frequencies arising from carbon vibrations), but also those resulting from the hydrogen vibrations. In most cases the hydrogen bands are readily identified, because of their position, and because of the fact that they repeat from molecule to molecule in the same pattern. For example, in the region covered by the charts, there are two infra-red bands at about 1380 cm^{-1} and 1470 cm^{-1}, and three Raman bands at about 1280 cm^{-1}, 1340 cm^{-1}, and 1460 cm^{-1}, which clearly repeat in all the spectra, and so may be classed as very likely caused by hydrogen vibrations, and excluded from further discussion. (See Chart II.)

On the whole, the observed skeletal frequencies show the same type of irregularity as is found for the calculated frequencies, and the general groupings are qualitatively alike. The lack of pattern in the experimental bands may be regarded as a definite correlation between experiment and theory, even though of a negative character. The absence of trends in the experimental spectra of the octanes might have seemed somewhat surprising, since in certain classes of spectra a particular atom and bond are known to give rise to a characteristic frequency, which persists even when terms are added to the molecules. This is observable in the case of the C−H vibrations, as well as in cases where a double bond occurs, such as C=C, the so-called ethylenic linkage, for example, the frequency for which persists throughout a series of compounds.

Possible correlation of bands in the theoretical and experimental spectra of the isomeric octanes for which all normal skeletal frequencies were evaluated is indicated in Chart II. The identification of lines is merely tentative. The following observations may be of interest.

N-octane.—The experimentally observed skeletal vibrations appear to fall into two main

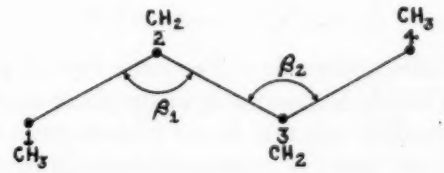

FIG. 8. Skeletal form of *n*-butane. $\beta_1^\circ=\beta_2^\circ=107°$.

[7] The infra-red spectra for all molecules are given by R. A. Oetjen, "The infrared spectra of the isomeric octanes," Thesis (University of Michigan, 1941). The Raman spectra for 2-5-dimethylhexane and 3-4-dimethylhexane are given by J. W. Murray, J. Chem. Phys. 2, 618 (1934). The Raman spectrum for *n*-octane is given by K. W. F. Kohlrausch, *Der Smekal-Raman-Effekt* (Verlagsbuchhandlung, Julius Springer, Berlin, 1938), p. 154.

TABLE IX. Table of characters.

C_{2h}	E	C_2	σ_h	i	Raman	Infra-red	No.
$\Gamma^{(1)}\sim A_G$	1	1	1	1	P	IA	5
$\Gamma^{(2)}\sim B_G$	1	−1	−1	1	DP	IA	1
$\Gamma^{(3)}\sim A_u$	1	1	−1	−1	F	A	2
$\Gamma^{(4)}\sim B_u$	1	−1	1	−1	F	A	4
ϕ_R	0	π	0	π			
U_R	6	0	6	0			
$\pm 1+2\cos\phi_R$	3	−1	1	−3			
$\chi(R)$	18	0	6	0			
Σ	12	2	6	0			

groups, corresponding to stretching and bending motions, as predicted. There seems to be some correlation of fundamental lines in the two spectra, as well as a possibility of establishing a correlation for the overtones in the infra-red. The two lines at 344.0 cm^{-1} and 396.6 cm^{-1} in the theoretical spectrum are repeated at 723 cm^{-1} and 768 cm^{-1} in the experimental spectrum, with decreased intensity. Whether this is an actual case of correlation or not is uncertain.

Infra-red	Calculated	Observed
	86.16	} Not measured
	344.0	
	396.6	
	2(344.0)	723
	2(396.6)	768
		882
		915
	986.3	970
	996.7	
	1104	1081
		1140

Raman	Calculated	Observed
	200.0	250
	224.3	
	443.4	420
		500
		810
		870
		890
	955.7	950
		1030
	1053	1060
	1054	1070
	1127	1130

2-5-dimethylhexane.—The same type of grouping of bands is observable in the theoretical and experimental spectra, in the regions covered by both, and there is a comparatively good possibility for correlation of lines.

Infra-red	Calculated	Observed
	152.6	} Not measured
	257.9	
	372.6	
	426.8	
		750
	883.7	922
		955
	1061	1046
		1091
	1124	1173
		1229

Raman	Calculated	Observed
	217.9	265
		313
	367.1	444
	376.0	
		778
	851.3	836
	1032	962
		1048
	1113	1150
	1146	1176
		1302

2-2-3-3-tetramethylbutane.—Possible correlation of lines in the theoretical and experimental spectra is given in the table below, including overtone bands, as indicated.

Infra-red	Calculated	Observed
	209.5	} Not measured
	484.1	
	657.4	
		788
	847.0	796
		803
	2(484.1)	931
		999
	1123	1184

4-methylheptane, 3-4-dimethylhexane, 2-3-4-trimethylpentane, and 2-methyl-3-ethylpentane.—The frequencies fall into two main groups, corresponding to stretching and bending motions, as before. Identification of lines is extremely uncertain, but the correlation indicated in Chart II is regarded as possible.

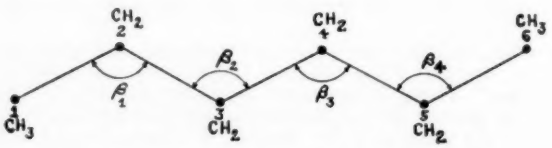

FIG. 9. Skeletal form of *n*-hexane.
$\beta_1^\circ=\beta_2^\circ=\beta_3^\circ=\beta_4^\circ=107°$.

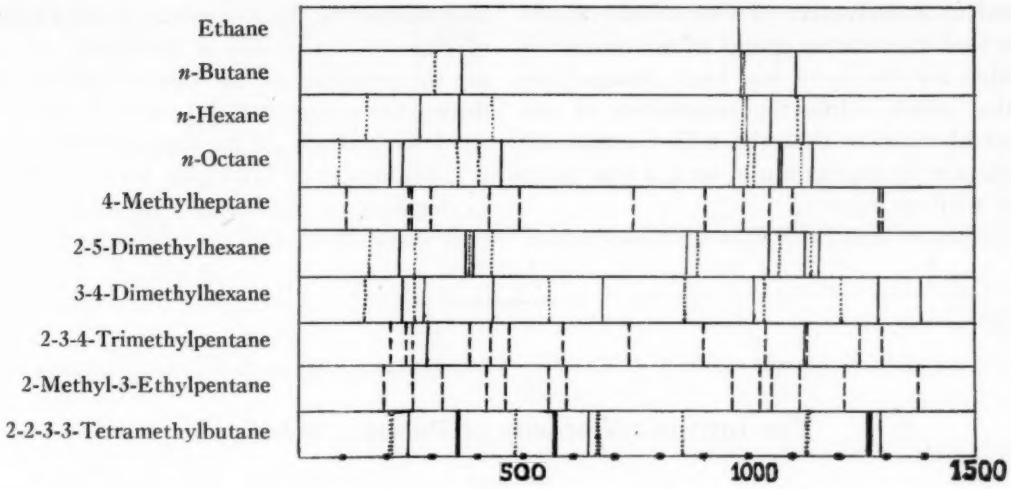

CHART I. Shows theoretical values of $1/\lambda$ in cm^{-1}. Infra-red active ⋮. Raman active |. Active in both |.

The agreement between theory and experiment is not very good, but in view of the fact that small changes in form, and possibly also small changes in the potential function constants, result in considerable shifts in the location of the bands, it is, perhaps, what might be expected. The lack of pattern in both the theoretical and experimental bands is a definite correlation.

The tentative correlation established by this research is valuable, since it can give the type of motion belonging to the observed spectral bands, and this knowledge may be of considerable value in interpreting the spectra of the derivatives of the octanes. For example, if it is known that a certain band corresponds to a given motion of the atoms of an octane, the disappearance of

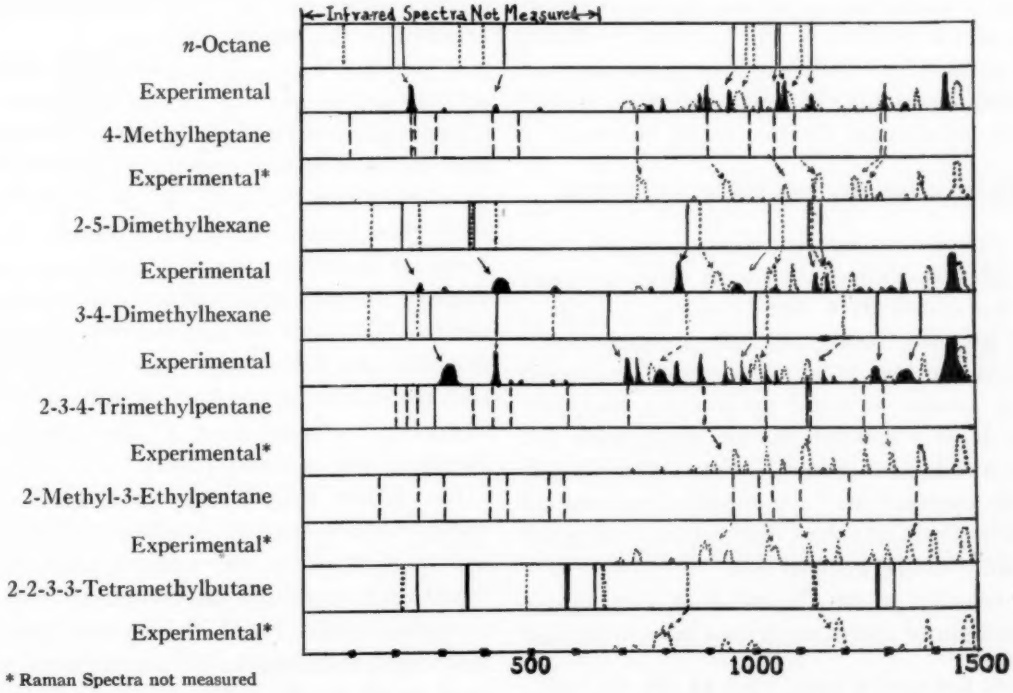

* Raman Spectra not measured

CHART II. Shows theoretical and experimental values of $1/\lambda$ in cm^{-1}. Infra-red active ⋮. Raman active |. Active in both |.

this band in a derivative of this octane would indicate that the atomic group whose motion is responsible for the band has been changed by the added terms, while the persistence of the band would indicate that the added terms are not connected to that group in such a way as to interfere with its motion.

The author wishes to express his appreciation to Professor D. M. Dennison, of the Department of Physics, University of Michigan, for suggesting the problem and for many helpful discussions during the progress of the research and to Professor J. C. Halford, of the Department of Chemistry, University of Michigan, for his collaboration in deciding on the forms that might best represent the structures of the molecules investigated.

THE JOURNAL OF CHEMICAL PHYSICS VOLUME 14, NUMBER 10 OCTOBER, 1946

The Intrinsic Viscosity of Polymer Solutions

P. DEBYE
Department of Chemistry, Cornell University, Ithaca, New York
(Received August 14, 1946)

1. INTRODUCTION

RECENTLY some articles have been published dealing with the behavior of polymers of the coiling type suspended in a flowing liquid.[1] One of the issues is to establish a physical reason for Staudinger's rule according to which the intrinsic viscosity of polymer solutions should be proportional to the molecular weight of the polymer. I would like to present here a detailed picture of the motion of the polymer molecule and its parts, which makes it easy to see why the rule should hold for the very simplified model currently substituted for the actual molecule.

2. MOTION OF THE POLYMER MOLECULE

The model is as usual a number of identical atomic groups connected to each other by rigid links, the consecutive ones making a definite angle with each other and able to turn freely around each other. It is also assumed that each of these groups is acted upon by a frictional force fv if in a solvent flowing along with the velocity v and that neither the links suffer friction from the medium nor any interaction between the different groups exists, due to their individual disturbance of the general flow.

The velocity of the liquid in a rectangular x, y, z system of coordinates may be represented by the vector $\mathbf{V}$ with the components

$$\mathbf{V}=\begin{cases}\alpha z=v_x\\ 0=v_y\\ 0=v_z\end{cases} \tag{1}$$

as it would result for instance from the motion of a plate in the x,y-plane moving with a constant velocity in the x-direction at a constant distance above another parallel plate at rest. The velocity gradient in the z-direction is α.

A polymer molecule suspended in this liquid will be set in motion by the frictional forces acting upon each atomic group of the chain. If now we confine our attention to the center of gravity of the molecule, it can easily be seen that this center of gravity (apart from its irregular Brownian motion) will move with the velocity of the liquid as it is at the position where this center is momentarily situated. In this way we have taken care of the condition that the sum of all the forces acting on the whole molecule, averaged over all the configurations the chain can acquire is zero.

Let us now take the center of gravity as the origin of our system of coordinates. Equation (1) will then represent the relative velocity of the liquid with respect to this center and will appear as represented in Fig. 1. It is evident from Fig. 1 that the still remaining frictional forces will now tend to rotate the molecule as a whole around the y-axis. Call the angular velocity of such a

[1] John G. Kirkwood, J. Chem. Phys. **14**, 180, 347 (1946); H. A. Kramers, J. Chem. Phys. **14**, 415 (1946), a sequence to an article by J. J. Hermans, Physica **10**, 777 (1943).

rotation ω. A group at the position x, y, z will, due to this rotation, have a velocity $\mathbf{v}$ with the component,

$$\mathbf{v}=\begin{cases}\omega z\\ 0\\ -\omega x\end{cases} \tag{2}$$

and the frictional force acting on such a group will be $\mathbf{F}=f(\mathbf{V}-\mathbf{v})$. In the steady state we will have to satisfy the condition that the average moment of this force around the center of gravity is zero. The instantaneous moment $\mathbf{M}$ has the components

$$\mathbf{M}=\begin{cases}f\omega \sum xy\\ f[(\alpha-\omega)\sum z^2-\omega\sum x^2],\\ -f(\alpha-\omega)\sum yz\end{cases} \tag{3}$$

the summation extending over all the groups of the molecule. Since in the average the products xy and yz are zero and

$$\text{Av}\,\langle x^2\rangle=\text{Av}\,\langle z^2\rangle=\text{Av}\left\langle\frac{r^2}{3}\right\rangle,$$

in which r is the distance of the group from the center of gravity, the average moment will only have a component in the y-direction and this will be equal to

$$\text{Av}\,\langle M_y\rangle=f(\alpha-2\omega)\,\text{Av}\left\langle\sum\frac{r^2}{3}\right\rangle. \tag{4}$$

In the steady state this average moment has to be zero and so we conclude that the molecule rotates as a whole with an angular velocity

$$\omega=\alpha/2. \tag{5}$$

But even so the liquid will still have relative velocities with respect to the different groups. For one of them this relative velocity $\mathbf{V}-\mathbf{v}$, will have the components

$$\mathbf{V}-\mathbf{v}=\begin{cases}\frac{\alpha}{2}z\\ 0\\ \frac{\alpha}{2}x\end{cases} \tag{6}$$

as follows from (1) and (2) with $\omega=\alpha/2$.

The flow lines of this relative flow of the liquid through the skeleton of the molecule are represented in Fig. 2. The frictional energy-losses connected with this flow will appear in the form of an increased viscosity of the solution.

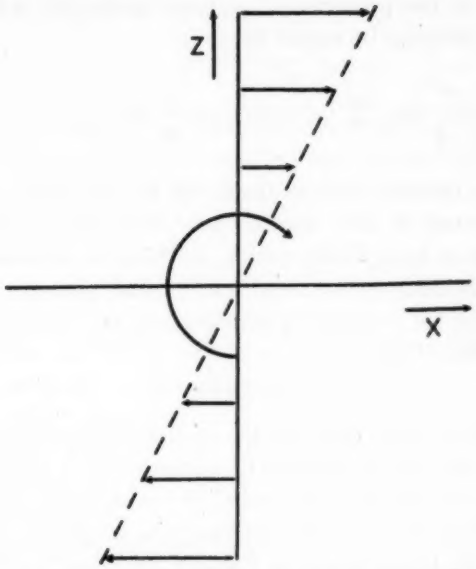

FIG. 1. Relative velocity of the medium with respect to the center of gravity of the molecule before rotation.

The flowlines themselves are hyperbolas with the equation

$$z^2-x^2=\text{const.}$$

and the absolute value of the velocity

$$\frac{\alpha}{2}(z^2+x^2)^{\frac{1}{2}}$$

is constant on circles around the y axis, increasing proportionally with the distance from this axis.

3. ENERGY LOSSES

In the flow represented by Fig. 2 and Eq. (6) the frictional force on one of the groups is

$$f\frac{\alpha}{2}(z^2+x^2)^{\frac{1}{2}}$$

and since this force is in the direction of the velocity, the work in unit time for one group is

$$f\frac{\alpha^2}{4}(z^2+x^2).$$

If n is the number of molecules per cc, the increase in energy losses per sec. and in 1 cc

due to the presence of polymer molecules will in the average be equal to

$$w=nf\frac{\alpha^2}{4}\text{Av}\,\langle\sum(z^2+x^2)\rangle=nf\frac{\alpha^2}{6}\,\text{Av}\,\langle\sum r^2\rangle. \quad (7)$$

This increase makes itself felt by an observable increase of the macroscopic viscosity from a value η to a higher value η'. Now in a medium of viscosity η the total energy loss per sec. and per cc for a velocity distribution as represented by Eq. (1) is

$$w=\eta\alpha^2. \quad (8)$$

This is easily checked by realizing that if one of the two parallel plates of surface S at a distance h is moving with the velocity $v=\alpha h$ with respect to the other, which is at rest, the frictional force on the upper plate is $F=\eta\alpha S$ and the displacement of this plate per unit time is $v=\alpha h$. Consequently the total amount of work dissipated in the volume Sh per sec. is $Fv=\eta\alpha^2 Sh$. If due to the presence of the polymer molecules the medium acts as if the viscosity is increased from η to η', the corresponding increase in dissipated energy will be

$$w=(\eta'-\eta)\alpha^2. \quad (9)$$

Equations (7) and (9) represent the same quantity in two different forms, so we conclude that

$$\eta'-\eta=\tfrac{1}{6}nf\sum\text{Av}\,\langle r^2\rangle. \quad (10)$$

It can now already be seen at once that the increase in viscosity will be proportional to the square of the number of links contained in the chain of the molecule. It is well known that the average of the square of the distance from beginning to end of the chain is proportional to N, denoting by N the total number of links. From this it follows immediately that the average of the square of the distance of one of the groups from the center of gravity of the whole molecule will also be proportional to N. On the other hand the number of terms in the sum of Eq. (10) is $N+1$. Neglecting terms of the relative importance $1/N$ against 1, we thus come to the conclusion that the sum is proportional to N^2. In a qualitative way this dependence is caused by the fact that in longer molecules the average distance of each group from the center of gravity is larger. Consequently each group comes into a region in which the relative velocity of the medium with respect to the rotating molecule is also larger. Increasing the length of the molecule therefore means not only increasing the number of centers which contribute to the energy losses but also increasing at the same time the individual energy loss due to each center.

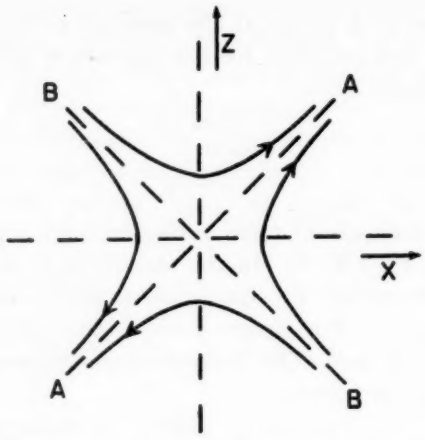

FIG. 2. Relative velocity of the medium with respect to the center of gravity of the rotating molecule.

4. INTRINSIC VISCOSITY

In order to complete the calculation indicated in Eq. (10), we have to know what the average square of the distance is of one of the groups from the center of gravity. Obviously this average will depend on the position of the group in the chain and we expect that for a group in the middle it will be smaller than for a group near the end of the chain. This is confirmed by a calculation not reproduced here, which although somewhat more involved proceeds along the same lines followed in calculating the average square of the distance from beginning to end, which is

$$R^2=\frac{1+p}{1-p}Na^2. \quad (11)$$

In Eq. (11) a is the length of a link and p is the cosine of the angle between two consecutive links ($\frac{1}{3}$ for C−C bonds).

If we number the $N+1$ groups of the chain from O to N and concentrate our attention on group number ν, it is found that the average square of the distance of this group from the

center of gravity is

$$r_\nu^2=\frac{1+p}{1-p}Na^2\left[\frac{1}{3}-\frac{\nu}{N}\left(1-\frac{\nu}{N}\right)\right]. \qquad (12)$$

The factor in front of the brackets being equal to R^2, we see that for $\nu=0$ or $\nu=N$ (the ends of the chain) $r^2=\frac{1}{3}R^2$, whereas a minimum value is reached for $\nu/N=\frac{1}{2}$ (the middle of the chain) equal to $r^2=\frac{1}{12}R^2$. Substituting (12) in (10) and performing the summation, which within the limits of accuracy can be represented by an integral, we find

$$\eta'-\eta=\frac{1}{6}nf\frac{1+p}{1-p}Na^2\sum_{\nu=0}^{\nu=N}\left[\frac{1}{3}-\frac{\nu}{N}\left(1-\frac{\nu}{N}\right)\right]$$

$$=\frac{1}{6}nf\frac{1+p}{1-p}N^2a^2\int_0^1\left[\tfrac{1}{3}-\xi(1-\xi)\right]d\xi \qquad (13)$$

$$=\frac{1}{36}nf\frac{1+p}{1-p}N^2a^2.$$

From the increase in viscosity we obtain the relative increase in dividing by η and the intrinsic viscosity $[\eta]$ in dividing by the concentration, which is nNm if m is the mass of one of the groups of the chain. The final result for the intrinsic viscosity is

$$[\eta]=\frac{1}{36}\frac{f/\eta}{m}\frac{1+p}{1-p}Na^2, \qquad (14)$$

which represents Staudinger's rule that the intrinsic viscosity is proportional to N and therefore to the molecular weight of the whole molecule. Should we represent each group by a sphere of radius ρ and apply Stokes law, according to which in this case $f=6\pi\eta\rho$, we will find

$$[\eta]=\frac{\pi}{6}\frac{\rho R^2}{m}. \qquad (14')$$

As is evident from the definition of $[\eta]$ it has the dimension of a specific volume and this is according to the theory represented here by the quotient of a volume which is $\pi/6$ times the product of the radius of the sphere, representing each group multiplied by the average square of the distance from beginning to end of the chain, divided by the mass of a single group. In order to show by an example that the order of magnitude is correct we take a polymer of molecular weight 500,000, each single group having the molecular weight 50. We now have $N=10{,}000$ and with $a=1.54$A (the C–C distance) it follows that $R^2=47{,}400.10^{-16}$ cm^2. Since $m=82.10^{-24}$ g we find that in order to explain a supposedly observed intrinsic viscosity $[\eta]=100$ cc/g (which in the customary practical units, 1 g and 100 cc, corresponds to the intrinsic viscosity (1) it is necessary to represent each group by a sphere of radius $\rho=0.33$A.

As to the streaming double refraction, which may be expected from the model, it is immediately evident from Fig. 2 that in a second approximation the molecule will in the average lose its central symmetry, be elongated in the direction AA, and compressed in the direction BB. With bonds having different polarizabilities parallel and perpendicular to their direction this will lead to observable double refraction of the solution in motion with axes under 45° against the direction of flow. At the same time it is also evident with respect to the viscous behavior of the solution that in a second approximation and due to the distortion of the molecule proportionality between the shearing stress and the velocity gradient will cease to exist.

Letters to the Editor

THIS section will accept reports of new work, provided these are terse and contain few figures, and especially few halftone cuts. The Editorial Board will not hold itself responsible for opinions expressed by the correspondents. Contributions to this section should not exceed 600 words in length and must reach the office of the Managing Editor not later than the 15th of the month preceding that of the issue in which the letter is to appear. No proof will be sent to the authors. The usual publication charge ($3.00 per page) will not be made and no reprints will be furnished free.

The Effect of Solvents on the Critical Concentration for Micelle Formation of Cationic Soaps*

M. L. CORRIN AND WILLIAM D. HARKINS
The University of Chicago, Chicago, Illinois
August 21, 1946

THE effect of various solvents upon the critical concentration for micelle formation has been discussed by Ward[1] and by Ralston and Hoerr.[2] The development of titrametric methods for the determination of critical concentrations has made it practical to extend such studies.[3] With the titration technique it is possible to measure a number of critical concentrations under varying conditions far more easily than if a conductometric method is used; by this latter procedure a large number of accurate measurements are required for a single determination. The work of Ward is restricted to sodium dodecyl sulfate, while Ralston and Hoerr consider only dodecylammonium chloride; the latter workers, however, do not report any values for the critical concentration. The work herein reported is restricted to cationic soaps since no indicator is available which gives a sharp end point with anionic materials in solutions containing organic solvents.

Data for the critical concentration of dodecylammonium chloride in various solvent-water mixtures are plotted in Fig. 1; the indicator was dichlorofluorescein. With decyl trimethyl ammonium bromide the measurements were extended in the region of low solvent concentration. These data are plotted in Fig. 2; the indicator employed was Sky Blue *FF*.

With decyl trimethyl ammonium bromide the decrease in critical concentration becomes more pronounced as the chain length of monohydric alcohol used as the solvent is increased. Dioxane also produces a slight initial decrease in critical concentration while no decrease was observed with ethylene glycol even at low solvent concentrations. A similar behavior was observed with dodecylammonium chloride. Isopropanol is but slightly different in its effect from *n*-propanol. At higher solvent concentrations the critical concentration of the detergent increases with dioxane, ethylene glycol, glycerol, and ethanol. At the highest concentrations of isopropanol, *n*-propanol, and *n*-butanol employed, the critical concentration was still decreasing.

On the basis of the above results it seems probable that Ward's hypothesis, which attributes the initial drop in critical concentration to adsorption of solvent molecules on the "surface of the micelle" is untenable.

It is, at present, difficult to correlate experimental observations with any dielectric constant data for the various solvent pairs. This is not unexpected since Ward has pointed out that a significant term in micelle formation is the dielectric environment about the polar head groups of the detergent molecules in the micelle; this quantity cannot, at the present time, be measured or even approximately calculated.

The term "interfacial energy" applied by many authors to the energy arising from an interaction of amphipathic molecules with surrounding solvent molecules is misleading and tends to obscure the actual processes involved in such systems. Interfacial energy is both defined and measured as the energy difference between the surface and bulk of a substance; there is no reason to consider that the interfacial energy represents the interaction energy of a

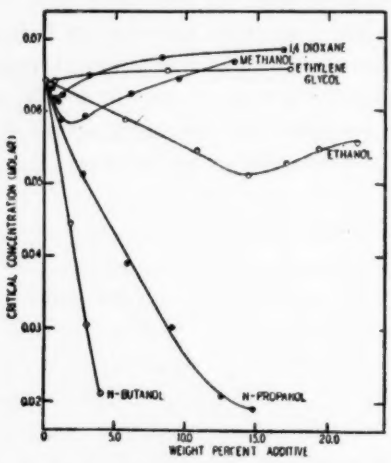

FIG. 1. The critical concentration for micelle formation in solutions of dodecylammonium chloride in various solvent-water mixtures.

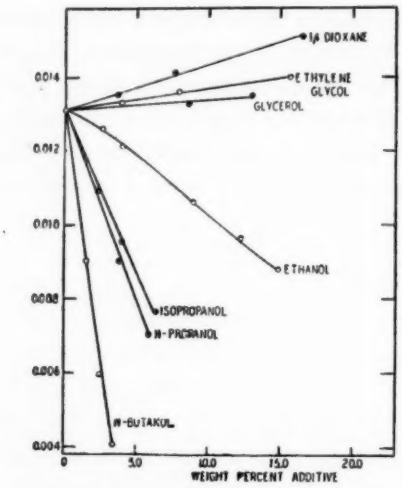

FIG. 2. The critical concentration for micelle formation in solutions of decyl trimethyl ammonium bromide in various solvent-water mixtures.

single molecule or portion of a molecule with the surrounding solvent molecules.

Since it is impossible at present to evaluate the energy terms involved in micelle formation, the experimental data herein reported can contribute only to the empirical knowledge of the properties of detergent solutions. It is hoped that the accumulation of further experimental information on a wide variety of properties of such solutions may eventually lead to a true understanding of their nature.

* The work reported in this paper was done in connection with the Government Research Program on Synthetic Rubber under contract with the Office of Rubber Reserve, Reconstruction Finance Corporation.

[1] A. F. H. Ward, Proc. Roy. Soc. **A176**, 412 (1940).
[2] A. W. Ralston and C. W. Hoerr, J. Am. Chem. Soc. **68**, 851 (1946).
[3] M. L. Corrin and W. D. Harkins, following letter.

Determination of Critical Concentrations for Micelle Formation in Solutions of Cationic Soaps by Changes in the Color and Fluorescence of Dyes*

M. L. Corrin and William D. Harkins
University of Chicago, Chicago, Illinois
August 26, 1946

In the first paper[1] on the use of dyes for the determination of the critical concentration for micelle formation, a titration method developed by the authors was mentioned. In this work with anionic soaps a cationic dye, pinacyanol chloride, was used. Attempts to use this same dye with cationic soaps were unsuccessful.

The following dyes, whose spectra in alcohol are visually distinguishable from those in water, were found to be ineffective with either anionic or cationic soaps: Orange *G* (*S*189), Azophloxin 2*G* (*S*40), Bordeaux *B* (*S*123), Congo Brown *G* (*S*280), New Methylene Blue (*S*1043), and Ponceau *G* (*S*37).

It was thought desirable to attempt to find dyes, one of whose several molecular forms is preferentially solubilized in soap micelles. This involved an extensive investigation in which it was discovered that the following dyes may be used as indicators with cationic soaps: Sky Blue *FF*, Eosin, Fluorescein, Dichlorfluorescein, and acidified 2,6-dichlorophenol indophenol. Another dye other than pinacyanol chloride applicable to anionic soaps, Rhodamine 6*G*, was also found. The values of critical concentrations determined by the use of these dyes are quite self consistent, as shown in Table I.

These results are also in agreement with literature values obtained by other, much more laborious methods. The critical concentration for dodecyl ammonium chloride is 0.0130 molar, as reported by Ralston and Hoerr,[2] and for decyl trimethyl ammonium bromide 0.065 molar by Scott and Tartar.[3]

Critical Concentration by Change in Fluorescence.—Cationic soap solutions containing eosin or fluorescein are highly fluorescent when micelles are present. This fluorescence is strongly quenched at concentrations below the critical; hence this property, as well as color, serves to determine the critical concentration, With eosin the color is orange above and red below the critical concentration. Both of these dyes are anionic and are effective with only cationic soaps.

Table I. The titrametric determination of critical concentrations with various dyes.

	Anionic Soaps			Cationic Soaps	
Dye	Potassium laurate	Sodium dodecyl sulfate	Sodium decyl sulfonate	Dodecyl ammonium chloride	Decyl trimethyl ammonium bromide
Pinacyanol chloride	0.0235	0.00602	0.0400		
Rhodamine 6*G*	0.0234	0.00612	0.0387		
Sky Blue *FF*				0.0643	0.0127
Eosin				0.0635	0.0136
Fluorescein				0.0610	0.0130
2,6-dichlorophenol-indophenol				0.0602	0.0124

Rhodamine 6*G*, a cationic dye and effective only with anionic soaps, also yields orange fluorescent solutions in the presence of micelles. When the soap concentration is reduced, the color changes to red and the fluorescence almost entirely disappears at the critical concentration.

* The work reported in this paper was done in connection with the Government Research Program on Synthetic Rubber under contract with the Office of Rubber Reserve, Reconstruction Finance Corporation.

[1] M. L. Corrin, H. B. Klevens, and W. D. Harkins, J. Chem. Phys. **14** 480 (1946).
[2] A. W. Ralston and C. W. Hoerr, J. Am. Chem. Soc. **64**, 772 (1942).
[3] A. B. Scott and H. V. Tartar, J. Am. Chem. Soc. **65**, 692 (1943).

On the Structure of Ozone

W. H. Eberhardt
Georgia School of Technology, Atlanta, Georgia
September 9, 1946

Using central-force-field methods, Glockler and Matlack[1] have recently presented a discussion of the bond energies and molecular structure of ozone based on a correlation of bond energy and interatomic distance suggested by other oxygen-oxygen bonds. Since their discussion is limited to acute angle models of the molceule, it is interesting to extend the technique to obtuse angle models.

From electron diffraction results[2] the ozone molecule has been reported to be an obtuse isosceles triangle with O−O bond length 1.26±0.02A and bond angle 127±3°. The separation of the base oxygen atoms is thus 2.25A. If one assumes the dependence of bond energy on interatomic distance as suggested by Glockler and Matlack, the energy of the two valence bonds is $2\times3.06=6.12$ electron volts. The contribution of the base O−O bond to the total binding energy will be small, and indeed may well be negative owing to the repulsion of the electron clouds of the two base oxygen atoms. Hence, it may be considered that adequate agreement with the total binding energy, 6.12 electron volts, may be obtained on the basis of this model as well as acute angle models.

[1] Glockler and Matlack, J. Chem. Phys. **14**, 505 (1946).
[2] Shand and Spurr, J. Am. Chem. Soc. **65**, 179 (1943).

Adsorption Isotherms for Hydrogen-Bonded Liquids on Charcoal

D. H. VOLMAN* AND I. M. KLOTZ
Northwestern University, Evanston, Illinois
August 28, 1946

IN van der Waal's adsorption on charcoal, a plot of the weight adsorbed as a function of the relative pressure (p/p_0) of the vapor gives a curve which is roughly the same for a large number of substances. A few exceptions are known, of which water is the outstanding example, in which marked deviations from the typical curve occur, particularly at low pressures. The underlying basis of these deviations becomes evident when it is realized that these exceptional substances all form strong hydrogen bonds in the liquid state. A stronger parallelism is then found to exist between adsorbability and condensation properties of a gas than has been realized previously.

A plot of boiling point as a function of van der Waal's a shows a region, bounded by the curves in Fig. 1, in which "normal" liquids are found. These are the substances which exhibit normal adsorption isotherms. In contrast, water, ammonia, and methyl alcohol, which show abnormal isotherms, also stand outside the normal region in Fig. 1, the distance being a rough measure of the deviation from the typical isotherm.

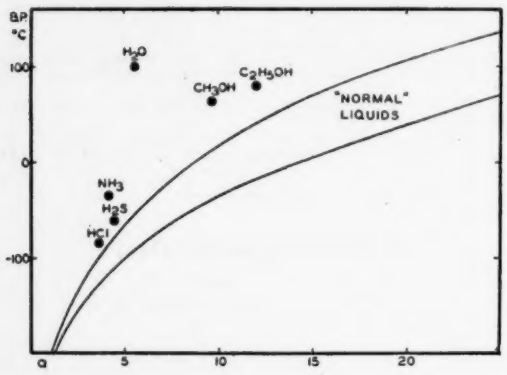

FIG. 1.

The deviation in the boiling-point curve is caused by the presence of strong hydrogen bonds in the liquid state, a condition which necessitates more energy to vaporize the molecules than would be required to overcome van der Waal's forces alone.

The deviations in the adsorption isotherm are also caused by hydrogen-bonding which may express itself in two different ways. In the region of low relative pressures (0.3–0.4), for water for example, the extent of adsorption appears to be unusually small. The apparent anomaly, is owing, however, to misleading values assigned to the relative pressure when one deals with a strongly hydrogen-bonded liquid. If there were no such bonding in liquid water, the boiling point and vapor pressure would be in line with those of the other hydrides of the sixth-group elements and would be near $-80°$ to $-100°$C, and about 20,000 mm (at room temperature), respectively. On the basis of this latter value for the vapor pressure if the liquid had no hydrogen bonds, the relative pressure of 0.3–0.4 is reduced to 0.0003–0.0004 and the observed adsorption is normal even though small. Since the adsorption at low pressures on charcoal (not containing specially-prepared, surface complexes) does not reflect in any way the hydrogen-bonding properties of water, this vapor behaves as if it came from a normal liquid with a vapor pressure of 20,000 mm.

Above relative pressures of 0.3–0.4 there is a steep rise in the water isotherm. Clearly this must be owing to the formation of a network of hydrogen-bonded water molecules, anchored initially by the few adsorbed molecules. Under these conditions the adsorbed phase does reflect the properties of the liquid and hence the isotherm rapidly approaches the normal curve.

* On leave, 1941–45, from University of California, Davis, California.